

NUCLEAR COMPRESSIBILITIES

J.P. BLAIZOT

*Commissariat à l'Énergie Atomique, Division de la Physique, Service de Physique Théorique,
CEN-Saclay, Boîte Postale No. 2, 91190 Gif-s/-Yvette, France*

Received February 1980

Contents:

| | | | |
|--|-----|---|-----|
| 1. Introduction | 173 | 5.1. Local description of the compression mode | 212 |
| 2. Equation of state of nuclear matter and static properties of nuclei | 174 | 5.2. The compressibility of the nuclear surface | 214 |
| 2.1. Some definitions | 175 | 6. Self-consistent calculations of the giant monopole resonance in nuclei | 219 |
| 2.2. Equilibrium state of a nucleus in a liquid drop model. Mass formulae | 177 | 6.1. The monopole strength function in spherical nuclei | 219 |
| 2.3. Phenomenological effective interactions | 180 | 6.2. The effective compression modulus for finite nuclei | 225 |
| 2.4. Results from nuclear matter theory | 190 | 6.3. The transition density | 228 |
| 3. Theory of collective excitations | 191 | 6.4. The transition potential | 231 |
| 3.1. Basic concepts | 191 | 6.5. Review of other calculations | 233 |
| 3.2. Linear response functions | 194 | 7. The effective mass | 234 |
| 3.3. Sum rules | 196 | 7.1. The concept of effective mass | 234 |
| 3.4. Comparison between various theories of collective motion | 199 | 7.2. Effective mass and static properties of nuclei | 235 |
| 4. Zero sound in nuclear matter and monopole excitation of nuclei | 201 | 7.3. Effective mass and giant quadrupole resonance | 237 |
| 4.1. Zero sound in nuclear matter | 201 | 7.4. Further remarks | 239 |
| 4.2. Giant monopole resonance in the harmonic oscillator model | 204 | 8. Present experimental data on the giant monopole resonance | 240 |
| 4.3. Giant monopole resonance in the liquid drop model | 207 | 8.1. Preliminary remarks | 240 |
| 5. From finite nuclei to nuclear matter | 212 | 8.2. Experiments | 241 |
| | | 8.3. Estimate of the compression modulus | 243 |
| | | 9. Conclusions | 245 |
| | | References | 246 |

Abstract:

We discuss the relation between the compressibility of nuclear matter and the frequencies of the collective monopole vibrations of nuclei. We analyse some of the problems which arise when one extrapolates from properties of finite nuclei to those of infinite nuclear matter. The best way to perform this extrapolation is to use a theory capable of describing both systems on the same footing. Self-consistent calculations using phenomenological effective interactions realize such a program. The general properties of these effective interactions are discussed. The theory we used is described; we emphasize that it accounts for both the properties of the ground states of nuclei and the small amplitude collective vibrations. Simple models of compression modes in infinite nuclear matter and in nuclei are presented; they illustrate various features of the collective modes in both systems. In particular we discuss the role of the shell structure and the effects of the nuclear surface. Results of extensive self-consistent calculations of the breathing mode of nuclei are presented and many features of the mode are analyzed. The role of the single particle spectrum on the frequencies of the collective modes is studied. Finally we briefly review the experimental situation on the monopole excitations of nuclei.

We show that experimental data are compatible with a well defined value of the compression modulus of nuclear matter: $K_x = 210 \pm 30$ MeV.

Single orders for this issue

PHYSICS REPORTS (Review Section of Physics Letters) 64, No. 4 (1980) 171–248.

Copies of this issue may be obtained at the price given below. All orders should be sent directly to the Publisher. Orders must be accompanied by check.

Single issue price Dfl. 32.50, postage included.

NUCLEAR COMPRESSIBILITIES

J.P. BLAIZOT

*Commissariat a l'Énergie Atomique, Division de la Physique, Service de Physique Théorique, CEN-Saclay,
Boite Postale No. 2, 91190 Gif-s/-Yvette, France*



NORTH-HOLLAND PUBLISHING COMPANY - AMSTERDAM

1. Introduction

Nuclear matter is an infinite system of nucleons, with a fixed ratio of neutron to proton numbers and no Coulomb interaction. Such a system has been considered mainly to test many-body theories but it presents in itself a real physical interest since nuclear matter exists in neutron stars. The first question which arises when one starts studying such a system is of course to obtain empirical information about its properties. This is not an easy task since nuclear matter does not exist in the laboratory and astrophysics measurements are rather indirect and therefore subject to large uncertainties. There are only two properties one can obtain rather directly from nuclei. The binding energy per nucleon E/A , which can be obtained by extrapolating the fits of nuclear masses, and the saturation density n_0 which is the density of nucleons inside medium and heavy nuclei. As we shall show in this report, the recent discovery of a giant monopole resonance in nuclei provides also direct information on the compressibility of nuclear matter.

The giant monopole resonance corresponds to a compression mode of the nucleus, the so-called "breathing mode". However the relation between the frequency of this mode and the compressibility of nuclear matter is not as straightforward as one might expect a priori. Even in nuclear matter there is not always a direct connection between the compressibility and the frequencies of the compression modes. Indeed, there exists in nuclear matter two kinds of compression modes, which differ by the nature of the associated restoring forces. These two modes are called zero and first sound. In first or ordinary sound, the restoring force is provided by the collisions between the nucleons. In the zero sound mode, the restoring force comes from the average potential felt by the nucleons; this potential varies when the density changes, trying to resist or to amplify the density fluctuations, depending on whether the interactions which generate this potential are repulsive or attractive. The velocity of ordinary sound is directly related to the square root of the compressibility, but this is not true in general for the zero sound, except when the interactions are such that the compression modulus is very large compared to its value in a non interacting Fermi system. In this particular case, the equations which govern zero sound reduce to those governing the conservation of particle number and momentum, i.e. the hydrodynamical equations. This simplification in the description of the zero sound mode is connected with the fact that the mode, in that case, dominates completely the response function, or equivalently it exhausts the sum rule. The nature of the restoring force in nuclei makes the compression modes of these systems very similar to the zero sound in nuclear matter. Furthermore, in heavy nuclei such modes exhaust the sum rule and it will be shown that this property is the key for the understanding of the relation between the frequencies of these modes and the compressibility of nuclear matter.

The results we shall present clearly indicate the needs for microscopic calculations in this context for several reasons. First of all, the single particle spectrum plays a dominant role in determining the existence and the structure of the collective modes in a nucleus; in particular the important property of depleting the sum rule depends to a large extent on the properties of the single particle spectrum. Secondly the compressibility of nuclear matter is certainly the main component of the restoring force in the compression of a nucleus; it would be the only one if the nuclear surface were sharp. However the diffuseness of the surface induces a strong reduction of the restoring force. Many other effects contribute to the restoring force although they are smaller than the effects associated with the surface. But as a result it turns out that the whole restoring force is hard to estimate without performing a complete microscopic calculation. In particular, simple models which provide analytical formulae from macroscopic arguments are not always correct.

Now it is important to emphasize that not all microscopic calculations of the giant monopole

resonances in nuclei can provide trustworthy information concerning nuclear matter. In particular a reliable calculation should contain as little phenomenological input as possible to allow the extrapolation from finite nuclei to nuclear matter without readjustment of the parameters or introduction of new ones. In other words it is clear that one must use a theory capable of describing nuclear matter as well as finite nuclei. Self-consistent calculations using phenomenological effective interactions have this advantage. They have of course some limitations which we shall indicate, but at least they allow a clear extrapolation to nuclear matter since the only phenomenological parameters which are fitted using the properties of nuclei, are those of the effective interaction. The present paper will be mainly devoted to the discussion of the results of these calculations.

The paper is organized as follows. In section 2 we analyze what can be learned about the equation of state of nuclear matter from static properties of nuclei. This serves as an elementary introduction in which some basic definitions are recalled and in which we critically review the empirical information one gets about nuclear matter by studying static properties of nuclei. In the same section we also discuss the properties of the phenomenological effective interactions which are used in self-consistent calculations of nuclei. In section 3 we present the theoretical framework in which we discuss collective motions in infinite and finite systems. A comparison to other theoretical approaches is given. Section 4 contains soluble models for compression modes in nuclear matter and in nuclei. The first is a simple model for zero sound in infinite nuclear matter: we discuss in particular under which condition the velocity of the zero sound is related directly to the compressibility. The second model describes the monopole vibration of a nucleus in the oscillator model with a monopole-monopole interaction and illuminates the role of the shell structure. We finally discuss the liquid drop model which relates in a simple way the compressibility of nuclear matter to the frequency of the compression modes of a nucleus. This model however, in its naive form, neglects important surface effects and it should not be used in a quantitative estimate of nuclear compressibility. The effects of the nuclear surface are analyzed in section 5, using a soluble model of semi-infinite nuclear matter. Section 6 contains the results of self-consistent calculations of monopole vibrations in closed shell nuclei. These calculations reveal the existence in medium and heavy nuclei of a very collective monopole mode of vibration which nearly exhausts the monopole sum-rule. The energy of this mode is shown to be determined to a great extent by the compressibility of nuclear matter through an effective compression modulus for finite nuclei K_A . To a good approximation the change of the density of a nucleus undergoing this collective oscillation is described by a homologous compression or dilatation of the ground state density. The transition potential associated with the vibration is analyzed. Finally we discuss other calculations of the breathing mode of nuclei. In section 7 the role of the effective mass is clarified and we present evidence based on the analysis of the frequency of giant quadrupole resonance for an effective mass close to unity in nuclei. The experimental situation is reviewed in section 8; the present empirical data are compatible with our calculations for a value of the compression modulus of the order of 210 MeV with an uncertainty of about 15%. Section 9 summarizes the conclusions.

2. Equation of state of nuclear matter and static properties of nuclei

The static properties of nuclei provide the first informations one can get about the equation of state of nuclear matter. In particular the mass formulae enable one to determine the binding energy, the saturation density, and the order of magnitude of the compressibility. These formulae appear in most

cases as expansions in two small quantities: $A^{-1/3}$ and $\delta = (N - Z)/A$ where N and Z are respectively numbers of neutrons and protons and $A = N + Z$. It is clear that such an expansion cannot account for the effects which are non analytic in A or δ , the shell effects being a typical example. Therefore some prescription is required to subtract these non-analytic effects from the data before fitting the parameters of the formula. This brings in uncertainties on the values of these parameters which will affect the extrapolated values of nuclear matter properties obtained by taking the limit $A \rightarrow \infty$ and dropping the Coulomb interaction.

An alternative to this approach is provided by the self-consistent calculations using phenomenological effective interactions, which reproduce a large number of static properties of nuclei. The same interactions can be used to calculate nuclear matter properties, within the same approximation as the one which is used for nuclei. Therefore in this approach, we can correlate, through the parameters of the effective interaction, the properties of nuclei to those of nuclear matter. This approach has the great advantage of being able to describe collective excitations. This will be discussed in the next sections. It is certainly not a complete many-body theory in the sense that the relation between the effective force in a nucleus and the nucleon-nucleon interaction in free space is not calculated. More important it is hard to estimate the corrections to the approximation which is used. However this approach has proved to be a very reliable tool in the study of the bulk properties of nuclei and the collective excitations.

The plan of this section is the following. First we recall a few definitions important for our discussion. Then we discuss how the static properties of finite nuclei are related to those of nuclear matter, first in a liquid drop model and then in self consistent calculations with effective interactions. The properties of these effective interactions are discussed in detail. Finally we say a few words about more fundamental theories of nuclear matter.

2.1. Some definitions

The total energy of nuclear matter at zero temperature can be written as [1]:

$$E = \Omega \mathcal{E}(n) \quad (2.1)$$

where Ω is the volume, assumed to be very large so that the surface effects can be neglected, $\mathcal{E}(n)$ is the energy density and n is the density of nucleons related to the Fermi momentum k_F by:

$$n = \frac{2}{3\pi^2} k_F^3. \quad (2.2)$$

The compressibility χ is defined by:

$$\chi = -\frac{1}{\Omega} \frac{\partial \Omega}{\partial P} = \frac{1}{n} \left(\frac{dP}{dn} \right)^{-1} \quad (2.3)$$

where the pressure P is related to the energy density by:

$$P = -\frac{\partial E}{\partial \Omega} = n \frac{d\mathcal{E}}{dn} - \mathcal{E} = n^2 \frac{dE/A}{dn}. \quad (2.4)$$

It is sometimes convenient to express χ in terms of the chemical potential μ :

$$\mu = \partial E / \partial A = d\mathcal{E} / dn. \quad (2.5)$$

From the preceding relations one gets easily:

$$1/\chi = n^2 d\mu / dn. \quad (2.6)$$

As will be discussed in the next section, microscopic theory leads to the following expression or χ :

$$\frac{1}{\chi} = \frac{2n}{3} \epsilon_F (1 + F_0) \quad (2.7)$$

where ϵ_F is the Fermi energy:

$$\epsilon_F = \hbar^2 k_F^2 / 2m^*. \quad (2.8)$$

The formula (2.7) separates the contributions to χ^{-1} into two parts. The term $2n\epsilon_F/3$ gives the compressibility of a system of non-interacting particles (with an effective mass m^*). The term proportional to F_0 is a correlation due to the interactions. F_0 is a so-called Landau parameter. It represents the coupling between changes in the self-consistent potential and the density fluctuations. The effective mass takes into account the contribution of the interactions to the energy of a particle with momentum k close to k_F , in the following approximate way:

$$\epsilon_k \sim \epsilon_F + (\mathbf{k} - \mathbf{k}_F) \cdot \mathbf{v}_F \quad (2.9)$$

where

$$v_F = \frac{1}{\hbar} \frac{d\epsilon_k}{dk} \Big|_{k=k_F} = \frac{\hbar k_F}{m^*}$$

is the Fermi velocity. The effective mass m^* is related to another Landau parameter, F_1 :

$$m^* = m(1 + F_1/3). \quad (2.10)$$

At the saturation density n_0 defined by:

$$\frac{dE/A}{dn} \Big|_{n=n_0} = 0, \quad (2.11)$$

the following relationships hold:

$$P(n_0) = 0, \quad \frac{dP}{dn} \Big|_{n_0} = n_0^2 \frac{d^2 E/A}{dn^2} \Big|_{n_0}, \quad \mu = E/A. \quad (2.12)$$

One furthermore defines a compression modulus by:

$$K_\infty = k_F^2 \frac{d^2 E/A}{dk_F^2} \Big|_{k_F=0} = 9n_o^2 \frac{d^2 E/A}{dn^2} \Big|_{n_o}. \quad (2.13)$$

A simple calculation shows that:

$$K_\infty = 3k_F \frac{d\mu}{dk_F} = \frac{9}{n_o \chi} = 6\epsilon_F(1 + F_o). \quad (2.14)$$

It is worth keeping in mind that the compression modulus is defined only at the saturation density, in particular its relation to the compressibility expressed by the eq. (2.14) is true only for $n = n_o$. Indeed, in general:

$$9n^2 \frac{d^2 E/A}{dn^2} = \frac{9}{n\chi} - \frac{18}{n} P \quad (2.15)$$

let us finally recall that the velocity c_1 of thermal found (or first sound) is related to the compressibility by:

$$c_1 = \frac{1}{\sqrt{\chi_o m n_o}} = \sqrt{\frac{K_\infty}{9m}}. \quad (2.16)$$

In order to have in mind orders of magnitude we list below typical numerical values of some physical quantities in nuclear matter.

| | | |
|--|---|---|
| Binding energy per nucleon | E/A | $-16 \pm 0.5 \text{ MeV}$ |
| Fermi momentum | k_F | $1.35 \pm 0.07 \text{ fm}^{-1}$ |
| Saturation density | $n_o = \frac{2}{3\pi^2} k_F^3$ | $0.166 \pm 0.027 \text{ fm}^{-3}$ |
| Average nucleon spacing | $r_o = \left(\frac{9\pi}{8}\right)^{1/3} \frac{1}{k_F}$ | $1.128 \pm 0.059 \text{ fm}$ |
| Compression modulus | K_∞ | $210 \pm 30 \text{ MeV}$ |
| Average kinetic energy per nucleon | $\langle T \rangle/A = \frac{3}{5}\epsilon_F$ | 23 MeV |
| Fermi energy | $\epsilon_F = \frac{\hbar^2 k_F^2}{2m^*}$ | $38 \text{ MeV} \text{ (for } m^* = m)$ |
| Fermi velocity in units of light velocity c | $v_F = \frac{\hbar k_F}{m^* c}$ | $0.3 \text{ (for } m^* = m)$ |
| Thermal sound velocity | c_1/c | 0.15 |

2.2. Equilibrium state of a nucleus in a liquid drop model. Mass formulae

The equilibrium state of a nucleus results from a delicate balance between several physical effects which

can be analyzed in a simple model. Let us assume that the density of a nucleus is constant, equal to n_o , inside a sphere of radius R_o and zero outside, and that the total energy can be written as follows:

$$E/A = \mathcal{E}(n_o)/n_o + 4\pi\sigma R_o^2/A + \frac{3}{5}Z^2e^2/AR_o + \delta^2 a_{\text{sym}}. \quad (2.17)$$

The four terms on the r.h.s. of eq. (2.17) are respectively the volume, the surface, the Coulomb and the symmetry energy. We assume that the neutrons and the protons occupy the same volume, i.e. we neglect the effects of a possible “neutron skin”. Minimizing E/A with respect to R_o yields:

$$P(n_o) = \frac{n_o}{3} \left[\frac{8\pi\sigma R_o^2}{A} - \frac{3Z^2e^2}{5AR_o} - 3n_o\delta^2 \frac{da_{\text{sym}}}{dn_o} - \frac{12\pi R_o^2 n_o}{A} \frac{d\sigma}{dn_o} \right]. \quad (2.18)$$

Thus, at equilibrium the pressure $P(n_o)$, which is generated by the compression of the nucleus, is compensated by four different terms:

- the pressure arising from the curvature of the surface
- the Coulomb pressure
- a pressure which arises from the density dependence of the symmetry energy coefficient a_{sym} and the surface energy coefficient σ .

$P(n_o)$ [†] can be obtained from the approximate equation of state

$$P(n) = (n - n_\infty)/\chi n_\infty. \quad (2.19)$$

Equations (2.18) and (2.19) determine the equilibrium density n_o , which, if the system is to be stable, has to be greater than the saturation density of nuclear matter n_∞ . Knowing $P(n_o)$ one can recalculate the binding energy in terms of $\delta R/R = -\frac{1}{3}(n - n_\infty)/n_\infty$ and nuclear matter constants. One gets:

$$\frac{E}{A} = \frac{\mathcal{E}(n_\infty)}{n_\infty} + \frac{1}{2}(n_o - n_\infty) \frac{d^2 E/A}{dn^2} + a_{\text{surf}} A^{-1/3} + \frac{3}{5} \frac{Z^2 e^2}{AR_o} + \delta^2 a_{\text{asym}} - \frac{n_o - n_\infty}{n_o^2} P(n_o) \quad (2.20a)$$

or:

$$E/A = -a_{\text{vol}} + a_{\text{surf}} A^{-1/3} + \delta^2 a_{\text{sym}} + \frac{3}{5} Z^2 e^2 / AR_o - \frac{1}{2} K_\infty (\delta R/R)^2, \quad (2.20b)$$

where we have set:

$$a_{\text{vol}} = -\mathcal{E}(n_\infty)/n_\infty, \quad a_{\text{surf}} = 4\pi r_o^2 \sigma, \quad R_o = r_o A^{1/3}. \quad (2.20c)$$

Formula (2.20b) provides a simplified mass formula which gives an idea about the accuracy with which nuclear parameters are determined by the fit to nuclear masses. For example K_∞ enters only in front of the small term $(\delta R/R)^2$ and cannot be precisely determined. r_o is more accurately determined if the fit incorporates also the fission barriers which are very sensitive to the ratio between Coulomb and

[†]We use throughout this paper the subscript o to denote equilibrium quantities. When these quantities are different from the corresponding nuclear matter ones, we denote the latter by the subscript ∞ .

surface energies and therefore to r_o . The mass formula developed by Myers and Swiatecki [2, 3] incorporates, besides the compressibility effects, the diffuseness of the surface and the possibility of a neutron skin, i.e. of having the radii of neutrons and protons distributions different. The values they get for the parameters we are interested in here are the following:

$$\begin{aligned} a_{\text{vol}} &= 15.96 \text{ MeV}, & K_\infty &= 240 \text{ MeV}, \\ a_{\text{surf}} &= 20.69 \text{ MeV}, & r_o &= 1.18 \text{ fm}, \\ a_{\text{sym}} &= 36.8 \text{ MeV}, & L = 3n_o da_{\text{sym}}/dn_o &= 100 \text{ MeV}. \end{aligned}$$

Other mass formulae give similar results [4a, 4b].

More direct information about the density is of course provided by electron scattering and the spectroscopic analysis of muonic atoms. If one defines an “effective sharp radius” for the proton distribution as:

$$R_P = \left[\frac{Z}{\frac{4}{3}\pi n_P} \right]^{1/3} \quad (2.21)$$

where n_P is the bulk density of the proton distribution, then both sets of empirical data are compatible with the average value [6]:

$$R_P = 1.13 A^{1/3} \quad (2.22)$$

which leads to a central density of protons:

$$n_P = 0.17 Z/A. \quad (2.23)$$

The droplet model reproduces this value with the nuclear radius parameter $r_o = 1.18 \text{ fm}$, which is the same as the parameter obtained by fitting nuclear masses. This value of r_o corresponds to $k_F = 1.29 \text{ fm}^{-1}$ which is smaller than the value traditionally adopted $k_F = 1.36 \text{ fm}^{-1}$ ($r_o = 1.12 \text{ fm}$). This last value is obtained from the formula (2.23) which indicates that if the neutrons and the protons occupy the same volume then the density of nuclear matter is $n_o = 0.17 \text{ nucleons/fm}^3$. Recent experimental determinations of the radii of the neutrons distribution [7] indicate that the “neutron skin” is smaller than that predicted by the droplet model, implying that the droplet model underestimates k_F .

Anyhow one has to emphasize that the determination of the properties of nuclear matter depends in a complicated way on the analytical form chosen for the mass formula, and in particular on the way one parametrizes the effects of the compressibility, the diffuseness of the surface, the neutron skin etc. As an example of ambiguities which one may encounter, let us consider the equilibrium condition (2.18) for our simple model. As will be shown in the section (5.2) the last term on the r.h.s. of (2.18) can be written:

$$d\sigma/dn_o = (n_o - n_\infty)\sigma K_\sigma/n_\infty^2 \quad (2.24)$$

where K_σ is a dimensionless coefficient, a typical value of which is -5 . Using (2.24), one can rewrite

(2.18) as follows:

$$\frac{n_o - n_\infty}{\chi n_\infty} \left[1 + \frac{3\sigma\chi K_\sigma}{R_o} \right] = \frac{n_o}{3} \left[\frac{8\pi\sigma R_o^2}{A} - \frac{3Z^2 e^2}{5AR_o} - 3n_o \delta^2 \frac{da_{sym}}{dn_o} \right]. \quad (2.25)$$

Now $3\sigma\chi K_\sigma/R_o \sim -0.7$ for typical values of the parameters and $R_o = 7$ fm. Therefore the equilibrium density n_o will be certainly different whether one sets $K_\sigma = 0$ or not. This ambiguity will obviously generate uncertainties in the nuclear matter constants r_o and K_∞ required to fit the masses of the nuclei.

2.3. Phenomenological effective interactions

The short range repulsion and the tensor component of the nucleon-nucleon potential strongly modify the interaction of two nucleons in the nucleus from what it is in free space [8, 9]. In particular it would make no sense to evaluate the potential energy of a nucleus as an expectation value of the nucleon-nucleon potential in an independent particle wave function. However there exists approximate schemes for the calculation of an effective interaction of nucleons in a nucleus, which is such that its expectation values in an independent particle wave function is close to the exact potential energy of the nucleus. Such approximate schemes are provided by the partial resummation of the perturbation expansion, e.g. Brueckner theory [8, 9, 10]. The effective interactions thus obtained have been used in the calculations of the bulk properties of nuclei. A few phenomenological adjustments are needed however in order to reproduce correctly the saturation properties of nuclear matter [11, 12, 13]. These adjustments affect mainly the short range part of the force, i.e. its density dependence to which the compression modulus is quite sensitive. These effective forces yield compression moduli typically in the range 190–250 MeV.

We shall not discuss these calculations any more but shall concentrate on more phenomenological theories which have been very successful in describing the bulk properties of nuclei and can be very easily extended to calculate the collective modes. In these theories the effective interaction is chosen phenomenologically, its parameters being fitted in order to reproduce the bulk properties of nuclei and some collective states. The form of the interaction is chosen so as to reproduce the main features of more fundamental effective interaction, e.g., it is density dependent. It has also to be simple enough to allow fast numerical computations. These interactions provide us the possibility of relating, within the same theoretical framework, a considerable amount of nuclear properties [5]. Furthermore, some of their parameters can be varied without affecting too much most of the properties which are fitted, except one or two. One can therefore relate, sometimes in a very clear way, observed properties of nuclei to what we are interested in here, properties of nuclear matter. Since the calculations which we shall mainly discuss here make use of these phenomenological interactions, we shall spend sometime discussing their properties.

The saturation of nuclear matter with these interactions is achieved mainly through three different mechanisms:

- density dependence = the interaction becomes less and less attractive (eventually repulsive) as the density increases
- velocity dependence = the attraction decreases when the relative momentum of the interacting nucleons increases, as it does when the density increases
- exchange forces which are attractive in even states and repulsive in odd states. The ratio of odd to even states increases with density.

2.3.1. Model examples

The compression modulus depends very much upon the saturation mechanism. In order to illustrate this point, we shall consider the following model examples, which will help in identifying the origin of the differences in the results obtained with various sets of forces. We shall consider three effective forces which saturate according to the three mechanisms just mentioned.

(i) Zero range force with density dependence

$$\langle \mathbf{k} | V | \mathbf{k}' \rangle = \frac{1}{\Omega} (t_0 + t_3 n^d). \quad (2.26)$$

(ii) Zero range force with velocity dependence†:

$$\langle \mathbf{k} | V | \mathbf{k}' \rangle = \frac{1}{\Omega} (t_0 + t_2 \mathbf{k} \cdot \mathbf{k}'). \quad (2.27)$$

(iii) Finite range force with exchange terms:

$$V(\mathbf{r}_1 - \mathbf{r}_2) = \frac{\exp\{-\mu|\mathbf{r}_1 - \mathbf{r}_2|\}}{\mu|\mathbf{r}_1 - \mathbf{r}_2|} (W + MP_x). \quad (2.28)$$

In the models under consideration, the energy of nuclear matter is calculated as the expectation value in a Slater determinant of the effective interaction. In table 1, we give, for each type of force, the expressions of the energy density, the pressure, the compressibility and the Landau parameters relevant to our discussion, F_0 and F_1 . Details concerning the calculations can be found for example in ref. [17].

The energy densities obtained with the three forces have a similar structure. They are composed of a kinetic energy term $\propto n^{5/3}$ and two potential terms, of which one has to be attractive and the other repulsive in order to get saturation. A plot of the binding energy per nucleon as a function of the Fermi momentum is given in the fig. 1. At very low density (small k_F) the kinetic energy dominates and the

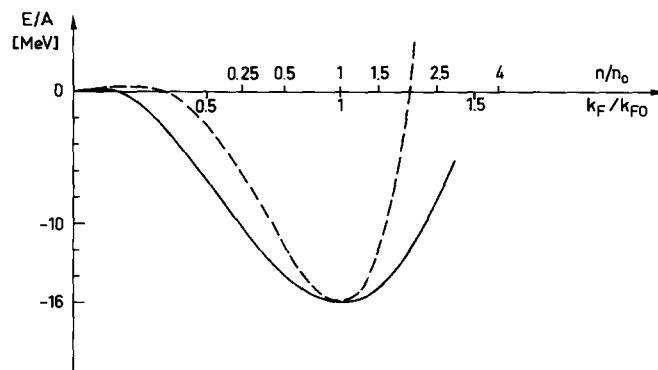


Fig. 1. Binding energy per nucleon in nuclear matter as a function of the Fermi momentum k_F or the density n . (—): finite range force with $\mu = 0.7 \text{ fm}^{-1}$. (---): density dependent force with $d = 2/3$.

† k and k' are the relative momenta of the interacting nucleons.

Table 1

Properties of nuclear matter with simple effective forces. $\mathcal{E}(n)$, $P(n)$, $\chi(n)$ are respectively the energy density, the pressure and the compressibility. $U(k)$ is the single particle potential. F_o and F_1 are Landau parameters. n_o is the saturation density. N_o is the density of single particle state at the Fermi surface: $N_o = 3n_o/2\varepsilon_F$. The function $I(x)$, proportional to the exchange integral, is:

$$I(x) = \frac{1}{12}[2(6 - (1/x^2)) + (1/2x^2)(1/x^2 + 12x^2)\log(1 + 4x^2) - (16/x)\arctg(2x)]$$

| | | |
|---|---|---|
| Force | $\langle k V k' \rangle = \frac{1}{\Omega} (t_o + t_3 n^d)$ | $\langle k V k' \rangle = \frac{1}{\Omega} (t_o + t_2 k \cdot k')$ |
| $\mathcal{E}(n)$ | $a \left(\frac{n}{n_o}\right)^{5/3} + b \left(\frac{n}{n_o}\right)^2 + c \left(\frac{n}{n_o}\right)^{d+2}$ | $a \left(\frac{n}{n_o}\right)^{5/3} + b \left(\frac{n}{n_o}\right)^2 + c \left(\frac{n}{n_o}\right)^{8/3}$ |
| $a; b; c$ | $\frac{3\hbar^2 k_{F0}^2}{10m} n_o; \frac{3}{8} t_o n_o^2; \frac{3}{8} t_3 n_o^{d+2}$ | $\frac{3\hbar^2 k_{F0}^2}{10m} n_o; \frac{3}{8} t_o n_o^2; \frac{3}{16} t_2 n_o^2 k_{F0}^2$ |
| $P(n)$ | $\frac{2}{3} a \left(\frac{n}{n_o}\right)^{5/3} + b \left(\frac{n}{n_o}\right)^2 + c(d+1) \left(\frac{n}{n_o}\right)^{d+2}$ | $\frac{2}{3} a \left(\frac{n}{n_o}\right)^{5/3} + b \left(\frac{n}{n_o}\right)^2 + \frac{5}{3} c \left(\frac{n}{n_o}\right)^{8/3}$ |
| $\frac{1}{\chi(n)}$ | $\frac{10}{9} a \left(\frac{n}{n_o}\right)^{5/3} + 2b \left(\frac{n}{n_o}\right)^2 + c(d+1)(d+2) \left(\frac{n}{n_o}\right)^{d+2}$ | $\frac{10}{9} a \left(\frac{n}{n_o}\right)^{5/3} + 2b \left(\frac{n}{n_o}\right)^2 + \frac{40}{9} c \left(\frac{n}{n_o}\right)^{8/3}$ |
| $U(k)$ | $\frac{3t_o n}{4} + \frac{3}{8} t_3 (d+2) n^{d+1}$ | $\frac{3t_o n}{4} + \frac{3t_2}{16} nk_F^2 + \frac{5}{16} t_2 nk^2$ |
| F_o | $N_o [\frac{3}{4} t_o + \frac{3}{8} t_3 (d+1)(d+2) n^d]$ | $N_o [\frac{3}{4} t_o + \frac{5}{8} t_2 k_F^2]$ |
| F_1 | 0 | $-3 \left[\frac{8\hbar^2}{5t_2 mn} + 1 \right]^{-1}$ |
| Force | $V(r_1 - r_2) = \frac{\exp[-\mu r_1 - r_2]}{\mu r_1 - r_2 } [w + MP_x]$ | |
| $\mathcal{E}(n)$ | $\frac{3\hbar^3 k_{F0}^2}{10m} n_o \left(\frac{n}{n_o}\right)^{5/3} + (W - M) n_o^2 \frac{\pi}{2\mu^3} \left(\frac{n}{n_o}\right)^2 - (W - 4M) \frac{3n_o k_{F0}}{4\pi} \left(\frac{n}{n_o}\right)^{4/3} I\left(\frac{k_F}{\mu}\right)$ | |
| F_o | $N_o \left\{ (W - M) \frac{\pi}{\mu^3} - \frac{\pi}{4\pi k_F^3} (W - 4M) \log\left(1 + 4 \frac{k_F^2}{\mu^2}\right) \right\}$ | |
| F_1 | $-N_o \frac{3\pi}{4k_F^2 \mu} (W - 4M) \left[\left(1 + \frac{\mu^2}{2k_F^2}\right) \log\left(1 + \frac{4k_F^2}{\mu^2}\right) - 2 \right]$ | |
| $U(k=0)$ | $(4W - M) \frac{\pi}{\mu^3} n - (W - 4M) \frac{2k_F}{\pi\mu} \left[1 - \frac{\mu}{k_F} \arctg\frac{k_F}{\mu}\right]$ | |
| $U(k=k_F)$ | $(4W - M) \frac{\pi}{\mu^3} n - (W - 4M) \frac{k_F}{\pi\mu} \left[1 - \frac{\mu}{k_F} \arctg\frac{2k_F}{\mu} + \frac{\mu^2}{4k_F^2} \log\frac{4k_F^2 + \mu^2}{\mu^2}\right]$ | |
| $\frac{m}{m^*} = 1 - \frac{\partial U}{\partial T_k}$ | $1 - \frac{m}{\hbar^2} \frac{W - 4M}{2\pi k_F \mu} \left[2 - \frac{\mu^2 + 2k_F^2}{2k_F^2} \log\left(1 + \frac{4k_F^2}{\mu^2}\right)\right]$ | |

system is unbound; then, as one increases the density, the energy starts to decrease, reaches a minimum and then increases again due to the repulsive part of the interaction. For the density dependent forces, the repulsion is achieved through the density dependent term if $d > 0$, and the attraction through the term proportional to the square of the density. Velocity dependent forces are in this respect equivalent to density dependent forces with $d = \frac{2}{3}$. In the case of the finite range forces, the term in n^2 is repulsive, the attraction being provided by the exchange term. Now if the range of the force $1/\mu$ is such that $\mu \sim k_{F0}/2$, then the exchange integral $I(k_F/\mu)$ (see table 1) goes as k_F/μ for $k_F \sim k_{F0}$. Thus the attractive term behaves (close to the saturation density) just as the kinetic energy (but with the opposite sign) in $n^{5/3}$. Therefore such forces with $\mu \sim k_{F0}/2$ behave like density dependent forces with $d = -\frac{1}{3}$.

Let us then study in more detail these density dependent forces as a function of the parameter d . First, using the saturation conditions one can express the parameters b and c of the energy density (see the table 1) in terms of d :

$$b = -Bn_o - a - \frac{1}{d} \left(Bn_o + \frac{a}{3} \right), \quad c = \frac{1}{d} \left(Bn_o + \frac{a}{3} \right), \quad (2.29)$$

where

$$B = -\mathcal{E}(n_o)/n_o.$$

Using these expressions one can get a simple formula for the compression modulus of nuclear matter in terms of the power d of the density dependent term in the effective interaction:

$$K_\infty = a/n_o + 9B + d(9B + 3a/n_o). \quad (2.30a)$$

For $k_F = 1.35 \text{ fm}^{-1}$ and $B = 16 \text{ MeV}$ one gets:

$$K_\infty = 167 + 212 d. \quad (2.30b)$$

Such a formula has already been given by L. Zamick [14]. We give below the values of K_∞ for some typical values of the parameter d :

| d | 1 | 2/3 | 1/3 | 1/6 | -1/3 |
|------------------------|-----|-----|-----|-----|------|
| $K_\infty(\text{MeV})$ | 379 | 308 | 238 | 202 | 96. |

These values turn out to be typical of what one obtains with more sophisticated forces which saturate with a term in n^d . It is interesting to note that the larger the range of the force the softer is the equation of state. For example in the table 2 we report results of calculations of the compression modulus using forces of the type (2.28) with different values of μ . One sees a clear increase of K_∞ with μ . This result is not however a trivial one. To understand it one has to remember the expression (2.14) of K_∞ in terms of the Landau parameters F_o and F_1 . Table 2 shows that F_1 remains roughly constant while F_o increases when μ increases, i.e., when the range of the force decreases. Now F_o is the sum of two terms, one which comes from the direct part of the interaction and which is repulsive, and one which comes from the exchange and which is attractive (see table 1). When the range of the force decreases the exchange integral decreases. In order to keep untouched the saturation properties $(E/A, n_o)$, the parameters

Table 2
Nuclear matter calculations with finite range forces (eq. (2.28)) for various values of the range μ^{-1} . W and M are the parameters of the interaction. U_o is the depth of the single particle potential. F_o , F_1 are Landau parameters, m^* and K_∞ are respectively the effective mass and the compression modulus

| μ (fm $^{-1}$) | $4W - M$ (MeV) | $W - 4M$ (MeV) | U_o (MeV) | F_o | F_1 | m^* | K_∞ |
|------------------------|-------------------|-------------------|----------------|-------|-------|-------|------------|
| 0.35 | 1.17 | 79.0 | -110 | -0.86 | -1.77 | 0.41 | 72.3 |
| 0.70 | 25.4 | 296 | -115 | -0.78 | -1.73 | 0.42 | 110.3 |
| 1.40 | 554 | 1810 | -117 | -0.67 | -1.74 | 0.42 | 170 |
| 2.80 | 13780 | 21361 | -114 | -0.56 | -1.79 | 0.40 | 238 |

$W - 4M$ and $4W - M$ increase, and this increase is such that the repulsive term in F_0 increases faster with μ than the attractive one.

The energy densities which are given by our schematic forces, as well as those obtained with more sophisticated effective interactions, make sense only for densities close to the saturation density. For higher densities, other degrees of freedom than those associated with nucleons only are expected to play an important role [15]. These extra degrees of freedom are clearly not taken into account in the present approach. At low densities one expects the normal phase of nuclear matter to be unstable against the formation of nuclei. A signal of this instability is the fact that the compressibility goes to infinity for densities in the range $0.5 n_0$ – $0.7 n_0$. This critical density n_c can be obtained by looking at the plot of F_0 versus n (fig. 2). One sees that F_0 goes through the value -1 for densities about $0.5 n_0$. This value of n_c is very insensitive to the compression modulus. Values of n smaller than n_0 are encountered in the surface of a nucleus. Of course, to explain the stability of the surface region, one has to take into account other contributions to the energy than those which are included in the local energy density. In particular non-local effects are important, and the concepts of local pressure, and compressibility lose part of their usefulness if not their meaning. However local concepts prove to be useful in obtaining semi-quantitative estimates of several quantities such as the restoring forces associated with the collective modes in nuclei [16] (see for example section 5).

Let us now consider the properties of the single particle spectrum with the different interactions. The energy of a particle with momentum k is given, within the approximation we use, by:

$$\epsilon(k) = \hbar^2 k^2 / 2m + U(k), \quad (2.31)$$

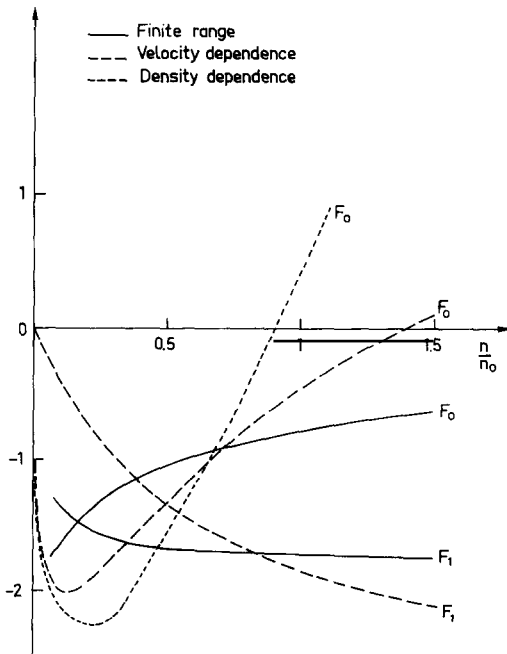


Fig. 2. Density dependence of the Landau parameters F_0 and F_1 (see table 1 for their analytical expressions). —, finite range force with $\mu = 0.7 \text{ fm}^{-1}$; ---, velocity dependent force; -·-, density dependent force with $d = 2/3$ ($F_1 = 0$ in this latter case). At small densities F_0 behaves like $n^{-2/3}$ while F_1 is linear in n .

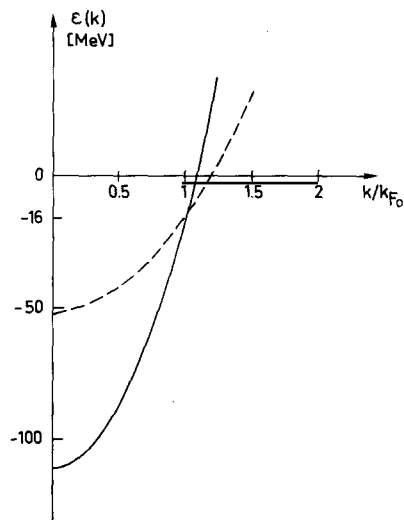


Fig. 3. Energies of the single particle states in nuclear matter as a function of the momentum k . ---, density dependent force with $d = 2/3$; —, velocity dependent force.

where $U(k)$ is the single particle potential which is in general a function of k . This k dependence of the single particle potential arises either from the velocity dependence of the effective interaction, or from the non locality of the average potential (exchange contribution). In fig. 3 we have drawn $\epsilon(k)$ versus k for two forces which lead to the same energy density, namely a density dependent force with $d = 2/3$ and a velocity dependent force. The two curves cross, as they should, at the point $\epsilon(k_F) = E/A$. The depth of the potential for $k = 0$ is very different in the two cases, about twice as large for a velocity dependent force than for a density dependent one. The slope for $k = k_F$ which is directly related to the effective mass is also much larger for the velocity dependent force: $m^*/m = 0.38$ for the velocity dependent force instead of 1 for the density dependent one. Finite range forces give a deep potential well and a small effective mass (see the table 2).

2.3.2. More realistic forces

In this section, we present a selection of the effective interactions we have used in our self-consistent calculations. These forces have been chosen because on one hand they allow one to reproduce accurately the ground state properties of nuclei while on the other hand they yield compression moduli in nuclear matter ranging from 190 to 365 MeV. Our choice has also been dictated by practical considerations for our numerical calculations, but there exists many other interactions which could have done as well. We believe that our choice is representative enough so that our main conclusions do not depend upon it.

The interactions we consider are the following:

- (i) The interaction D1 of Gogny [18];
 - (ii) The interaction Sk_a of Köhler [19];
 - (iii) The Skyrme forces S III and S IV of the Orsay group [20];

Table 3
Explicit form of the effective interactions used in the self-consistent calculations and numerical values of their parameters

| Skyrme type interactions | | | | | | | | |
|--------------------------|---------------------------------|-------|---------------------------------|---------------------------------|---|--------|----------|---------------------------------|
| | t_0 (MeV fm ³) | x_0 | t_1 (MeV fm ⁵) | t_2 (MeV fm ⁵) | t_3 (MeV fm ^{3+3\alpha}) | x_3 | α | W_0 (MeV fm ⁵) |
| S III | -1128.75 | 0.45 | 395 | -95 | 14000 | 1 | 1 | 120 |
| S IV | -1205.6 | 0.05 | 765 | 35 | 5000 | 1 | 1 | 150 |
| Sk _a | -1602.78 | -0.02 | 570.88 | -65.70 | 8000 | -0.286 | 1/3 | 125 |

Finite range interactions

| W_1 (MeV) | B_1 (MeV) | H_1 (MeV) | M_1 (MeV) | μ_1 (fm) | W_2 (MeV) | B_2 (MeV) | H_2 (MeV) | M_2 (MeV) | μ_2 (fm) | t_3 (MeV fm $^{3+3\alpha}$) | x_3 | α | W_o (MeV fm 5) |
|----------------|----------------|----------------|----------------|-----------------|----------------|----------------|----------------|----------------|-----------------|-----------------------------------|-------|----------|-------------------------|
| D1 -402.4 | -100 | -496.2 | -23.56 | 0.70 | -21.3 | -11.77 | 37.27 | -68.81 | 1.2 | 1350 | 1 | 1/3 | 115 |
| B1 595.55 | 0 | 0 | -206.05 | 0.70 | -72.21 | 0 | 0 | -68.39 | 1.4 | 0 | 0 | 0 | 115 |

$$V_{12} = \sum_{i=1,2} \exp{-(r/\mu_i)^2} (W_i + B_i P_\sigma - H_i P_\tau - M_i P_\sigma P_\tau) + t_3(1+x_3 P_\sigma) \rho^\alpha(\mathbf{R}) \delta(r) + i W_0 (\sigma_1 + \sigma_2) k' \times \delta(r) k$$

Table 4
Nuclear matter properties calculated with various effective interactions. For the definitions, see text

| | B1 | D1 | Sk _a | S IV | S III |
|---|---------|---------|-----------------|---------|---------|
| E/A | -15.7 | -16.3 | -16.0 | -15.98 | -15.87 |
| k_{Fo} | 1.45 | 1.355 | 1.32 | 1.31 | 1.29 |
| (n_0) | (0.206) | (0.168) | (0.155) | (0.152) | (0.145) |
| K_∞ | 193 | 228 | 263 | 325 | 356 |
| m^*/m | 0.43 | 0.67 | 0.61 | 0.47 | 0.76 |
| ε_F | 101.4 | 56.8 | 59.2 | 75.7 | 45.4 |
| F_o | -0.673 | -0.326 | -0.266 | -0.269 | 0.299 |
| F_1 | -1.650 | -0.990 | -1.178 | -1.594 | -0.708 |
| a_{sym} | 60.6 | 30.7 | 32.8 | 31.2 | 28.2 |
| $L = 3n_o \frac{da_{\text{sym}}}{dn_o}$ | 163 | 18.4 | 75.07 | 63.58 | 10.132 |
| $K_{\text{sym}} = 9n_o^2 d^2 a_{\text{sym}} / dn_o^2$ | -24.8 | -278 | -79.124 | -140.07 | -392.35 |
| $n_o d^2 \mathcal{G} / dn^2$ | 21.4 | 25.3 | 29.2 | 36.1 | 39.6 |
| $n_o^2 d^2 \mathcal{G} / dn^3$ | 39.6 | 59.4 | 76.6 | 105.6 | 122.2 |

(iv) The interaction B1 of Brink and Boeker [21] to which is added a zero range spin-orbit term.

The form of these interactions is given in table 3 together with the values of the parameters. The interaction B1 is a finite range interaction which saturates with the exchange terms. The interaction D1 contains also a finite range part but it saturates mainly through its density dependent part which is zero range. The other forces are essentially zero range and saturate with a mixture of velocity and density dependence.

Nuclear matter properties derived with these interactions are listed in table 4. In all cases the binding energy per nucleon is very close to 16 MeV. One notices a regular decrease of the saturation Fermi momentum k_{F0} with increasing compression modulus K_∞ . It was noticed in the ref. [22] that this apparent relation between K_∞ and k_{F0} applies to a wider class of effective interactions than those selected here. This is illustrated by the fig. 4 from which one sees that the effective forces which yield a given Fermi momentum k_F yield compression moduli differing by at most 50 MeV. This, of course, is

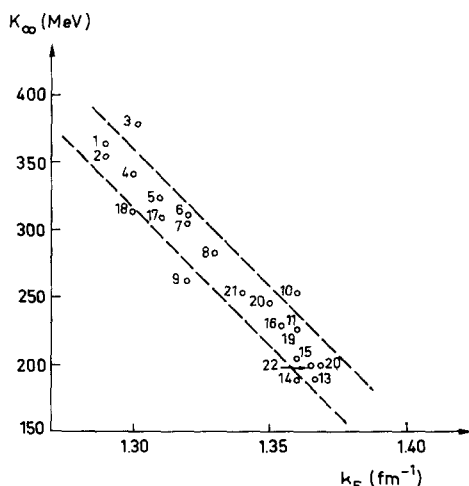


Fig. 4. Nuclear matter compression modulus K_∞ versus the saturation Fermi momentum k_F for various effective interactions. The dashed lines are given to guide the eye and delineate a region where most of the interactions are found. The references corresponding to each effective interaction can be found in [22].

not an absolute law, B1 being a particular exception. But it reveals some general trend in the properties of the effective interactions. For a given density dependent interaction, one can understand why K_∞ decreases if k_F increases: indeed K_∞ is directly related to the strength of the density dependence which is the repulsive part of the force one generally decreases in order to increase the saturation density. This effect is visible on the Skyrme forces S III and S IV: when k_F increases t_3 decreases (see the table 3). The correlations observed for various effective interactions of different forms are induced by the fit of the parameters to properties of nuclei, in particular the radii. For a given k_F the relation between K_∞ and the nuclear radii is the resultant of two opposite effects. Indeed K_∞ determines the magnitude of the compression or dilatation of the nucleus due to the combined effects of the surface tension, and the Coulomb repulsion and the diffuseness of the nuclear surface. The value of the r.m.s. radius $\langle r^2 \rangle / A$ depends on both quantities, as can be seen from the following formula:

$$\langle r^2 \rangle / A \approx \frac{3}{5} R_o^2 + \pi^2 a^2, \quad (2.32)$$

where we have assumed a Fermi shape $(1 + \exp\{(r - R_o)/a\})^{-1}$ for the density distribution. R_o is related to the central density n_o by: $4\pi n_o R_o^3 = 3A$. A small value of K_∞ favors large changes in R_o . On the other hand, a , the diffuseness of the surface, becomes larger for small K_∞ (see section 5.2) and this tends to increase the r.m.s. radius. It happens that in most cases the effect of the diffuseness dominates so that for a given k_F , the radii increase when K_∞ decrease. Taking into account that for a given K_∞ , the radii decrease when k_F increases, this explains the fig. 4 where all the forces which have been quoted yield almost the same radii, except however B1 which gives too small radii in ^{208}Pb .

The variation of K_∞ from one force to the other is easily understood from the discussion of the preceding section. The decrease in K_∞ from S IV to SK_a is mainly due to the decrease in the power of the density (1 for S IV, 1/3 for SK_a). The decrease of K_∞ between SK_a and D1 is due to the finite range of D1 and B1 gives a lower K_∞ because it has no density dependence at all. It is also important to notice that the effective mass varies quite a lot from one force to another, but this variation is not correlated with that of K_∞ except for the two Skyrme forces S III and S IV which belong to the same family.

The other quantities of the table 4 are given for completeness.[†] They are used at different times of the discussion.

We present in the table 5 some ground state properties of nuclei obtained with the various interactions. The experimental binding energies are reproduced equally well by the various interactions (except B1 which is not really suited for heavy nuclei). There are slight discrepancies between the different forces concerning the radii which can be traced back to the variation of k_F from one force to another. These variations in k_F induce variations in the bulk density, as can be seen in fig. 5a, where the protons distributions calculated with three different forces are shown. One could be tempted to relate the amplitude of the oscillations of the density to the nuclear compressibility. However the variation of the amplitude from one force to another is too small to be significant. And anyway experimental analysis of high energy electron scattering do not show up these oscillations. These oscillations are actually significantly reduced by the inclusion of the correlations induced by the collective modes [23, 24] (see fig. 5b).

The single particle properties are quite important for the discussion of the collective excitations. In particular the single particle energies appear explicitly in the calculation of the energies of the collective modes. They are displayed in the fig. 6 for the nucleus ^{208}Pb and three different forces. The exact position of a given level depends on many factors, an important one being the strength of the spin orbit

[†] I am grateful to M. Farine and M. Pearson for the calculation of K_{sym} with finite range forces.

Table 5

E/A is the binding energy per nucleon and r_c is the charge radius. The references for the experimental values can be found in ref. [22]

| Nucleus | Force | E/A (MeV) | E/A (exp) (MeV) | r_c (fm) | r_c (exp) (fm) |
|-------------------|-----------------|----------------|----------------------|---------------|---------------------|
| ^{16}O | B1 | -6.28 | -7.98 | 2.76 | 2.73 |
| | D1 | -8.19 | | 2.76 | |
| | Sk _a | -7.97 | | 2.78 | |
| | S IV | -8.02 | | 2.74 | |
| | S III | -8.00 | | 2.75 | |
| ^{40}Ca | B1 | -6.61 | -8.55 | 3.47 | 3.49 |
| | D1 | -8.67 | | 3.47 | |
| | Sk _a | -8.54 | | 3.50 | |
| | S IV | -8.52 | | 3.48 | |
| | S III | -8.53 | | 3.50 | |
| ^{90}Zr | B1 | -6.64 | -8.71 | 4.21 | 4.27 |
| | D1 | -8.75 | | 4.26 | |
| | Sk _a | -8.64 | | 4.30 | |
| | S IV | -8.62 | | 4.30 | |
| | S III | -8.64 | | 4.33 | |
| ^{208}Pb | B1 | -5.73 | -7.87 | 5.36 | 5.50 |
| | D1 | -7.90 | | 5.46 | |
| | Sk _a | -7.80 | | 5.53 | |
| | S IV | -7.80 | | 5.53 | |
| | S III | -7.80 | | 5.59 | |

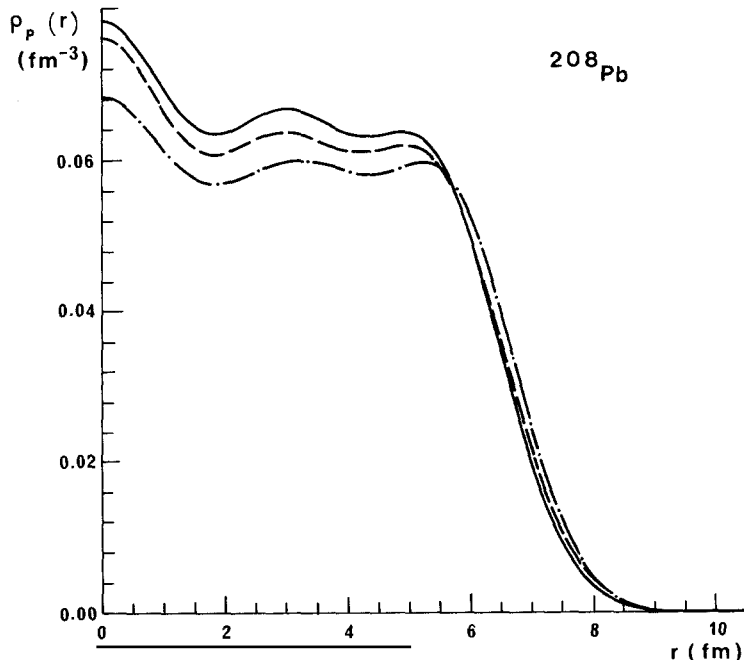


Fig. 5a. Protons densities in ^{208}Pb calculated within the Hartree-Fock approximation with the forces D1 (—), S III (---) and S IV (—·—).

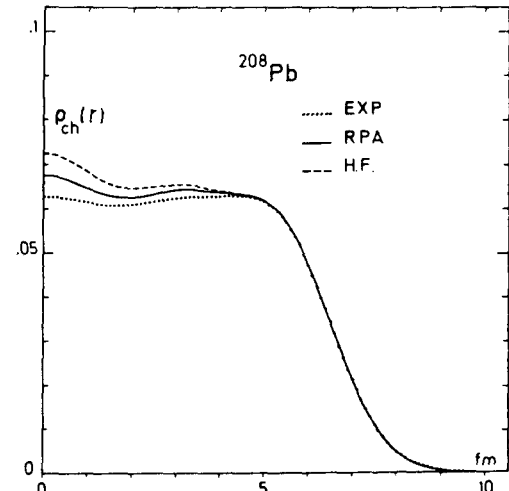


Fig. 5b. Charge density of ^{208}Pb , calculated with the interaction D1 with inclusion of the RPA ground state correlations (—), and experiment (···) [24]. I acknowledge J. Dechargé and D. Gogny for communication of this figure.

potential. But fig. 6a suggests that forces which yield a small effective mass in nuclear matter yield a spread single particle spectrum. This is clearly seen in fig. 6b where we have plotted as a function of m^* an average energy gap $\Delta\epsilon$ given by the formula:

$$\Delta\epsilon = \frac{\sum_p (2j_p + 1)\epsilon_p}{\sum_p (2j_p + 1)} - \frac{\sum_h (2j_h + 1)\epsilon_h}{\sum_h (2j_h + 1)}, \quad (2.33)$$

where the sums run over the single particle proton states shown in fig. 6 in the case of ^{208}Pb (plus the state $3 p_{1/2}$). For ^{40}Ca the sums run over the states belonging to the f-p shell and the s-d shell. p-states are above the Fermi level and h-states below. It is interesting to note that experimental data favor an effective mass close to unity in heavy nuclei but are compatible with a smaller value in light nuclei such as ^{40}Ca . A similar conclusion is obtained from the analysis of the giant quadrupole resonance in

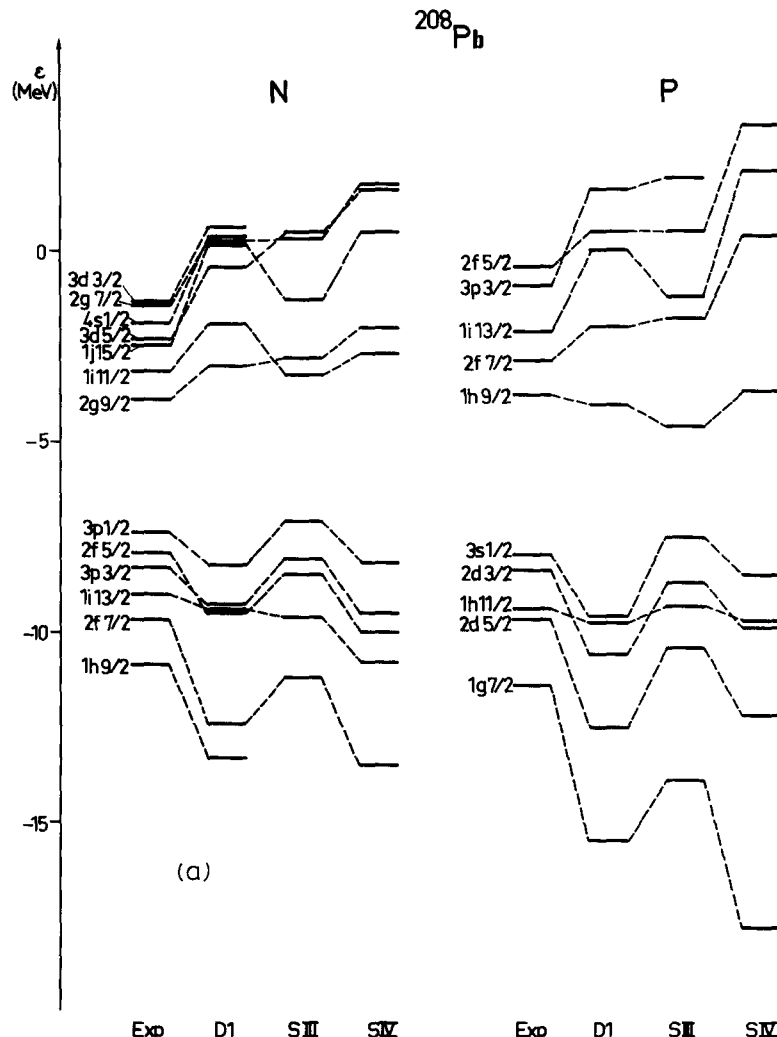


Fig. 6a. Single particle spectrum in ^{208}Pb , calculated with the forces D1, S III and S IV, and compared with the experimental one.

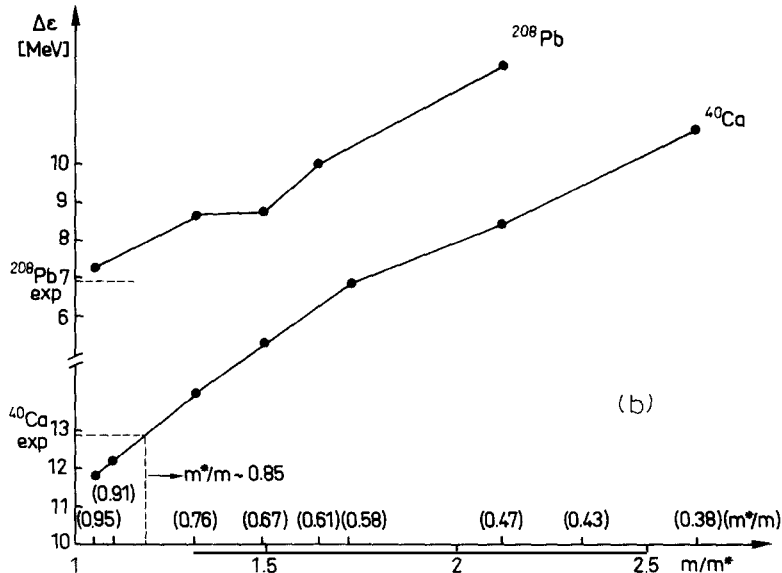


Fig. 6b. Average energy gap (eq. (2.33)) in ^{40}Ca and ^{208}Pb as a function of m^* .

section 7.3. It is worth recalling that the density dependence of the effective interaction is quite useful in order to get a more compressed single particle spectrum. Indeed a repulsive density dependent component in the effective interaction diminishes the role in the saturation of the velocity dependent components and of the exchange term which both tend to decrease the effective mass (see also the discussion in section 7.2).

2.4. Results from nuclear matter theory

The aim of nuclear matter theory is to calculate the properties of nuclear matter starting from a nucleon-nucleon potential which fits the phase shifts of the nucleon-nucleon scattering and the properties of the deuteron [11]. Unfortunately such a program has not succeeded yet. As a rule, the calculations based upon the Brueckner theory predict either too low binding or too large density at saturation. The compression modulus obtained from these calculations is in general of the order of 100 to 150 MeV. The variational calculations which have been recently so successful in dealing with boson systems are still confronted with technical difficulties for fermion systems and are not yet in a position of predicting trustable values for nuclear matter properties [25]. However, direct calculations of Landau parameters, starting from a Brueckner G -matrix seem to be more successful. These calculations are based on the fact that the particle-hole interaction in nuclear matter can be divided into two parts [26]. The first one, called the direct term, is approximated by the G -matrix (plus actually other terms which can be calculated from the G -matrix). The second term is the interaction induced by the exchange of a collective excitation between the particle and the hole. This induced interaction is an important contribution to the particle-hole interaction. It is in general repulsive in the $S = 0$, $T = 0$ channel, and it increases appreciably the value of F_0 . Furthermore, calculations involving the induced interaction turn out to be rather insensitive to the original input (i.e. to the approximation used for the direct term). Such calculations have been performed by Sjöberg [27] and give the following results:

$$F_1 = -0.69, \quad m^* \sim 0.77 m, \quad K_\infty = 184 \text{ MeV}, \quad F_0 = -0.373.$$

This calculation has been performed for a value of $k_F = 1.35 \text{ fm}^{-1}$ which is the saturation density for the potential used. The corresponding binding energy is only -9.25 MeV .

For completeness let us mention an estimate of the density dependence of the symmetry energy coefficient from Brueckner theory. According to ref. [28], one has:

$$a_{\text{sym}}(n) = 32(n/n_o)^{2/3}$$

which implies

$$L = 3 n_o \frac{da_{\text{sym}}}{dn} \Big|_{n_o} = 64 \text{ MeV}$$

which has to be compared with the phenomenological values of the section (2.2) and the values obtained with phenomenological forces (table 4).

3. Theory of collective excitations

As we have seen in the preceding section, a study of the static properties of nuclei does not allow a very accurate determination of the compression modulus of nuclear matter. This quantity can be expected to be related to the restoring force associated with collective compression modes in both infinite and finite systems. It is therefore of great interest to study under which conditions such collective compression modes exist, i.e. are sufficiently undamped to allow their detection, and to see to which extent their frequencies are determined by the nuclear compressibility.

In this section, we review the formal framework in which we wish to discuss these questions. The same theory of collective excitations is used in nuclear matter and in finite nuclei, which makes transparent the similarities and the differences between both systems. A comparison between various approaches currently used in actual calculation is presented at the end.

3.1. Basic concepts

We shall assume that for the excitations we are interested in, the energy can be written as a functional of the one-body density matrix ρ defined by:

$$\rho_{\alpha\beta} = \langle \Phi | a_\beta^+ a_\alpha | \Phi \rangle \quad (3.1)$$

where $|\Phi\rangle$, the state of the system is supposed to be an independent particle state, which implies that ρ satisfies the equation:

$$\rho^2 = \rho. \quad (3.2)$$

The functional $E[\rho]$ contains all the information which is needed to calculate the collective excitations [29, 30, 17]. First $E[\rho]$ has a minimum for $\rho = \rho_o$ corresponding to the ground state of the system. Expanding $E[\rho]$ around ρ_o one gets:

$$E[\rho] = E[\rho_o] + \sum_{\alpha\beta} \frac{\delta E}{\delta \rho_{\alpha\beta}} \delta \rho_{\alpha\beta} + \frac{1}{2} \sum_{\alpha\beta\gamma\delta} \frac{\delta^2 E}{\delta \rho_{\alpha\beta} \delta \rho_{\gamma\delta}} \delta \rho_{\alpha\beta} \delta \rho_{\gamma\delta}. \quad (3.3)$$

The functional derivatives of $E[\rho]$ have the following physical interpretation. The first derivative:

$$\delta E / \delta \rho_{\alpha\beta} = h_{\beta\alpha} \quad (3.4)$$

is the single particle Hamiltonian. The second derivative:

$$\frac{\delta^2 E}{\delta \rho_{\alpha\beta} \delta \rho_{\gamma\delta}} = \frac{\delta h_{\beta\alpha}}{\delta \rho_{\gamma\delta}} \quad (3.5)$$

which describes how the single particle potential reacts to a density matrix fluctuation is the particle-hole interaction.

The equilibrium density matrix ρ_o is solution of the Hartree-Fock equations:

$$[h[\rho_o], \rho_o] = 0. \quad (3.6)$$

We call hole states, the single particle states which are occupied in the ground state, and particle states the others. The condition (3.2) written to lowest order in $\delta\rho = \rho - \rho_o$ implies that only the particle-hole matrix elements of $\delta\rho$ appear in the expansion (3.3). Thus (3.3) can be written as:

$$E[\rho] = E[\rho_o] + \sum_{ph, p'h'} \{ A_{ph, p'h'} \delta\rho_{ph}^* \delta\rho_{p'h'} + \frac{1}{2} B_{ph, p'h'} \delta\rho_{ph}^* \delta\rho_{p'h'}^* + \frac{1}{2} B_{ph, p'h'}^* \delta\rho_{ph} \delta\rho_{p'h'} \} \quad (3.7)$$

where the matrices A and B are given by:

$$A_{ph, p'h'} = (\epsilon_p - \epsilon_h) \delta_{pp'} \delta_{hh'} + \frac{\delta^2 E}{\delta \rho_{hp} \delta \rho_{p'h'}} \quad (3.8)$$

$$B_{ph, p'h'} = \frac{\delta^2 E}{\delta \rho_{hp} \delta \rho_{h'p'}}$$

ϵ_p and ϵ_h are respectively the particles and holes energies.

In order to get equations of motion for the collective modes, one considers the energy (3.7) as the Hamiltonian governing the time evolution of the density matrix fluctuations $\delta\rho_{ph}$, considered as complex classical coordinates. Thus the equations of motion are:

$$i \delta \dot{\rho}_{ph} = \partial E / \partial (\delta \rho_{ph}^*). \quad (3.9)$$

The equation of motion in the presence of an external time dependent potential $U(t) = U(\omega) e^{-i\omega t}$ is trivially obtained from (3.9) by replacing E by

$$\hat{E} = E + \text{Tr } \rho U. \quad (3.10)$$

Written in the space of the particle-hole configurations, the equation (3.9) (with an external field) takes the following form:

$$\begin{pmatrix} A - \hbar\omega - i\eta & B \\ B^* & A^* + \hbar\omega + i\eta \end{pmatrix} \begin{pmatrix} \delta\rho_{ph}(\omega) \\ \delta\rho_{hp}(\omega) \end{pmatrix} = - \begin{pmatrix} U_{ph}(\omega) \\ U_{hp}(\omega) \end{pmatrix}. \quad (3.11)$$

For $U=0$, the equations (3.11) reduce to the well known RPA eigenvalue problem [31].

When discussing nuclear matter properties, it is convenient to use the Wigner transform of $\delta\rho$ [32], which we note $\delta n_{\mathbf{k}}(\mathbf{R})$:

$$\delta n_{\mathbf{k}}(\mathbf{R}) = \int d^3r \exp\{-i\mathbf{k} \cdot \mathbf{r}\} \delta\rho\left(\mathbf{R} + \frac{\mathbf{r}}{2}, \mathbf{R} - \frac{\mathbf{r}}{2}\right). \quad (3.12)$$

$E[\rho]$ (eq. (3.3)) can be reexpressed in terms of $\delta n_{\mathbf{k}}$:

$$E[\rho] = E[\rho_0] + \int d^3R \left\{ \sum_{\mathbf{k}} (\epsilon_{\mathbf{k}}^0 - \mu) \delta n_{\mathbf{k}}(\mathbf{R}) + \frac{1}{2} \sum_{\mathbf{k}\mathbf{k}'} f(\mathbf{k}, \mathbf{k}', \mathbf{R}) \delta n_{\mathbf{k}}(\mathbf{R}) \delta n_{\mathbf{k}'}(\mathbf{R}) \right\} \quad (3.13)$$

where we have set:

$$\begin{aligned} \sum_{\mathbf{k}} &= 4 \int \frac{d^3k}{(2\pi)^3} \\ \epsilon_{\mathbf{k}}^0 &= h^0(\mathbf{R}, \mathbf{k}) = \left. \frac{\delta E}{\delta n_{\mathbf{k}}(\mathbf{R})} \right|_{\rho_0} \end{aligned} \quad (3.14)$$

and we assume that the particle hole interaction takes the form:

$$\delta h(\mathbf{R}, \mathbf{k})/\delta n_{\mathbf{k}}(\mathbf{R}) = \delta(\mathbf{R} - \mathbf{R}') f(\mathbf{k}, \mathbf{k}', \mathbf{R}). \quad (3.15)$$

In all practical applications, this short range approximation turns out to be sufficient. The chemical potential μ is introduced in the equation (3.13) to ensure particle number conservation. We have retained in (3.13) only that part which does not depend on the spins and isospins, which is the part of relevance in the present discussion. In nuclear matter, due to the translational invariance, all the quantities which appear in (3.13) are independent of \mathbf{R} . The expansion (3.13) is then formally identical to that introduced by Landau to describe liquid ${}^3\text{He}$ [33].

One gets further simplifications when one considers only long wavelength excitations or equivalently particle-hole excitations with momentum $|\mathbf{q}| = |\mathbf{k}_p - \mathbf{k}_h| \ll k_F$, \mathbf{k}_p and \mathbf{k}_h being the momenta of the particle and the hole respectively. Then the equation of motion for $\delta n_{\mathbf{k}}$ can be easily obtained from the equation (3.11). In the limit $q \rightarrow 0$ the momenta \mathbf{k}_p and \mathbf{k}_h become equal in magnitude to the Fermi momentum and the variation of the density matrix $\delta\rho_{ph}$ reduces to the change $\delta n_{\mathbf{k}}$ in the occupation of the single particle state \mathbf{k} . Taking carefully the limit of the equation (3.11) one gets the following equation for $\delta n_{\mathbf{k}}$:

$$(\omega - i\eta + \mathbf{q} \cdot \mathbf{v}_{\mathbf{k}}) \delta n_{\mathbf{k}} + \frac{\partial n_{\mathbf{k}}^0}{\partial \epsilon_{\mathbf{k}}} \mathbf{q} \cdot \mathbf{v}_{\mathbf{k}} \sum_{\mathbf{k}'} f(\mathbf{k}, \mathbf{k}') \delta n_{\mathbf{k}'} = -U \frac{\partial n_{\mathbf{k}}^0}{\partial \epsilon_{\mathbf{k}}} \mathbf{q} \cdot \mathbf{v}_{\mathbf{k}}, \quad (3.16)$$

where $n_{\mathbf{k}}^0$ is the Wigner transform of the ground state density matrix:

$$n_{\mathbf{k}}^0 = \theta(\epsilon_{\mathbf{k}}^0 - \mu). \quad (3.17)$$

The equation (3.16) can be cast into a more convenient form. First one notices that $f(\mathbf{k}, \mathbf{k}')$ is needed

only for $|\mathbf{k}| = |\mathbf{k}'| = k_F$, and is therefore a function only of the angle between \mathbf{k} and \mathbf{k}' . It is then natural to expand $f(\mathbf{k}, \mathbf{k}')$ in Legendre polynomials:

$$f(\mathbf{k}, \mathbf{k}') = \frac{1}{N_o} \sum_l F_l P_l(\hat{\mathbf{k}}, \hat{\mathbf{k}}'), \quad (3.18)$$

where N_o is the density of single particle state at the Fermi surface:

$$N_o = \frac{3}{2} n_o / \epsilon_F \quad (3.19)$$

and F_l are the so-called Landau parameters already encountered in the previous section. Similarly we write:

$$\delta n_{\mathbf{k}} = -\frac{\partial n_k^0}{\partial \epsilon_{\mathbf{k}}} \nu_{\mathbf{k}}, \quad (3.20)$$

$\nu_{\mathbf{k}}$ measures the displacement (in energy units) of the Fermi surface along the direction \mathbf{k} . Again it is a function of the direction of \mathbf{k} only and $\nu_{\mathbf{k}}$ can be expanded in Legendre polynomials:

$$\nu_{\mathbf{k}} = \sum_l \nu_l P_l(\hat{\mathbf{k}} \cdot \hat{\mathbf{q}}). \quad (3.21)$$

Using the equations (3.17–3.21) one can rewrite (3.16) as follows:

$$\sum_l \left[(x - s) + \frac{x}{2l+1} F_l \right] \nu_l P_l(x) = -Ux, \quad (3.22)$$

where $x = \hat{\mathbf{q}} \cdot \hat{\mathbf{k}}$ and $s = \omega/qv_F$.

This equation will be used in section 4.1 when we discuss the zero sound mode in nuclear matter [38].

Finally formula (3.14) enables us to calculate the energy variation associated with a fluctuation δn in the density. We use (3.20) and (3.21) and take into account that only the zeroth harmonic distortion of the Fermi surface ν_o is involved in a static density change. A straightforward calculation yields:

$$\frac{E}{A} = \frac{E_o}{A} + \frac{\epsilon_F}{3} (1 + F_o) \frac{(\delta n)^2}{n_o^2} \quad (3.23)$$

from which the formula (2.14) for the compression modulus follows.

3.2. Linear response functions

The change in the density matrix $\delta\rho_{ik}(\omega)$ produced by an external potential $U(\omega)$ can be written:

$$\delta\rho_{ik}(\omega) = \sum_{lj} R_{ik,lj}(\omega) U_{lj}(\omega) \quad (3.24)$$

where the response function $R(\omega)$ is minus the inverse of the matrix which stands on the left hand side of the equation (3.11). Notice that only the p-h and h-p matrix elements of $\delta\rho$ are given by (3.11) and accordingly (3.24). The other matrix elements are negligible in the linear approximation. It is often

convenient to express the response of the system with the expectation value of the operator U itself:

$$\langle U(\omega) \rangle = \text{Tr } U(\omega) \delta\rho(\omega) = \frac{1}{\hbar} \sum_{N>0} |\langle 0 | U | N \rangle|^2 \left\{ \frac{1}{\omega - \omega_N + i\eta} - \frac{1}{\omega + \omega_N + i\eta} \right\}. \quad (3.25)$$

In (3.25) the sum $\sum_{N>0}$ runs over all the RPA eigenstates N with positive eigenfrequencies ω_N . The poles of $\langle U(\omega) \rangle$ are the excitation energies of the system while the residues in these poles are proportional to the transition probabilities between the ground state and the excited states. In the case of the response to a local scalar field which is proportional to the density operator:

$$U(\omega, q) = U(\omega) \rho_q^+ \quad (3.26)$$

with:

$$\rho_q^+ = \sum_i e^{iq \cdot r_i} = \int e^{iqr} \psi^+(r) \psi(r) d^3r \quad (3.27)$$

one gets:

$$\langle U(\omega, q) \rangle = |U(\omega)|^2 \chi(q, \omega) \quad (3.28)$$

where $\chi(q, \omega)$ is the familiar response function used in the study of infinite systems [1]:

$$\chi(q, \omega) = \frac{1}{\hbar} \sum_{N>0} \left\{ \frac{|\langle 0 | \rho_q | N \rangle|^2}{\omega - \omega_N + i\eta} - \frac{|\langle 0 | \rho_q^+ | N \rangle|^2}{\omega + \omega_N + i\eta} \right\}. \quad (3.29)$$

Particularly important is the imaginary part of $\chi(q, \omega)$ (or more generally $\langle U(\omega) \rangle$), which is directly related to the energy loss in the interaction with the external field U . One has indeed, applying the Fermi golden rule

$$dF/dt = 2\pi\omega |U|^2 S(q, \omega), \quad (3.30)$$

where

$$S(q, \omega) = -\frac{\hbar}{\pi} \text{Im } \chi(q, \omega) = \sum_{N>0} |\langle N | \rho_q^+ | 0 \rangle|^2 \delta(\omega - \omega_N). \quad (3.31)$$

In finite systems, it is often convenient, not to consider $S(q, \omega)$ but its expansion in multipoles. For that purpose one uses:

$$e^{iq \cdot r} = 4\pi \sum_{LM} j_L(qr) Y_{LM}(\hat{k}) Y_{LM}(\hat{r}). \quad (3.32)$$

For small values of q (long wavelength limit: $2\pi/q \gg R$):

$$j_L(qr) \sim \frac{q^l r^l}{(2l+1)!!} \quad (3.33)$$

and only the multipole operators $r^l Y_m^l(\hat{r})$ are relevant. In that case we define strength functions in analogy with (3.31) by:

$$S_L(\omega) = \sum_{N>0} |\langle N | r^L Y^L | 0 \rangle|^2 \delta(\omega - \omega_{N_0}). \quad (3.34)$$

3.3. Sum rules

Important for our discussion, will be the following sum rules defined with the help of the moments of the strength function $S(q, \omega)$ or $S_L(\omega)$:

$$m_k(\rho_q^+) = \int d\omega \omega^k S(q, \omega) \quad (3.35)$$

$$m_k(r^L Y^L) = \int d\omega \omega^k S_L(\omega). \quad (3.36)$$

These moments are helpful to characterize how the oscillator strength is distributed as a function of the excitation energy. Of particular relevance will be the lowest moments m_{-1} , m_o , m_1 , m_2 and m_3 . For example one can define an average excitation energy by

$$\bar{E}_{\text{RPA}} = m_1/m_o. \quad (3.37)$$

We shall also use a similar quantity \bar{E}_{ph} calculated with the moments of the unperturbed strength function. m_2 and m_o can be used to define a mean quadratic spreading of the distribution:

$$\sigma = \sqrt{m_2/m_o - (m_1/m_o)^2}. \quad (3.38)$$

m_1 is the so-called energy-weighted sum-rule. In the case of a local operator U , it does not depend explicitly on the interactions. One has indeed:

$$m_1(U) = \frac{1}{2} \langle [U, [T, U]] \rangle_o = \frac{\hbar^2}{2m} \langle (\nabla U)^2 \rangle_o. \quad (3.39)$$

For example, with the monopole operator $U = \sum_i r_i^2$, one finds:

$$m_1 = \frac{2\hbar^2}{m} \langle r^2 \rangle_o. \quad (3.40a)$$

In nuclear matter, with the operator $\rho_q^+ = \sum_i \exp(i\mathbf{q} \cdot \mathbf{r}_i)$, one has:

$$m_1 = A\hbar q^2/8m. \quad (3.40b)$$

The moment m_{-1} is more sensitive to the interactions; it is directly related to the static polarisability or the compressibility of the system. This can be seen in the following way. In a static external field U ,

the change in the expectation value of U is given by (3.25) (for $\omega = 0$):

$$\langle U \rangle = \langle U \rangle_o - 2\lambda m_{-1} \quad (3.41)$$

where $\langle U \rangle_o = \text{tr } U \rho_o$.

From the stationarity of the total energy $\hat{E} = E + \lambda U$ one gets

$$dE/d\lambda + \lambda d\langle U \rangle/d\lambda = 0, \quad (3.42)$$

i.e.

$$dE/d\langle U \rangle = -\lambda. \quad (3.43)$$

Using (3.41–3.43) one then gets:

$$\frac{d^2E}{d\langle U \rangle^2} = \left[\frac{d^2E}{d\lambda^2} \Big|_{\lambda=0} \right]^{-1} = \frac{1}{2m_{-1}}. \quad (3.44)$$

In the particular case where $U = \sum_{i=1}^A r_i^2$ we define:

$$K_A = \frac{2\langle r^2 \rangle_o^2}{Am_1} = \eta_o^2 \frac{d^2E/A}{d\eta^2} \Big|_{\eta_o} \quad (3.45)$$

where $\eta_o = \langle r^2 \rangle_o / A$. K_A can be considered as an effective compression modulus for the finite nuclei. In nuclear matter one has, for $U = \rho_q^+$:

$$K_\infty = \frac{9}{8} A \hbar/m_{-1}. \quad (3.46)$$

The usefulness of the sum rules appears mainly when a single collective mode dominates the response function. Then the sum rules can be used to calculate the properties of this collective mode; for example its energy can be written:

$$\hbar\omega = \sqrt{m_1/m_{-1}}. \quad (3.47)$$

In a finite system where a single mode saturates the response associated with the operator r^2 , one has:

$$\hbar\omega = \sqrt{\frac{\hbar^2}{m} \frac{AK_A}{\langle r^2 \rangle_o}}. \quad (3.48)$$

In nuclear matter, a single mode which depletes the sum rule associated with the density operator ρ_q^+ , has the frequency:

$$\omega = q \sqrt{\frac{K_\infty}{9m}} = c_1 q. \quad (3.49)$$

The formula (3.47) is of course not unique and many other combinations of moments of the strength function could be used to get the frequency of a mode which exhausts a sum rule. However formula (3.47) has a very simple physical interpretation: it gives the frequency of the collective mode as the ratio between a mass parameter and a restoring force constant which can also be obtained from a hydrodynamical description of the collective mode. If an excitation exhausts the sum rule associated with a local operator U , it is indeed possible to associate to the operator U a velocity field:

$$\mathbf{v}(\mathbf{r}, t) = \dot{\alpha}(t) \nabla U(\mathbf{r}), \quad (3.50)$$

where $\alpha(t)$ is a small time dependent amplitude, and $\dot{\alpha}$ its time derivative. The energy of the system can be written as follows:

$$E = E_0 + \frac{1}{2} B_\alpha \dot{\alpha}^2 + \frac{1}{2} C_\alpha \alpha^2, \quad (3.51)$$

where B_α and C_α are respectively a mass parameter and a restoring force constant. The kinetic energy is given by:

$$\frac{1}{2} B_\alpha \dot{\alpha}^2 = \frac{1}{2} m \dot{\alpha}^2 \int n_0 (\nabla U)^2 d^3 r \quad (3.52)$$

hence the mass parameter B_α :

$$B_\alpha = m \langle (\nabla U)^2 \rangle_0 = \frac{2m^2}{\hbar^2} m_1(U) \quad (3.53)$$

where we have used eq. (3.39). To get the potential energy one uses the continuity equation which gives the density variation in terms of α and U :

$$\delta n = -\alpha \nabla (n_0 \nabla U). \quad (3.54)$$

Then one has:

$$\frac{1}{2} C_\alpha \alpha^2 = \frac{1}{2} \frac{d^2 E}{d \langle U \rangle^2} \left[\int d^3 r U \delta n \right]^2. \quad (3.55)$$

Hence C , using (3.39) and (3.44)

$$C_\alpha = \frac{2m^2}{\hbar^4} \frac{[m_1(U)]^2}{m_{-1}(U)}. \quad (3.56)$$

The frequency $\sqrt{C/B}$ is equal, as it should, to that given by (3.47). It is sometimes useful to have the expression of the energy (3.51) in terms of the expectation value Q of the operator U :

$$Q = \int U \delta n d^3 r = -\alpha \frac{2m}{\hbar^2} m_1(U). \quad (3.57)$$

One has:

$$E = E_o + \frac{1}{2}B_O \dot{Q}^2 + \frac{1}{2}C_O \ddot{Q}^2,$$

where:

$$B_O = \frac{\hbar^2}{2m_1(U)}, \quad C_O = \frac{1}{2M_{-1}(U)}. \quad (3.58)$$

Finally, when studying the monopole vibrations of a nucleus, it is convenient to express the energy in terms of the r.m.s. radius η . Then the mass parameter is equal to the total mass of the nucleus and the restoring force is equal to AK_A/η_o^2 .

The expression (3.45) defines K_A as the restoring force for a collective motion along the trajectory defined by a constrained Hartree-Fock calculation. One could also consider a mode corresponding to a homologous transformation of the coordinates, $r \rightarrow e'r$, under which the density matrix becomes:

$$\rho_\nu = \exp\{-\nu[H, r^2]\} \rho_o \exp\{\nu[H, r^2]\}. \quad (3.59)$$

Then it can be easily shown [34] that:

$$m_3(r^2) = \frac{1}{2} \frac{\partial^2}{\partial \nu^2} E[\rho_\nu] \quad (3.60)$$

from which one can define:

$$K_A = \frac{2}{A} \left(\frac{m}{2\hbar^2} \right)^2 m_3(r^2). \quad (3.61)$$

It is readily seen that the definitions (3.61) and (3.45) coincide when a single mode depletes the sum rule associated with the operator r^2 . When this is not the case, the definition (3.45) yields a smaller K_A than (3.61) [34].

3.4. Comparison between various theories of collective motion

Many theories of collective excitations in nuclei (and other systems) lead to equations of motion which are identical. It is therefore of some relevance here to briefly summarize their main ingredients in order to show which ones are the most appropriate to the problem we are interested in, namely extract for nuclear matter informations from what we know about nuclei. These theories have in common two basic ingredients.

(i) The assumption that elementary excitations are quasiparticle like, which is true in nuclear matter for long wavelength excitations; in nuclei this assumption is supported by the validity of the shell model. In other words one assumes that the correlations between the nucleons do not play an important role in the dynamics of the excitations we consider; they can be approximately accounted for by using an effective interaction acting between uncorrelated particles (or quasiparticles).

(ii) The second ingredient is the small amplitude approximation: one assumes that the departure from equilibrium is small and then linearizes the equations of motion.

The theory we discuss in detail here starts by parametrizing $E[\rho]$ with the help of a phenomenological effective interaction which is supposed to simulate the main effects of the short range correlations between the nucleons. Namely:

$$E[\rho] = \langle \Phi | T + V[\rho] | \Phi \rangle \quad (3.62)$$

$|\Phi\rangle$ being assumed to be a Slater determinant. Then all the quantities which appear in the equations (3.11) are calculated: the single particle energies by solving the Hartree-Fock equations and the particle-hole interaction by using (3.18). Therefore all the parameters of the theory are those of the effective interaction, and the same theory, with the same parameters, gives definite prediction for finite nuclei and nuclear matter.

On the other hand, Migdal, generalizing the Landau theory of Fermi liquid, obtains the RPA equations using the Green functions formalism [35]. In Migdal's theory, the single particle energies are given by the excitation energies of the $A \pm 1$ systems relative to the ground state of the A -system. Therefore, in principle, they can be obtained from experiment. Unfortunately Migdal's theory does not provide a prescription for calculating the single particle wave functions which have to be chosen empirically. The particle-hole interaction is not either given by the theory and has to be adjusted to experiment. Moreover it is density dependent and there is no experimental evidence, as yet, which could decide which is the correct density dependence of the particle hole interaction. This makes difficult the extrapolation to nuclear matter for which one needs the interaction inside the nucleus. This criticism concerning the density dependence of the particle-hole interaction could be applied as well to the self consistent calculations. However in this case the density dependence is that of the effective interaction which can be deduced either from the effective interaction in nuclear matter via a local density approximation, or from constraints obtained in the fit to the static properties of nuclei. Other RPA calculations, which use the experimental single particle energies and an adjustable effective interaction are not either suited to predict properties of nuclear matter. It should be said however that those calculations are expected to be more successful than the self-consistent approaches in predicting the correct energies of the excited states, since they contain much more phenomenological information [37]. And indeed they are; but in the present context, the most important is to have a consistent approach which can be used from nuclei to nuclear matter. It is clear in particular that Migdal's theory cannot be applied to nuclear matter unless one measures in such a system the properties of the single particle excitations and the frequencies of the collective modes in order to adjust the particle-hole interaction in nuclear matter as we do in nuclei.

The same kind of criticism, as far as nuclear matter properties are concerned, could be applied to the Copenhagen approach to the theory of the collective modes [36]. In this approach one parametrizes the variation of the one body potential in the following form

$$\delta V = \kappa \alpha F \quad (3.63)$$

where F is a one body operator characterizing the excited mode, α the amplitude of the density fluctuation ($\alpha = \text{Tr } \delta \rho F$) and κ a coupling constant. Very simple arguments can be used to obtain the strength of the coupling constant in the case of surface mode; e.g. one assumes that the equi-densities and the equi-potential suffer the same deformation in the course of the excitation. The application of

similar arguments for the compression mode requires a delicate (and somewhat ambiguous) separation of δV into a volume part and a surface part, which introduces some inaccuracy in the predictions (see the discussion in section 6.4).

Macroscopic approaches, such as the hydrodynamic models, where the nuclei are considered as small pieces of nuclear matter, might be thought to be more appropriate to our problem. These models, however, give a rather poor description of the nuclear surface. Furthermore, since they do not take properly into account the single particle properties which play such an important role in the collective excitations of a nucleus, they cannot really predict whether or not a collective mode with a given structure can exist in a nucleus. Their usefulness appears mostly when the microscopic calculations do predict the existence of a collective mode which exhausts the sum rule associated with some local operator. Then hydrodynamics concepts become quite useful in analyzing and understanding the results of the microscopic calculations.

Let us finally mention that the generator coordinate method and the time-dependent Hartree-Fock approximation allows to go beyond the small amplitude approximation (see the discussion in section 6.5).

4. Zero sound in nuclear matter and monopole excitation of nuclei

In this section, we shall briefly illustrate with the help of simple analytically soluble models the main characteristics of the collective compression modes in infinite and finite systems. The aim of this discussion is both to provide an explicit application of the formalism developed in the preceding section and to prepare the foregoing presentation of the results. First we study the structure of the collective mode in nuclear matter (zero sound). We show that the relation between the compressibility and the frequency of the mode becomes simple only when the mode nearly exhausts the sum rule. In finite system, the quantization of the single particle motion brings essential new features which are very important for explaining the existence of the collective modes and their properties. These features are studied in the harmonic oscillator model. This model does not provide any relation between the frequency of the collective monopole mode and the compression modulus of nuclear matter. The liquid drop model which we describe at the end of this section provides such a relation which we critically discuss.

4.1. Zero sound in nuclear matter

The equation for the zero sound in nuclear matter can be obtained from eq. (3.22) which can be written:

$$\sum_l \left[\delta_{ll'} + \Omega_{ll'}(s) F_l \frac{\nu_{l'}}{2l'+1} \right] = -\Omega_{l0}(s) U \quad (4.1)$$

where:

$$\Omega_{ll'}(s) = \frac{1}{2} \int_{-1}^{+1} dx P_l(x) \frac{x}{x-s} P_{l'}(x). \quad (4.2)$$

The calculation of the response function $\chi(q, \omega)$ requires the calculation of δn , the density fluctuation,

and therefore of the zeroth harmonic distortion ν_o . This calculation is easy when only one or two Landau parameters are non zero. Let us start by considering that only $F_o \neq 0$ in which case one gets:

$$\nu_o = \frac{-\Omega_{oo}}{1 + F_o \Omega_{oo}} U, \quad \nu_1 = 3s\nu_o, \quad (4.3)$$

and

$$S(q, \omega) = \frac{N_o \hbar}{4 \pi} \frac{2a_s}{[2 + F_o g(s)]^2 + F_o^2 a_s^2} \quad (4.4)$$

where $a_s = s\pi$ if $s < 1$
 $= \eta$ if $s > 1$, η being an infinitesimal positive number

$$g(s) = 2 + s \log \left| \frac{1-s}{1+s} \right|. \quad (4.5)$$

We shall briefly study this form factor in the two domains $s > 1$ and $0 < s < 1$

(i) $0 < s < 1 \quad (-1 < F_o < 0)$

$$S(q, \omega) = \frac{\hbar}{2} N_o \frac{s}{[2 + F_o g(s)]^2 + F_o^2 \pi^2 s^2} \quad (4.6)$$

$S(q, \omega) = 0$ for $s = 0$ and $s = 1$.

If $F_o = 0$, $S(q, \omega)$ is a linear function of s

$$S(q, \omega) = \frac{\hbar N_o}{8} s \quad (0 < s < 1). \quad (4.7)$$

If $F_o < 0$ the denominator in (4.6) modifies the shape of $S(q, \omega)$ in a sensible way, as can be seen on the fig. 7. If F_o is too negative (particle-hole interaction too attractive) then the system becomes unstable.

(ii) $s > 1 \quad F_o > 0$.

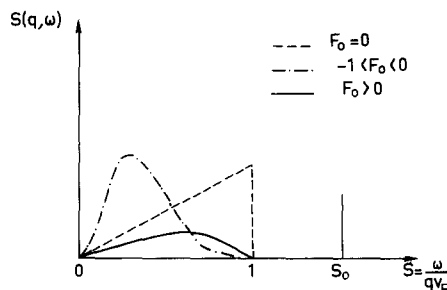


Fig. 7. Qualitative behaviour of the strength function $S(q, \omega)$ in nuclear matter, as a function of the magnitude of the Landau parameter F_o .

The form of $S(q, \omega)$ becomes qualitatively different. Indeed in that case $S(q, \omega)$ has a pole for the value s_o solution of the equation

$$\frac{1}{2}g(s_o) = 1 + \frac{s_o}{2} \log \left| \frac{1-s_o}{1+s_o} \right| = -\frac{1}{F_o}. \quad (4.8)$$

In the vicinity of this pole, $S(q, \omega)$ has the following form

$$S(q, \omega) = \frac{\hbar N_o}{2F_o^2} \frac{\delta(s - s_o)}{|g'(s_o)|}. \quad (4.9)$$

This pole just corresponds to the zero sound mode. It can be obtained analytically from (4.8) in the limiting case $F_o \gg 1$, one has indeed:

$$g(s) \underset{s \gg 1}{\sim} -\frac{2}{3s^2} \quad (4.10)$$

and therefore:

$$s_o \sim \sqrt{F_o/3} \quad \text{for } F_o \gg 1. \quad (4.11)$$

The deformation ν_k of the Fermi surface associated with this mode can be obtained directly from (3.16):

$$\nu_k(s_o) \sim \frac{\hat{k} \cdot \hat{q}}{s_o - \hat{q} \cdot \hat{k}}. \quad (4.12)$$

The expression (4.12) shows that the zero sound wave has in general a very complicated structure (many harmonics ν_l contribute to ν_k). However, when s_o is very large then only the monopole, dipole and quadrupole distortions of the Fermi surface are important.

The poles of $S(q, \omega)$ when both F_o and F_1 are different from zero are given by the solutions of a slightly more complicated equation:

$$\frac{1}{2}s \log \frac{s-1}{s+1} + 1 \left/ \left\{ F_o + \frac{F_1}{1+F_1/3} s^2 \right\} \right. = -1. \quad (4.13)$$

The solution of this equation can again be obtained simply in the case where $s \gg 1$:

$$s_o^2 \sim \frac{F_o}{3} \left(1 + \frac{F_1}{3} \right) \quad (F_o \gg 1). \quad (4.14)$$

Using (2.10) and (2.14) and remembering that $s_o = c_o/v_F$ where c_o is the velocity of the zero sound wave, one can rewrite (4.14) as follows

$$c_o^2 = \frac{6\epsilon_F F_o}{9m} \sim \frac{K_\infty}{9m} \quad (F_o \gg 1). \quad (4.15)$$

Comparing (4.16) and (2.16) one sees that in the limit of a very repulsive particle-hole interaction, the zero sound velocity becomes equal to that of ordinary sound. The simplest way to see the connection between first and zero sound is to consider the two conservation laws of particle density and momentum, which are just the $l = 0$ and $l = 1$ moments of eq. (3.22)

$$s\nu_0 = \frac{1}{3}\nu_1(1 + F_1/3) \quad (4.16)$$

$$s\nu_1 = (1 + F_0)\nu_0 + \frac{2}{5}(1 + F_2/5)\nu_2 + U. \quad (4.17)$$

In the hydrodynamic regime, the collisions between (quasi) particles wash out the high multipole distortions of the Fermi surface and therefore $\nu_2 = 0$.

Then the two equations (4.19) can be solved for s (putting $U = 0$). One finds

$$s^2 = \frac{1}{3}(1 + F_0)(1 + F_1/3) \quad (4.18)$$

from which one easily recovers the first found velocity c_1 , given by (2.16). In the more complicated case of zero sound ν_2 is never negligible compared to ν_0 . It can be calculated by solving the equations (4.1). If F_0 is large enough (and F_2 not too large) then $s_1 - s_0$ is small, the difference between the first and zero sound velocities being approximately given by [38]:

$$\frac{c_0^2 - c_1^2}{c_1^2} = \frac{4}{5} \frac{1 + F_2/5}{1 + F_0}. \quad (4.19)$$

Let us now summarize the main points we wish to extract from this discussion.

(i) The existence of a collective mode in nuclear matter requires a repulsive particle-hole interaction. This is simply connected to the continuous character of the single particle spectrum at the Fermi surface.

(ii) When the particle-hole interaction is strong enough, the velocity of the zero sound becomes equal to that of ordinary sound. One should not however assimilate these two very different modes. The restoring forces have completely distinct origins in the two cases, quasiparticle collisions for the ordinary sound, response of the selfconsistent potential to the density fluctuations for the zero sound. When F_0 is very large, it happens that only the lowest moments of the equations of motion for zero sound are required, and these are just the equation of hydrodynamics which govern ordinary sound.

(iii) If F_0 is large, the zero sound mode exhausts the sum rule, which is a corollary of the preceding statement. This can be verified using the form (4.9) for $S(q, \omega)$ and the asymptotic form (4.10) of $g(s)$. In that case (but this is not true in general) the velocity of the zero sound is directly related to the compressibility of nuclear matter and does not depend explicitly on the value of the effective mass (provided F_1 is not too large).

Calculations of zero sound in nuclear matter have been performed recently [41], using phenomenological effective interactions.

4.2. Giant monopole resonance in the harmonic oscillator model

In finite systems, due to the quantization of the single particle motion, it is relatively easier to create collective modes than in infinite systems. In particular, the existence of a gap in the single

particle spectrum allows the existence of undamped collective mode with attractive particle-hole interactions. In order to get some insight into the nature of the compression modes of a finite system, it is useful to consider a simple model of the nucleus in which, in the ground state, the nucleons fill the levels of a spherical harmonic oscillator. Furthermore, we shall assume that the single particle potential reacts only to the lowest moments of the density fluctuations, i.e. to changes in the radius of the system, taking into account the fact that the number of particles must be conserved. Thus the model is characterized by the following energy functional [89]:

$$E[\rho] = \langle H_o \rangle + \frac{\kappa}{2} [\langle r^2 \rangle - \langle r^2 \rangle_o]^2 \quad (4.20)$$

where

$$H_o = \sum_i \frac{P_i^2}{2m} + \frac{1}{2} m \Omega_o^2 r_i^2 \quad (4.21)$$

and $\langle r^2 \rangle_o$ is the expectation value of $\sum_i r_i^2$ in the ground state. The single particle Hamiltonian is then:

$$h = \frac{P^2}{2m} + \frac{1}{2} m \Omega_o^2 r^2 + \kappa [\langle r^2 \rangle - \langle r^2 \rangle_o] r^2 \quad (4.22)$$

h has the form of a harmonic oscillator Hamiltonian with a variable frequency Ω such that:

$$\Omega^2 = \Omega_o^2 + \frac{2\kappa}{m} [\langle r^2 \rangle - \langle r^2 \rangle_o]. \quad (4.23)$$

Thus if $\kappa < 0$, the “radius” of the potential ($\sim 1/\omega$) increases when $\langle r^2 \rangle$ increases. If $\kappa > 0$ the opposite happens.

It is instructive to consider the response function for the operator r^2 , in the model. Since all the particle-hole configurations which can be excited by r^2 are degenerate, all the strength is concentrated in one single peak located at the frequency $\omega_o = 2\Omega_o$. This is in contrast with the nuclear matter case, where, in absence of particle-hole interaction, the oscillator strength is spread over a finite frequency domain (see fig. 7).

The energy associated with the collective excitation can be written:

$$E = E_o + \frac{1}{2} B \dot{q}^2 + \frac{1}{2} C q^2 \quad (4.24)$$

where $q = \langle r^2 \rangle - \langle r^2 \rangle_o$ and the parameters B and C are given by the formulae (3.58). If $\kappa = 0$ (no particle-hole interaction) the sum rules are easily evaluated and one finds:

$$C_o = \frac{1}{2m_{-1}(r^2)} = \frac{m \Omega_o^2}{\langle r^2 \rangle_o} \quad (4.25)$$

$$B_o = \frac{\hbar^2}{2m_1(r^2)} = \frac{m}{4\langle r^2 \rangle_o}$$

When the particle-hole interaction is turned on, the response function remains dominated by a single collective mode. Now the particle-hole interaction cannot change the sum rule $m_1(r^2)$ and therefore does not affect the mass parameter. It only increases the restoring force parameter C_o by an amount κ , as is obvious from the formula (4.20). Therefore the parameters B and C which enters the expression (4.24) are:

$$B = B_o, \quad C = C_o + \kappa \quad (4.26)$$

and the frequency of the collective mode becomes:

$$\omega = \omega_o \sqrt{1 + \kappa/C_o}. \quad (4.27)$$

The collective mode we are considering can be described in terms of a local velocity field of the type (3.50) with $U(r) = r^2$. It follows that in this mode the transition density is:

$$\delta n(r, t) = -\alpha(t)(3n_o(r) + r dn_o(r)/dr) \quad (4.28)$$

where $n_o(r)$ is the ground state density. This transition density is obtained by displacing each equi-density by an amount $\alpha(t)r$, r being the distance of the equi-density to the center of the nucleus, and normalizing to keep constant the number of particles. The transition potential is obtained from (4.22):

$$\delta h(r, t) = \alpha(t)\kappa \langle r^2 \rangle_o r^2. \quad (4.29a)$$

It has the simple form of a time dependent harmonic oscillator Hamiltonian. Actually, in the small amplitude approximation where only the particle-hole matrix elements of h are taken into account, the transition potential is proportional to the transition density†:

$$\delta h(r, t) \approx \frac{\kappa}{C_o} \delta n(r, t). \quad (4.29b)$$

One can give another expression for the frequency of the collective mode in terms of the effective compression modulus K_A defined by (3.45). A simple calculation yields:

$$K_A = 4m\Omega_o^2 \frac{\langle r^2 \rangle_o}{A} \left(1 + \frac{\kappa}{C_o}\right) = 4 \frac{\langle r^2 \rangle_o C}{A}. \quad (4.30)$$

Combining (4.27) and (4.30) one recovers immediately the formula (3.48).

It is interesting to compare the formula (4.30) with the corresponding one for nuclear matter (eq. (2.14)): $K_\infty = 6\varepsilon_F(1 + F_o)$. If one neglects the particle-hole interaction ($\kappa = 0, F_o = 0$) one gets $K_\infty = 228$ MeV and $K_A = 133$ MeV (using $\hbar\Omega_o = 40A^{-1/3}$, $\langle r^2 \rangle_o/A = \frac{3}{5}r_o^2 A^{2/3}$ and $r_o = 1.2$ fm). Therefore in the

†Note however that $\delta h(r, t)$ given by (4.29b) is the diagonal part of a *non-local* operator which has the same particle-hole matrix elements as the *local* operator given by (4.29a).

absence of particle-hole interaction, the effective compression modulus K_A which is here independent of A appears to be much lower than that of nuclear matter. The connection between K_A and K will be discussed in greater detail later but we can at this stage make a remark. If κ and F_0 are set equal to zero, K_A and K_∞ can be expressed in terms of the average kinetic energy per particle:

$$K_A = 8\langle T \rangle/A, \quad K_\infty = 10\langle T \rangle/A. \quad (4.31)$$

The large difference between K_A and K_∞ comes partly from the difference in the evaluations of $\langle T \rangle/A$ in the oscillator model (~ 17 MeV) and in nuclear matter (~ 23 MeV), and partly from the different numerical constants in (4.31).

The strength of the particle-hole interaction, κ , has to be adjusted to experiment and we cannot say much about it. However more detailed calculations and experimental data show that the observed frequency is slightly lower than the unperturbed one, which implies $\kappa < 0$. κ is bounded by the value $\kappa = -C_0$ for which the effective compression modulus vanishes.

Finally let us use this model to give an order of magnitude of the zero point amplitude a associated with the time evolution of $q = \langle r^2 \rangle - \langle r^2 \rangle_0$:

$$a = \sqrt{\hbar/2B\omega}. \quad (4.32)$$

Neglecting the particle-hole interaction, one gets easily:

$$a = \langle r^2 \rangle_0 \sqrt{\frac{\hbar}{m\Omega_0 \langle r^2 \rangle_0}} \sim 1.1 \langle r^2 \rangle_0 A^{-2/3} \quad (4.33)$$

i.e. $a/\langle r^2 \rangle_0 \sim 0.1$ for ^{40}Ca and ~ 0.03 for ^{208}Pb . These numbers give an idea of the accuracy of the small amplitude approximation.

4.3. Giant monopole resonance in the liquid drop model [36, 39]

In this model, the state of the nucleus at a given time is entirely characterized by the values of the local current and density which are determined by the linearized equations of hydrodynamics†:

$$\partial \delta n / \partial t + \nabla(\mathbf{n}_0 \cdot \mathbf{v}) = 0 \quad (4.34)$$

$$m \mathbf{n}_0 \cdot \partial \mathbf{v} / \partial t + \nabla \delta P = 0 \quad (4.35)$$

where $\mathbf{n}_0(\mathbf{r})$ is the ground state density, $\mathbf{v}(\mathbf{r}, t)$ is the velocity field and $\delta n(\mathbf{r}, t)$ is the local density fluctuation:

$$\delta n(\mathbf{r}, t) = n(\mathbf{r}, t) - \mathbf{n}_0(\mathbf{r}). \quad (4.36)$$

†We assume that the quadrupole distortion of the momentum distribution does not play an important role in the breathing mode. In this case the equations for zero sound reduces to the equation for ordinary sound, i.e. hydrodynamical equations.

The density $n(\mathbf{r}, t)$ is assumed to be of the form:

$$n(\mathbf{r}, t) = \tilde{n}(\mathbf{r}, t) \theta(r - R(t)), \quad (4.37)$$

where \tilde{n} is a regular function of r . In equilibrium, $\tilde{n}(r) = n_o$ and $R = R_o$. It follows that to lowest order in $R = R - R_o$, δn can be written:

$$\delta n(\mathbf{r}, t) = \delta \tilde{n}(\mathbf{r}, t) \theta(r - R_o) + n_o(R - R_o) \delta(r - R_o), \quad (4.38)$$

where $\delta \tilde{n}(r, t) = \tilde{n}(r, t) - n_o$. The conservation of the number of particles implies the following relation between δR and $\delta \tilde{n}$:

$$\delta R = R - R_o = -\frac{1}{n_o R_o^2} \int_0^{R_o} \delta \tilde{n} r^2 dr. \quad (4.39)$$

The variation of the pressure inside the nucleus ($r < R$) is assumed to derive from a local energy density. Thus:

$$\delta P = n_o \left. \frac{d^2 \mathcal{E}}{dn^2} \right|_{n_o} \delta \tilde{n} = mc_1^2(n_o) \delta \tilde{n}. \quad (4.40)$$

The equations (4.34) and (4.35) can be combined into a single wave equation:

$$\frac{\partial^2}{\partial t^2} (\delta \tilde{n}) - \nabla^2 (mc_1^2 \delta \tilde{n}) = 0. \quad (4.41)$$

The solutions of (4.41) with spherical symmetry and finite at the origin are of the form:

$$\delta \tilde{n}(\mathbf{r}, t) = \alpha(t) n_o j_o(qr), \quad (4.42)$$

where $\alpha(t)$ is a dimensionless amplitude, harmonic function of time with the frequency:

$$\omega = c_1 q. \quad (4.43)$$

To determine completely the solution, one has to specify the boundary conditions, i.e. the value of $\delta \tilde{n}(R)$. This is obtained by writing that the compressional pressure at the surface is compensated by the pressure generated by the curvature of the surface (see eq. (2.18); we retain here, to simplify the discussion, only the effect of the surface tension):

$$P(R) = 2\sigma/R. \quad (4.44)$$

$P(R)$ can be obtained from the approximate equation of state (2.19), and (4.44) becomes:

$$\frac{\tilde{n}(R) - n_\infty}{\chi n_\infty} = \frac{2\sigma}{R}. \quad (4.45)$$

Expanding this condition is lowest order in R and taking into account the equilibrium condition, one gets:

$$\delta\tilde{n}(R) = -\frac{2\sigma\chi n_\infty}{R_o^2} \delta R. \quad (4.46)$$

Since the difference between $\delta\tilde{n}(R)$ and $\delta\tilde{n}(R_o)$ is of second order in δR , one can replace $\delta\tilde{n}(R)$ by $\delta\tilde{n}(R_o)$ in the left hand side of this equation. Using the equation (4.39) to eliminate δR and the explicit form (4.42) of the solution, the boundary condition can finally be written:

$$j_o(qR_o) = \frac{2\sigma\chi j_1(qR_o)}{R_o q R_o}. \quad (4.47)$$

Now, typical values of the parameters appearing in the equation (4.49) are $\sigma \sim 1.237 \text{ MeV fm}^{-2}$, $\chi \sim 0.258 \text{ MeV}^{-1} \text{ fm}^3$, $R_o \sim 1.13 A^{-1/3}$ so that $2\sigma\chi/R_o \sim 0.565 A^{-1/3}$. For large enough nuclei this is a small quantity and to a good approximation the wave numbers q_ν are determined by the equation:

$$\sin q_\nu R_o \sim \frac{2\sigma\chi}{\nu\pi R_o} \quad (\nu \geq 1) \quad (4.48)$$

i.e.

$$q_\nu \sim \frac{\nu\pi}{R_o} \left(1 - \frac{2\sigma\chi}{\nu^2\pi^2 R_o} \right). \quad (4.49)$$

Thus, the frequency of the lowest mode ($\nu = 1$) is:

$$\omega_1 = \sqrt{\frac{\pi^2}{15} \frac{AK_\infty}{m\langle r^2 \rangle_o}} \left(1 - \frac{12a_{\text{surf}} A^{-1/3}}{\kappa_\infty \pi^2} \right). \quad (4.50)$$

To obtain this formula, one has assumed that the speed of sound c_1 is the same in the nucleus as in nuclear matter. In fact this is correct only up to terms in $A^{-1/3}$ as can be seen from the following expansion (obtained from the definition (4.40) of c_1^2):

$$c_1^2(n_o) = c_1^2(n_\infty) + \frac{2\sigma}{R_o n_o} + \frac{2\sigma\chi}{R_o} n_\infty^2 \frac{d^3\mathcal{E}}{dn^3} + \dots \quad (4.51)$$

A proper inclusion of these terms would modify the term in $A^{-1/3}$ in (4.53). These terms actually disappear if one constructs the energy density from the equation of state (2.19), through the formula:

$$\frac{\mathcal{E}(n)}{n} = \int_{n_\infty}^n P(n) \frac{dn}{n^2}. \quad (4.52)$$

We shall not do that here but simply remark that the terms in $A^{-1/3}$ represent in this model a very small correction, of the order of $0.1A^{-1/3}$.

The transition density of the lowest mode can be obtained from (4.38), using $\delta R = -\alpha R_o/\pi^2$:

$$\delta n(r, t) = \alpha(t) \left[n_o j_o(qr) \theta(r - R_o) - \frac{n_o R_o}{\pi} \delta(r - R_o) \right]. \quad (4.53)$$

Using the continuity equation (4.34) the velocity potential Φ is easily found to be:

$$\Phi = -\frac{\dot{\alpha}}{q^2} j_o(qr). \quad (4.54)$$

The expressions for the mass parameter B_α and the restoring force C_α entering the expression (3.51) of the energy are easily found by integrating the equations of motions (4.35) after multiplication by $\mathbf{u} = \nabla\Phi$. One gets:

$$\ddot{\alpha} \int nm_o u^2 - \alpha \int m\mathbf{u} \cdot \nabla c_1^2 \delta\tilde{n} = 0 \quad (4.55)$$

from which the identification of B_α and C_α follows (within a normalization factor):

$$B_\alpha = \int mn_o u^2 = \frac{3AmR_o^2}{2\pi^4} \left(1 + \frac{18a_{\text{surf}} A^{-1/3}}{K_\infty \pi^2} \right) \quad (4.56)$$

$$\begin{aligned} C_\alpha &= \int n_o c_1^2 (\nabla \cdot \mathbf{u})^2 + 4\pi R_o^2 u(R_o) mc_1^2 \delta\tilde{n}(R_o) \\ &= \int n_o c_1^2 (\nabla \cdot \mathbf{u})^2 - 2a_{\text{surf}} A^{2/3} \frac{u(R_o)}{R_o^2} \delta R \\ &= \frac{AK_\infty}{6\pi^2} \left(1 + \frac{6a_{\text{surf}}}{K_\infty \pi^2} A^{-1/3} \right). \end{aligned} \quad (4.57)$$

One can relate $\alpha(t)$ to the expectation value η^2 of r^2 in the density (4.53). One has indeed:

$$\eta^2 - \eta_o^2 = \frac{1}{A} (\langle r^2 \rangle - \langle r^2 \rangle_o) = -\frac{18R_o^2}{\pi^4} \alpha(t). \quad (4.58)$$

Then from (4.57) one gets (neglecting $A^{-1/3}$ terms):

$$K_A = \eta_o^2 \frac{d^2(E/A)}{d\eta^2} \Big|_{\eta_o} = \frac{\pi^6}{1350} K_\infty. \quad (4.59)$$

Again it is worth-emphasizing the ambiguity in the definition of K_A . Had one defined K_A as $R_o^2 (d^2(E/A)/dR^2)|_{R_o}$, one would have obtained $K_A = (\pi^2/6)K$, which is larger than K_∞ while K_A given by (4.59) is smaller than K_∞ . The relative values of K_A obtained by the two definitions can be qualitatively understood from the fig. 8 where we have drawn the transition densities normalized to a given $\langle r^2 \rangle$ or a given R . It is seen that the compression of the matter inside the nucleus is larger if one constrains R rather than $\langle r^2 \rangle$.

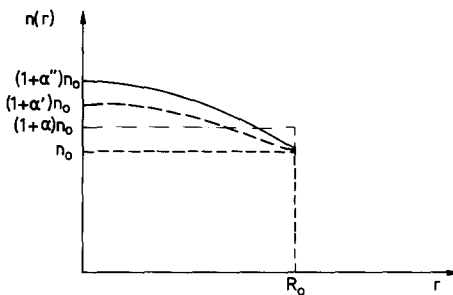


Fig. 8. Variations of the density in the liquid drop model; ---, ground state density n_0 ; — — —, density obtained by performing a scale transformation; ——, density obtained by adding to n_0 the transition density (4.53) with an amplitude α' normalized so as to get the same r.m.s. radius $\langle r^2 \rangle$ as in the scaled density ($\alpha' = (\pi^4/45)\alpha$); ——, same as before but α'' is normalized so as to get the same change in the radius R as in the scaled density ($\alpha'' = (\pi^2/3)\alpha$).

It is interesting to compare these results with those obtained by using the approximate velocity potential:

$$\Phi = \dot{\alpha} r^2/6. \quad (4.60)$$

In this case the transition density is:

$$\delta n(r) = n_0 \theta(r - R_0) - n_0 \frac{R_0}{3} \delta(r - R_0). \quad (4.61)$$

The relation between α and η in this case is:

$$\eta^2 - \eta_0^2 = -\frac{2}{5} R_0^2 \alpha \quad (4.62)$$

and

$$C_\alpha = AK_\infty/9. \quad (4.63)$$

Thus, for this special mode, one has:

$$K_A = \eta^2 \frac{d^2(E/A)}{d\eta^2} \Big|_{n_0} = R_0^2 \frac{d^2(E/A)}{dR^2} \Big|_{R_0}. \quad (4.64)$$

It is also easily verified in this case that the mass parameter associated with the collective coordinate η is simply the total mass of the nucleus, Am , while in the exact case it is larger, equal to $(\pi^4/90)Am$. It must be noticed that the approximate velocity field $\dot{\alpha}r/3$ does not satisfy the proper boundary condition since its divergence does not vanish at the surface, as it should. The frequency obtained with this velocity field is:

$$\omega = \sqrt{K_\infty/m\eta_0^2} \quad (4.65)$$

which is larger than the exact frequency given by (4.50) by a factor $\sqrt{\pi^2/15}$.

It is seen in fig. 8 that the change in the density obtained with the velocity field $\dot{\alpha}r$ is drastically

different from the one resulting from the exact solution of the wave equation. The boundary condition imposed on the exact solution, which follows from the fact that the pressure must vanish at the surface of the nucleus, forces the density to change more at the center than close to the surface. As will be seen in section 6, the transition density of the breathing mode in heavy nuclei exhibits this characteristic increase in the center. In fact, in ^{208}Pb , the formula (4.50) reproduces rather well the results of self-consistent RPA calculations which show indeed that $K_A \sim \frac{2}{3}K_\infty$, a value quite close to that obtained in eq. (4.59). However, calculating K_A with the assumption that the velocity field is proportional to r , yields almost the same value, in contrast with what happens in the liquid drop model (see eq. (4.65)). This is because the liquid drop model ignores some important effects of the nuclear surface which will be discussed in the next section. Very likely, the biggest nuclei which we know are not large enough to guarantee the validity of the liquid drop picture. It would be interesting to investigate for which value of the mass number the model would give a complete description of the breathing mode. In ^{208}Pb and lighter nuclei it will be shown that other effects are important and therefore the apparent agreement of microscopic calculations with formula (4.50) seems to be accidental.

Let us finally mention that hydrodynamical equations for giant resonances, including a proper treatment of the nuclear surface and of the higher distortion of the Fermi surface have recently been developed [85, 86].

5. From finite nuclei to nuclear matter

In section 5.1 we present a local density approximation [16] which will be helpful to understand the results which are discussed in section 6. In particular we analyse the contribution of the nuclear surface to the restoring force for the compression modes. One drawback of this approach is that it neglects all the non local effects which are responsible for the stability of the surface. Those effects, however, are expected to contribute very little to the restoring force. This is confirmed by the analysis of a soluble model of semi-infinite nuclear matter which we present in section 5.2.

5.1. Local description of the compression mode

The starting point for that description is the formula (3.13). One assumes that the ground state of the nucleus can be described by a local Fermi surface:

$$n_k^0(\mathbf{R}) = \theta(\varepsilon_k^0(\mathbf{R}) - \mu) \quad (5.1)$$

with

$$\varepsilon_k^0(\mathbf{R}) = \frac{\hbar^2 k^2}{2m^*(\mathbf{R})} + U_o(\mathbf{R}) \quad (5.2)$$

and

$$\mu = \frac{\hbar^2 k_F^2(\mathbf{R})}{2m^*(\mathbf{R})} + U_o(\mathbf{R}) = \varepsilon_F(\mathbf{R}) + U_o(\mathbf{R}). \quad (5.3)$$

The local Fermi momentum $k_F(\mathbf{R})$ is related to the local density through (2.2). Furthermore local Landau parameters are defined through (3.18) with N_o calculated with the local quantities. This approximate scheme is of the same level of accuracy as the Thomas–Fermi approximation for the kinetic energy.

Now, since the giant monopole mode nearly exhausts the sum rule associated with the operator $\Sigma_i r_i^2$ we can interpret r^2 as a velocity potential for the collective flow (see section 3.3). This is equivalent to the scaling assumption discussed previously. Then we can obtain a simple physical picture of the collective mode by considering the deformation of the local Fermi surface. Let us write the velocity field as

$$\mathbf{v}(\mathbf{R}) = \dot{\alpha}(t) \mathbf{u}(\mathbf{R}) \quad (5.4)$$

where $\alpha(t)$ is a small time dependent amplitude and $\mathbf{u}(\mathbf{R})$ can be interpreted as a displacement field (here $\mathbf{u} = \mathbf{R}$). This velocity field produces the following changes in the distribution function:

(a) Displacement in \mathbf{R} -space of the local Fermi surface. This gives rise to the following variation

$$\delta n_{\mathbf{k}}^{(a)}(\mathbf{R}) = n_{\mathbf{k}}^0(\mathbf{R} + \alpha \mathbf{u}) - n_{\mathbf{k}}^0(\mathbf{R}) = \delta(|\mathbf{k}| - k_F(\mathbf{R})) \alpha \mathbf{u} \cdot \nabla k_F(\mathbf{R}). \quad (5.5)$$

By integrating eq. (5.5) over \mathbf{k} one gets that piece of the transition density which is associated with the displacement of the surface, i.e.

$$\delta n(\mathbf{R}) = \alpha \mathbf{u} \cdot \nabla n^0(\mathbf{R}) = \alpha R \frac{dn^0(R)}{dR}. \quad (5.6)$$

(b) Displacement in \mathbf{k} -space of the local Fermi surface. Due to the collective flow, the momenta of all the particles at point \mathbf{R} are shifted by the amount mv/\hbar . This results in a dipolar distortion of the Fermi surface:

$$\delta n_{\mathbf{k}}^{(b)}(\mathbf{R}) = -\frac{mv(\mathbf{R})}{\hbar} \cdot \hat{\mathbf{k}} \delta(|\mathbf{k}| - k_F(\mathbf{R})). \quad (5.7)$$

(c) Deformation of the local Fermi surface. This is a non local effect which can be understood from the following argument. If the system is squeezed in one direction, the components along this particular direction of the momenta of the particles will increase. Thus a multipole deformation of the nucleus induces multipole deformations of the Fermi surface. In the present case only monopole deformations have to be considered; they lead to

$$\delta n_{\mathbf{k}}^{(c)}(\mathbf{R}) = \alpha k_F(\mathbf{R}) \delta(|\mathbf{k}| - k_F(\mathbf{R})). \quad (5.8)$$

Integrating (5.8) over \mathbf{k} one gets that part of the transition density which really describe a local compression of the nucleus

$$\delta n(\mathbf{R}) = 3\alpha n^0(\mathbf{R}). \quad (5.9)$$

The sum of (5.9) and (5.6) is the transition density associated with the breathing mode which have been obtained previously in section 4 (eq. (4.28)).

One can now calculate the energy up to second order in α and $\dot{\alpha}$; indeed only the first order expressions of δn_k are required for such a calculation. One gets from (3.13)

$$E = E_o + \frac{1}{2}B\dot{\alpha}^2 + \frac{1}{2}C\alpha^2 \quad (5.10)$$

where

$$B = m\langle r^2 \rangle_o \quad (5.11a)$$

$$C = 6\langle \epsilon_F(1 + F_o) \rangle_o \quad (5.11b)$$

where $\langle \dots \rangle_o$ denotes the following operation:

$$\langle f \rangle_o = \int d^3r f(r) n^0(r).$$

A similar formula has been obtained by other authors [63, 64]. This formula can be compared with the expression (4.57) obtained in the liquid drop model.

5.2. The compressibility of the nuclear surface

In this section, we analyse the properties of the nuclear surface in a soluble model of semi infinite nuclear matter.

Let us assume that the total energy of the system can be written as:

$$E = \int \left(\mathcal{E}(n) + C \frac{(\nabla n)^2}{n} \right) d^3r \quad (5.12)$$

with:

$$\mathcal{E}(n) = Bn_o \left[-2 \left(\frac{n}{n_o} \right)^{1/d+1} + \left(\frac{n}{n_o} \right)^{2/d+1} \right]. \quad (5.13)$$

This particular form of the energy density $\mathcal{E}(n)$ has been chosen in order to get simple analytical formulae for the surface properties [65]. The parameters B and n_o are chosen respectively equal to the binding energy per nucleon and the saturation density of nuclear matter. The extra parameter, d , determines the compression modulus:

$$K_\infty = 18B/d^2. \quad (5.14)$$

The term which contains the gradient of the density has been added phenomenologically in order to control the surface properties of the system.

The equilibrium density is solution of the variational problem:

$$\delta(E - \mu N) = 0 \quad (5.15)$$

or:

$$\mu = d\mathcal{E}/dn + C[(\nabla n)^2/n - 2 \nabla^2 n/n]. \quad (5.16)$$

For a semi-infinite geometry, with plane equidensities perpendicular to the x -axis, this equation reduces to:

$$\mathcal{E} - \mu n - C \dot{n}^2/n = 0 \quad (5.17)$$

where $\dot{n} = dn/dx$.

We look for solutions which satisfy the following boundary conditions:

$$x \rightarrow -\infty, \quad \dot{n} \rightarrow 0, \quad n \rightarrow n_o. \quad (5.18)$$

Thus the chemical potential μ is the same as in nuclear matter:

$$\mu = \frac{d\mathcal{E}}{dn} \Big|_{n_o} = \frac{\mathcal{E}(n_o)}{n_o}. \quad (5.19)$$

This can be understood from the fact that a plane surface does not generate any pressure and therefore does not affect the equilibrium of the bulk. Equation (5.17) with the boundary conditions (5.18) can be integrated and one gets:

$$n/n_o = (1 + e^{\alpha x/d})^{-d} \quad (5.20a)$$

$$\alpha = \sqrt{B/C}. \quad (5.20b)$$

The surface energy E_{surf} is the difference between the actual energy of the system and the energy it would have if all the particles were at the density n_o :

$$E_{\text{surf}} = S \int_{-\infty}^{+\infty} \left\{ \mathcal{E}(n) + C \frac{\dot{n}^2}{n} - \frac{\mathcal{E}(n_o)}{n_o} n \right\} dx \quad (5.21)$$

where $S = \int dx dy$ is the (infinite) area of the surface of the system. It is convenient to introduce a surface energy per unit area: $\sigma = E_{\text{surf}}/S$. σ is related to the surface energy coefficient of the mass formula by the relation (2.20c). It follows from equations (5.17) and (5.19) that σ is stationary with respect to all variations in the density. Indeed, setting:

$$\hat{\mathcal{E}} = \mathcal{E} + C \dot{n}^2/n \quad (5.22)$$

one has:

$$\delta\sigma = \int \left(\frac{\partial \hat{\mathcal{E}}}{\partial n} \delta n + \frac{\partial \hat{\mathcal{E}}}{\partial \dot{n}} \delta \dot{n} - n \frac{\partial \mathcal{E}}{\partial n_o} \frac{\delta n_o}{n_o} + n \frac{\mathcal{E}(n_o)}{n_o^2} \delta n_o - \frac{\mathcal{E}(n_o)}{n_o} \delta n \right).$$

The terms proportional to δn_o vanish because of (5.19) and the terms proportional to δn vanish because of (5.17).

Using eq. (5.17) one gets a simpler form for σ :

$$\sigma = 2C \int_{-\infty}^{+\infty} \frac{\dot{n}^2}{n} dx = 2 \int_{-\infty}^{+\infty} [\mathcal{E}(n) - \mu n] dx. \quad (5.23)$$

In this model, half of the surface energy comes from the gradient terms and half from the lack of binding due to the diffuse surface. From (5.23), using the explicit solution (5.20), a simple integration yields:

$$\sigma = \frac{2n_o}{1+d} \sqrt{CB}. \quad (5.24)$$

We wish to calculate the variation of the total energy up to second order in the density variation δn , in order to get an estimate of the surface compression modulus. We shall consider first a variation of the form:

$$\delta n = \alpha n + \beta \dot{n} \quad (5.25)$$

where α and β are two constants. It is easy to show that the energy does not depend on β . One has indeed:

$$\begin{aligned} \delta^2 E = & \frac{\alpha^2}{2} \int \left(\frac{\partial^2 \hat{\mathcal{E}}}{\partial n^2} n^2 + 2n\dot{n} \frac{\partial^2 \hat{\mathcal{E}}}{\partial n \partial \dot{n}} + \dot{n}^2 \frac{\partial^2 \hat{\mathcal{E}}}{\partial \dot{n}^2} \right) + \frac{\beta^2}{2} \int \left(\frac{\partial^2 \hat{\mathcal{E}}}{\partial n^2} \dot{n}^2 + 2\dot{n}\ddot{n} \frac{\partial^2 \hat{\mathcal{E}}}{\partial n \partial \ddot{n}} + \ddot{n}^2 \frac{\partial^2 \hat{\mathcal{E}}}{\partial \ddot{n}^2} \right) \\ & + \alpha\beta \int \left(n\dot{n} \frac{\partial^2 \hat{\mathcal{E}}}{\partial n^2} + (\dot{n}^2 + n\ddot{n}) \frac{\partial^2 \hat{\mathcal{E}}}{\partial n \partial \dot{n}} + \dot{n}\ddot{n} \frac{\partial^2 \hat{\mathcal{E}}}{\partial \dot{n}^2} \right). \end{aligned} \quad (5.26)$$

The terms in front of the β 's can be eliminated by using the equation:

$$\frac{d\mu}{dx} = 0 = \frac{\partial^2 \hat{\mathcal{E}}}{\partial n^2} \dot{n} + \frac{\partial^2 \hat{\mathcal{E}}}{\partial n \partial \dot{n}} \ddot{n} - \frac{d}{dx} \left(\frac{\partial^2 \hat{\mathcal{E}}}{\partial n \partial \dot{n}} \dot{n} + \frac{\partial^2 \hat{\mathcal{E}}}{\partial \dot{n}^2} \ddot{n} \right).$$

Since $\delta n = \beta \dot{n}$ corresponds to a mere displacement of the surface, the disappearance of the terms in β^2 reflects the fact that in a semi-infinite system there is no restoring force associated with such a displacement. The vanishing of the term proportional to $\alpha\beta$ indicates that the variations proportional to n and \dot{n} are independent (in the sense of normal modes). The variation of the energy corresponding to the density variation (5.25) is therefore:

$$\delta^2 E = \frac{\alpha^2}{2} \int \left(\frac{\partial^2 \hat{\mathcal{E}}}{\partial n^2} n^2 + 2n\dot{n} \frac{\partial^2 \hat{\mathcal{E}}}{\partial n \partial \dot{n}} + \dot{n}^2 \frac{\partial^2 \hat{\mathcal{E}}}{\partial \dot{n}^2} \right) dx. \quad (5.27)$$

It turns out in the present case that we have a further cancellation. Indeed for $\hat{\mathcal{E}}$ given by (5.22) one

has:

$$\frac{\partial^2 \hat{\mathcal{E}}}{\partial n^2} n^2 + 2n \dot{n} \frac{\partial^2 \hat{\mathcal{E}}}{\partial n \partial \dot{n}} + \dot{n}^2 \frac{\partial^2 \hat{\mathcal{E}}}{\partial \dot{n}^2} = \frac{\partial^2 \hat{\mathcal{E}}}{\partial n^2} n^2 = \frac{d^2 \mathcal{E}}{dn^2} n^2.$$

Therefore:

$$\delta^2 E = \frac{\alpha^2}{2} \int \frac{d^2 \mathcal{E}}{dn^2} n^2 dx. \quad (5.28)$$

We can extract from $\delta^2 E$ a volume and a surface contribution:

$$\delta^2 E = \frac{\alpha^2}{2} \Omega n_o^2 \frac{d^2}{dn^2} \Big|_{n_o} + \frac{\alpha^2}{2} S \int_{-\infty}^{+\infty} \left(\frac{d^2 \mathcal{E}}{dn^2} n^2 - n_o n \frac{d^2 \mathcal{E}}{dn^2} \Big|_{n_o} \right) dx. \quad (5.29)$$

The term proportional to the surface area is nothing but the second order variation of the surface energy coefficient. This can be easily shown by expanding σ in second order in α and remembering that a variation $\delta n = \alpha n$ involves a variation $\delta n_o = \alpha n_o$ of the bulk density, which means that we have to take properly into account the variation of the term $\mathcal{E}(n_o)/n_o$.

Writing $\delta n = 3\alpha n$ to make apparent the desired factor 9, using $\Omega = \frac{4}{3}\pi r_o^3 A$ and $S = 4\pi r_o^2 A^{2/3}$, one gets:

$$\delta^2(E/A) = \frac{\alpha^2}{2} \left(K_\infty + 36\pi r_o^2 n_o^2 \frac{d^2 \sigma}{dn_o^2} A^{-1/3} \right) \quad (5.30)$$

where the last term is what we call K_{surf} in section 6.2. It is convenient to introduce the dimensionless parameter K_σ by writing:

$$K_{\text{surf}} = 9a_{\text{surf}} K_\sigma. \quad (5.31)$$

Thus

$$K_\sigma = \frac{n_o^2}{\sigma} \frac{d^2 \sigma}{dn_o^2}. \quad (5.32)$$

K_σ can be obtained easily by using the explicit solution (5.20a) to calculate σ by eq. (5.21). One gets:

$$K_\sigma = -\frac{1+3d+d^2}{d^2} = -\left(1 + \frac{K_\infty}{18B} \sqrt{\frac{K_\infty}{2B}}\right). \quad (5.33)$$

One notices that K_σ is negative. Therefore the surface energy coefficient is *maximum* at the saturation density. K_σ depends only on the parameter d and is thus determined by the properties of the bulk, i.e. the compression modulus K_∞ . For values of d close to 1, K_σ as a function of K_∞ , has the following linear behaviour:

$$K_\sigma \sim -\frac{5}{2}(1 + K_\infty/18B). \quad (5.34)$$

The same is true of K_{surf} given by (5.31) if the parameter C is adjusted in order to keep constant the surface energy when d varies.

It is remarkable that K_σ does not depend, in this model, on more specific surface properties; in particular, it does not depend on the value of the parameter C , or equivalently on the surface energy coefficient σ . Of course some surface properties will vary with d . This can be seen from the formula:

$$\alpha\sigma = 2Bn_o/(1+d) \quad (5.35)$$

which indicates that for fixed σ , α decreases when d increases. Thus, because of (5.14) the surface thickness, proportional to α^{-1} is a decreasing function of K_∞ (for fixed σ). These properties clearly show up in the detailed results given in table 6.

Let us now consider another possible density variation, obtained by a homologous transformation of the ground state density. In such a transformation, $r \rightarrow r/\lambda$, and the parameters n_o and α , which enter the ground state density (see eq. (5.20a)), transform as follows:

$$n_o \rightarrow \lambda^3 n_o, \quad \alpha \rightarrow \lambda \alpha.$$

Therefore this density variation involves at the same time a compression of the bulk and a stretching of the surface. Now we have:

$$K_{\text{surf}} = a_{\text{surf}} \frac{1}{\sigma} \left. \frac{d^2\sigma}{d\lambda^2} \right|_{\lambda=1}$$

and:

$$\left. \frac{d^2\sigma}{d\lambda^2} \right|_{\lambda=1} = 9n_o^2 \frac{\partial^2\sigma}{\partial n_o^2} + 6n_o\alpha \frac{\partial^2\sigma}{\partial \alpha \partial n_o} + \frac{\partial^2\sigma}{\partial \alpha^2}. \quad (5.36)$$

Table 6

Properties of the semi-infinite nuclear matter as a function of the parameter d . C is the parameter in front of the gradient terms in eq. (5.12). It is adjusted in order to keep constant the surface energy coefficient (see eq. (5.24)). n_c is the density at which the compressibility becomes infinite. γ is the slope of the density at half the saturation density: $\gamma = \dot{n}/n_o|_{n=n_o/2}$. K_∞ is the compression modulus of nuclear matter. K_{surf}^1 and K_{surf}^2 are the surface compressibility coefficients corresponding to the formulae (5.38) and (5.33) respectively

| d | c | n_c/n_o | γ | K_∞ | $K_{\text{surf}}^1/a_{\text{surf}}$ | $K_{\text{surf}}^2/a_{\text{surf}}$ |
|-----|-------|-----------|----------|------------|-------------------------------------|-------------------------------------|
| 0.8 | 3.224 | 0.702 | -0.645 | 450 | -49.8 | -56.8 |
| 0.9 | 3.593 | 0.683 | -0.567 | 356 | -43.1 | -50 |
| 1.0 | 3.981 | 0.667 | -0.501 | 288 | -38.0 | -45 |
| 1.1 | 4.389 | 0.651 | -0.446 | 238 | -34.0 | -41 |
| 1.2 | 4.817 | 0.638 | -0.400 | 200 | -30.7 | -37.8 |
| 1.3 | 5.264 | 0.625 | -0.360 | 170 | -28.1 | -35.1 |
| 1.4 | 5.732 | 0.614 | -0.326 | 147 | -25.9 | -32.9 |
| 1.5 | 6.220 | 0.604 | -0.297 | 128 | -24.0 | -31 |
| 1.6 | 6.727 | 0.594 | -0.271 | 112 | -22.4 | -29.4 |
| 1.7 | 7.255 | 0.585 | -0.249 | 99.6 | -21.0 | -28 |

Again the derivatives can be calculated easily using (5.20a) and (5.21). One finds:

$$\frac{\alpha n_o}{\sigma} \frac{\partial^2 \sigma}{\partial \alpha \partial n_o} = 1, \quad \frac{\alpha^2}{\sigma} \frac{\partial^2 \sigma}{\partial \alpha^2} = 1 \quad (5.37)$$

and the second derivative $\partial^2 \sigma / \partial n_o^2$ is given by (5.33). One then gets:

$$\frac{K_{\text{surf}}}{a_{\text{surf}}} = \frac{1}{\sigma} \frac{d^2 \sigma}{d \lambda^2} \Big|_{\lambda=1} = -\frac{1}{d^2} (2d^2 + 27d + 9). \quad (5.38)$$

The inclusion of the surface stretching does not strongly modify the preceding conclusions, namely the linear dependence of K_{surf} on K_∞ (for the values of d close to 1, the slope is the same). The derivatives of σ with respect to α are positive however. Therefore the inclusion of the surface stretching will tend to decrease the absolute value of K_{surf} and therefore to increase the effective compression modulus of the whole system.

One important conclusion of this section is that the nuclear surface has a large negative contribution to the compression modulus of a semi-infinite system. The same conclusion can be extrapolated to finite nuclei, where the surface contribution appears as an $A^{-1/3}$ correction (see eq. (5.30)). The fact that the nuclear surface energy is maximum at saturation density is fairly model independent. This can be understood from the following arguments. The major part of the restoring force is given by the local approximation developed in section 5.1. In the semi-infinite model of section 5.2 this local approximation gives even the exact answer: the formulae (5.11b) and (5.28) are easily shown to be equivalent. Now we observe that if the nuclear density had a sharp surface, there would be no surface contribution to the restoring force. As is the case for the surface energy, the surface contribution to the compression modulus comes from the difference between a system with a diffuse surface, and a system with a sharp surface. This is clearly seen on formula (5.29). As we have discussed in section 2, the Landau parameter F_o is a decreasing function of the density near saturation density n_∞ and is smaller than -1 for densities smaller than $0.6n_\infty$. In other words, the quantity $n^2 d^2 \mathcal{E}/dn^2$ is always smaller than its value for $n = n_\infty$, and formula (5.29) shows therefore that the second derivative of the surface energy with respect to the density of the bulk is negative. Furthermore it is important to realize that the surface compression modulus K_{surf} is a large quantity (see table 6), much larger than the correction in $A^{-1/3}$ obtained in the liquid drop model discussed in section 4. It is also useful to remember that it has a very regular behaviour as a function of K_∞ . More realistic calculations of nuclear surface properties performed recently lead to identical conclusions [87].

6. Self-consistent calculations of the giant monopole resonance in nuclei

We now present results of self-consistent calculations of the giant monopole resonance in spherical nuclei. Most of the material of this section has already been published [22]. Therefore we shall not discuss the details of the calculations, but rather concentrate on the interpretation of the results.

6.1. The monopole strength function in spherical nuclei

The RPA equations (3.11) have been solved in their matrix form, in the space of the particle-hole configurations. The continuum of the single particle states has been discretized in an oscillator basis.

This procedure has been shown to be reliable for the calculation of the giant resonances [29]. A very powerful check of our numerical calculation is provided by the sum rule m_1 (eq. (3.39)) which can be evaluated exactly and using the RPA strength function: in our calculations, both evaluations agree within less than 1%. Another justification for this approximate numerical scheme is provided by a comparison with calculations treating more correctly the continuum (see fig. 19 and the discussion at the end of section 6.5).

A typical RPA strength function is shown in fig. 9. The collectivity of the giant monopole resonance is then spectacular. The unperturbed strength lies between 23 and 35 MeV with an average value $\bar{E}_{ph} = 30.2$ MeV. The particle-hole interaction shifts the strength by more than 14 MeV. All the oscillator strength is collected in a single resonance. This represents a somewhat ideal case. Detailed results are reported in table 7 which shows how things vary with the mass of the nucleus and the effective interaction used in the calculation.

The first important result of the calculations is to suggest the systematic existence of a giant isoscalar monopole resonance in spherical nuclei. This resonance is more and more pronounced as the nucleus becomes heavier. This result is independent of the interaction used and can be viewed in different ways:

- (i) A direct examination of the RPA strength function (see fig. 10) reveals that the strength becomes more and more concentrated as the nucleus becomes heavier.
- (ii) The percentage of energy weighted sum rule carried by the resonance increases with the number of nucleons in the system. It reaches 95% in ^{208}Pb .

(iii) The mean square spreading σ_{RPA} defined in eq. (3.38) decreases from 7.8 MeV in ^{16}O to 1.5–2 MeV in ^{208}Pb . This quantity σ is given here only to get an idea of how the monopole strength is distributed; it should not be naively identified with the width of the resonance (e.g. this would make no sense for the case displayed in fig. 9).

(iv) The collectivity of the excitation can also be inferred from the examination of its particle-hole components (see table 8a,b). These are such that the individual particle-hole monopole transitions add up coherently in the resonance.

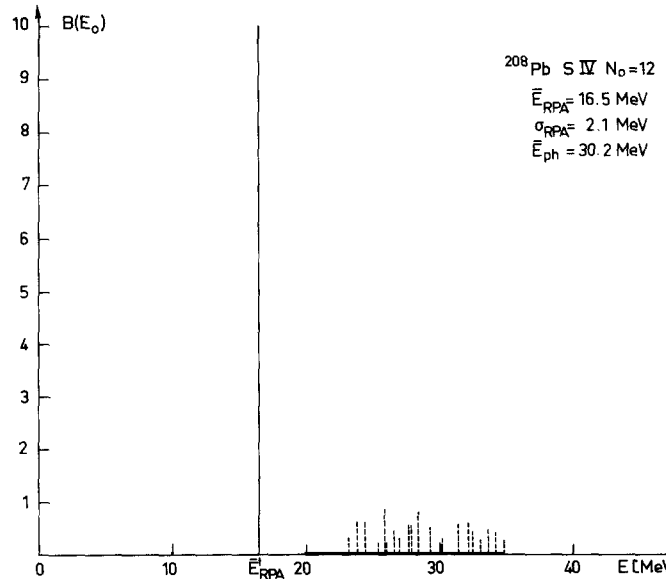


Fig. 9. Monopole strength function in ^{208}Pb calculated with the interaction S IV.

Table 7
Detailed results of RPA calculations of the breathing mode in spherical nuclei (all the quantities are defined in the text)

| | B1 | D1 | Sk _a | S IV | S III |
|---|------|-------|-----------------|------|-------|
| K_∞ (MeV) | 190 | 228 | 263 | 325 | 356 |
| m^*/m | 0.43 | 0.67 | 0.61 | 0.47 | 0.76 |
| The nucleus ^{16}O | | | | | |
| η (fm) | 2.64 | 2.63 | 2.65 | 2.61 | 2.62 |
| K_A (MeV) | 76.5 | 101 | 117 | 138 | 147 |
| $\hbar\omega$ (MeV) | 21.4 | 24.6 | 26.3 | 29.0 | 29.8 |
| E_{RPA} (MeV) | 21.6 | 25.1 | 26.5 | 29.4 | 30.3 |
| E_{TDA} (MeV) | 22.4 | 26.2 | 28.7 | 33.1 | 34.1 |
| E_{ph} (MeV) | 39.9 | 31.3 | 31.7 | 39.9 | 29.8 |
| σ_{RPA} (MeV) | 4.5 | 6.7 | 6.8 | 8.5 | 8.75 |
| The nucleus ^{40}Ca | | | | | |
| η (fm) | 3.37 | 3.35 | 3.39 | 3.37 | 3.38 |
| K_A (MeV) | 99 | 132 | 144 | 171 | 186 |
| $\hbar\omega$ (MeV) | 19.0 | 22.1 | 22.8 | 25.0 | 26.0 |
| E_{RPA} (MeV) | 19.1 | 22.2 | 23.0 | 25.3 | 26.3 |
| E_{TDA} (MeV) | 19.8 | 22.8 | 24.1 | 27.3 | 28.2 |
| E_{ph} (MeV) | 38.0 | 29.6 | 29.7 | 36.9 | 27.1 |
| σ_{RPA} (MeV) | 3.4 | 4.1 | 4.6 | 6.1 | 5.9 |
| The nucleus ^{90}Zr | | | | | |
| η (fm) | 4.21 | 4.22 | 4.28 | 4.27 | 4.29 |
| K_A (MeV) | 112 | 146.5 | 160 | 197 | 217 |
| $\hbar\omega$ (MeV) | 16.2 | 18.5 | 19.1 | 21.2 | 22.1 |
| E_{RPA} (MeV) | 16.2 | 18.5 | 19.1 | 21.2 | 22.1 |
| E_{TDA} (MeV) | 16.8 | 18.9 | 19.7 | 22.2 | 22.9 |
| E_{ph} (MeV) | 35.8 | 27.6 | 27.8 | 34.8 | 25.0 |
| σ_{RPA} (MeV) | 2.5 | 2.9 | 3.0 | 3.3 | 3.3 |
| The nucleus ^{208}Pb | | | | | |
| η (fm) | 5.51 | 5.48 | 5.59 | 5.58 | 5.59 |
| K_A (MeV) | 114 | 150 | 161 | 204 | 224 |
| $\hbar\omega$ (MeV) | 12.5 | 14.4 | 14.6 | 16.5 | 17.3 |
| E_{RPA} (MeV) | 12.5 | 14.4 | 14.7 | 16.5 | 17.2 |
| E_{TDA} (MeV) | 12.9 | 14.9 | 15.0 | 16.9 | 17.5 |
| E_{ph} (MeV) | 28.2 | 23.2 | 24.1 | 30.2 | 21.9 |
| σ_{RPA} (MeV) | 1.4 | 1.7 | 1.3 | 2.1 | 1.9 |

Since most of the strength is concentrated in the giant monopole resonance we can characterize the energy of this resonance by the formula (3.48) deduced from sum-rule arguments:

$$\hbar\omega = \sqrt{\hbar^2 A K_A / m \langle r^2 \rangle_0}.$$

Actually the energy $\hbar\omega$ given by (3.48) is also equal to \bar{E}_{RPA} (eq. (3.37)) (within 0.3 MeV) even in light nuclei. It coincides in heavy nuclei with the energy of the most important peak. This justifies the

Table 8

Main particle-hole components of the most collective states in ^{40}Ca (a) and ^{208}Pb (b), calculated with the interaction D1. The state $N = 1$ in ^{40}Ca has an energy of 20.9 MeV and carries 76% of the sum rule m_1 . The states $N = 1, N = 2, N = 3$ in ^{208}Pb have energies of 13.7, 14.7, 15.6 MeV and carry 85%, 4% and 9% of the sum rule, respectively. The $B(E_\alpha)$ of the individual p-h configurations are given in percentage of the total strength. The configurations listed exhaust 88% of the monopole strength for ^{40}Ca and 96% for ^{208}Pb

| (a) | | | | (b) | | | | | | | |
|---------------------|---------------------------|---------------|----------------|---------------|---------------------------|---------------|----------------|------|--------|--------|--------|
| Configuration | $\epsilon_p - \epsilon_h$ | $B(E_\alpha)$ | $X_{ph}^{N=1}$ | Configuration | $\epsilon_p - \epsilon_h$ | $B(E_\alpha)$ | $X_{ph}^{N=1}$ | | | | |
| $3s_{1/2} 2s_{1/2}$ | n | 28.8 | 7.78 | 0.374 | $2d_{5/2} 2d_{5/2}$ | n | 22.0 | 4.79 | -0.206 | | |
| | p | 22.2 | 8.54 | 0.608 | | p | 23.6 | 5.00 | -0.203 | | |
| $3p_{3/2} 1p_{3/2}$ | n | 33.0 | 7.33 | -0.134 | $3d_{3/2} 2d_{3/2}$ | n | 21.0 | 3.11 | 0.144 | 0.130 | |
| | p | 33.6 | 7.52 | -0.128 | | p | 22.5 | 3.36 | -0.154 | -0.084 | |
| $2p_{1/2} 1p_{1/2}$ | n | 32.4 | 3.64 | -0.090 | $4s_{1/2} 3s_{1/2}$ | n | 20.1 | 1.88 | 0.122 | -0.111 | |
| | p | 31.9 | 3.72 | -0.080 | | p | 21.5 | 1.97 | -0.134 | | |
| $2d_{5/2} 1d_{5/2}$ | n | 29.4 | 13.6 | -0.260 | $3f_{7/2} 2f_{7/2}$ | n | 18.8 | 6.97 | -0.263 | -0.161 | |
| | p | 28.1 | 14.0 | -0.262 | $4f_{7/2} 2f_{7/2}$ | n | 28.7 | 1.38 | -0.106 | | |
| $2d_{3/2} 1d_{3/2}$ | n | 24.4 | 10.8 | -0.342 | $2f_{7/2} 1f_{7/2}$ | p | 26.9 | 3.63 | 0.153 | 0.090 | |
| | p | 23.1 | 11.5 | -0.415 | $3f_{5/2} 2f_{5/2}$ | n | 16.6 | 5.88 | -0.230 | -0.101 | -0.355 |
| | | | | | $4f_{5/2} 2f_{5/2}$ | n | 27.2 | 1.10 | -0.084 | | |
| | | | | | $2f_{5/2} 1f_{5/2}$ | p | 26.8 | 2.63 | 0.126 | | |
| | | | | | $4p_{3/2} 3p_{3/2}$ | n | 15.3 | 5.23 | -0.420 | -0.386 | 0.80 |
| | | | | | $5p_{3/2} 3p_{3/2}$ | n | 26.3 | 0.98 | 0.092 | | |
| | | | | | $3p_{3/2} 2p_{3/2}$ | p | 24.6 | 2.97 | -0.157 | | |
| | | | | | $4p_{1/2} 3p_{1/2}$ | n | 14.5 | 2.80 | -0.431 | 0.877 | 0.184 |
| | | | | | $3p_{1/2} 2p_{1/2}$ | p | 24.4 | 1.48 | -0.106 | | |
| | | | | | $2g_{9/2} 1g_{9/2}$ | n | 25.7 | 4.54 | 0.176 | 0.113 | |
| | | | | | | p | 27.3 | 4.82 | 0.166 | 0.100 | |
| | | | | | $2g_{7/2} 1g_{7/2}$ | n | 24.9 | 3.39 | 0.144 | 0.096 | |
| | | | | | | p | 25.9 | 3.80 | 0.143 | 0.088 | |
| | | | | | $2h_{11/2} 1h_{11/2}$ | n | 24.9 | 5.61 | 0.182 | 0.116 | |
| | | | | | | p | 26.9 | 5.73 | 0.182 | 0.102 | |
| | | | | | $2h_{9/2} 1h_{9/2}$ | n | 21.6 | 4.68 | 0.154 | 0.102 | |
| | | | | | $2i_{13/2} 1i_{13/2}$ | n | 21.5 | 6.26 | 0.188 | 0.128 | |
| | | | | | $3i_{13/2} 1i_{13/2}$ | n | 30.5 | 1.68 | -0.105 | | |

usefulness of the quantity K_A defined by eq. (3.45). The formula (3.48) shows that the measurement of $\hbar\omega$, the energy of the giant monopole resonance determines the effective compression modulus of finite nuclei K_A . We discuss in section 6.2 the dependence of K_A on A , m^* and K_∞ .

It is worth-emphasizing the very different behaviour of the unperturbed and RPA strength functions obtained for the various interactions. The large variations of \bar{E}_{ph} from one force to another (see table 7 and fig. 11a) follows remarkably the variations of the effective mass m^* . The energy \bar{E}_{ph} decreases roughly linearly by 10 MeV when the effective mass increases from 0.43 to 0.76. On the contrary, the variations of \bar{E}_{RPA} follow regularly the changes of the compression modulus K_∞ and are rather insensitive to the variation of the effective mass alone.

The energy shift $\bar{E}_{ph} - \bar{E}_{RPA}$ follows also the variations of the effective mass (see fig. 11b). This is not unexpected since, quite generally, one expects the energy shift to be proportional to the unperturbed energies and, as shown in fig. 11, $\bar{E}_{ph} \sim m/m^*$. Here, one also expects $\bar{E}_{ph} - \bar{E}_{RPA}$ to be proportional to some average of the Landau parameter $F_o(r)$ over the nuclear volume (see eq. (5.11b)). Therefore one expects $\bar{E}_{RPA} - \bar{E}_{ph} \sim \langle F_o \rangle / m^*$.

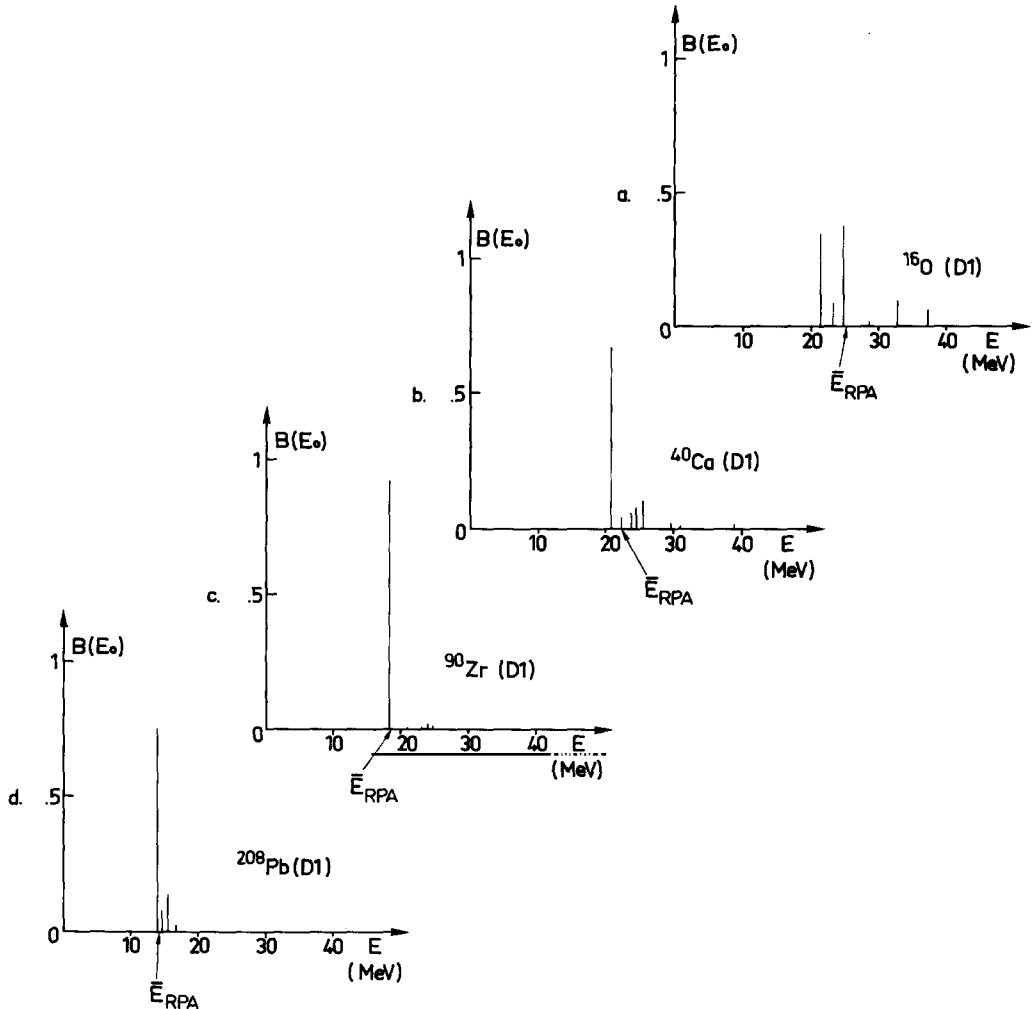


Fig. 10. Monopole strength function in the nuclei ^{16}O , ^{40}Ca , ^{90}Zr , ^{208}Pb calculated with the interaction D1.

Fig. 11b shows that the variations of the energy shift are mostly determined by the variations of the effective mass. The variation of $\langle F_o \rangle$, roughly proportional to the variation of F_o , explains the deviations from a linear law in (m/m^*) . All these effects, associated with the variations of m^* and F_o , partly compensate each other in the final energy \bar{E}_{RPA} , in such a way that this quantity is determined by that combination of F_o and m^* which corresponds to the compression modulus of nuclear matter. It is important to remark the large cancellation of the effect associated with m^* . This cancellation will be further discussed in section 7.

The A dependence of the energy shift is more delicate to analyse. The average particle-hole-energy \bar{E}_{ph} and the RPA energy \bar{E}_{RPA} decrease roughly as $A^{-1/3}$, but the energy shift $\bar{E}_{ph} - \bar{E}_{RPA}$ increases, roughly like $A^{-1/3}$ (see fig. 11c).

The analysis of the energy shift is complicated by the fact that \bar{E}_{ph} and \bar{E}_{RPA} are defined with the help of the moment m_o of the strength function, for which there is no simple closed expression, contrary to what happens for m_1 or m_{-1} . An analysis in terms of the moments m_1 and m_{-1} , or m_1 and m_3 would be probably instructive, but it has not been done yet.

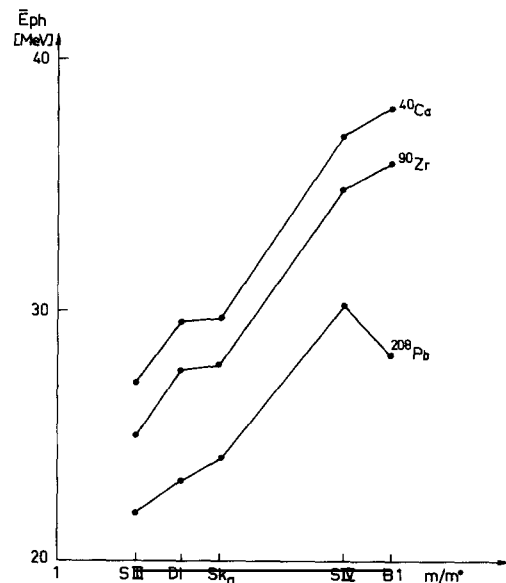


Fig. 11a. Average particle-hole energies \bar{E}_{ph} (see eq. (3.29)) for the nuclei ${}^{40}\text{Ca}$, ${}^{90}\text{Zr}$ and ${}^{208}\text{Pb}$. The forces S III, D1, Sk_a, S IV and B1, with which the calculations are done, are indicated in abscissa, on a scale proportional to the inverse of the effective mass.

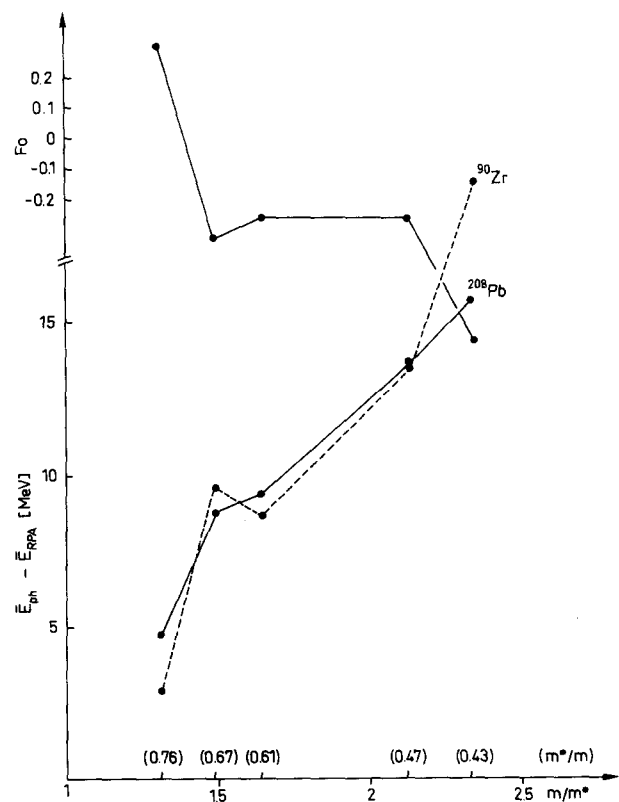


Fig. 11b. Average energy shift $\bar{E}_{ph} - \bar{E}_{RPA}$ in ${}^{90}\text{Zr}$ and ${}^{208}\text{Pb}$, and Landau parameter F_0 . The scale in abscissa is as in fig. 11a.

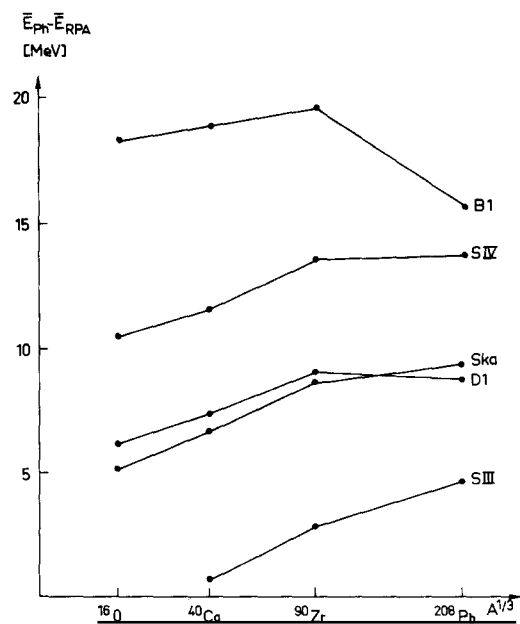


Fig. 11c. Average energy shift $\bar{E}_{ph} - \bar{E}_{RPA}$ as a function of $A^{1/3}$.

6.2. The effective compression modulus for finite nuclei

The compression modulus K_A has been calculated from the formula (3.45) and using the RPA results for m_{-1} . Both methods agree within 2 or 3%. Figures 12, 13 illustrate the variation of K_A with K_∞ and A respectively. It is remarkable that the compression modulus of the heaviest nuclei (^{208}Pb , ^{90}Zr) does not depend in a sensitive way on the mass number A , and it never exceeds the value $\frac{2}{3}K_\infty$ (for the heaviest nucleus we have calculated, i.e. ^{208}Pb). The variation of K_A with K_∞ is also very regular, K_A increasing almost linearly with K_∞ . However some irregularities can be noticed; they occur mainly for the interaction D1 which gives higher values for K_A compared to what could be extrapolated from the values given by the other forces.

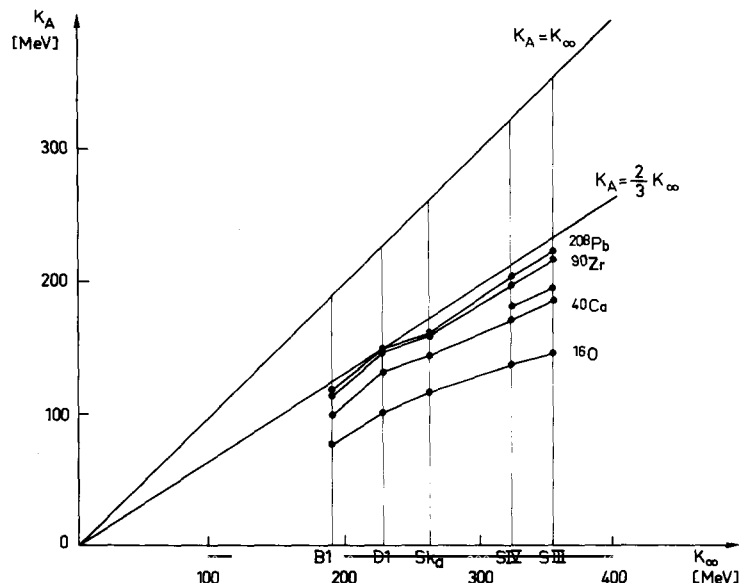


Fig. 12. The effective compression modulus K_A (definition (3.45)) as a function of the compression modulus of nuclear matter K_∞ .

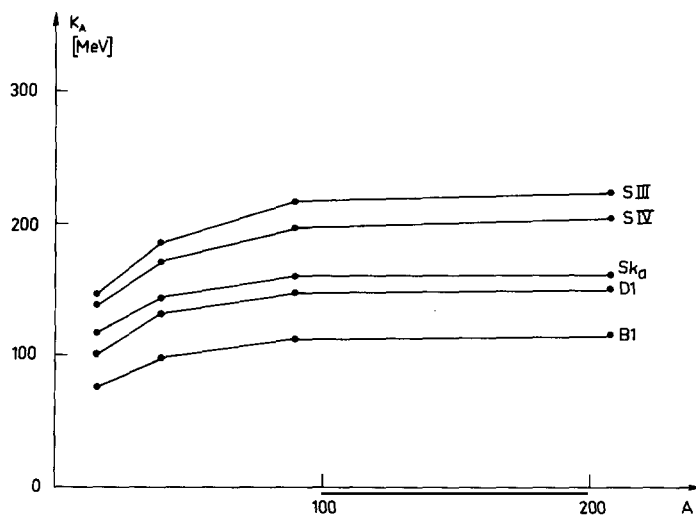


Fig. 13. The effective compression modulus K_A as a function of A .

The behaviour of K_A as a function of A and K_∞ can be understood in the simple model developed at the beginning of section 2. Let us indeed calculate K_A in this model by taking the second derivative of E/A , given by eq. (2.17), with respect to R_o . One gets:

$$K_A = R_o^2 \frac{d^2(E/A)}{dR_o^2} = 9 \frac{dP(n_o)}{dn_o} + \frac{12}{5} \frac{Z^2 e^2}{AR_o} - \frac{8\pi\sigma R_o^2}{A} + 8\delta^2 n_o^2 \frac{d^2 a_\tau}{dn_o^2} + 18n_o \delta^2 \frac{da_\tau}{dn_o} + \frac{36\pi R_o^2}{A} n_o^2 \frac{d^2 \sigma}{dn_o^2}. \quad (6.1)$$

There are no terms in $d\sigma/dn_o$ in the above expression. Such terms indeed vanish, as shown in section 5.2. Now $dP(n_o)/dn_o$ would be equal to $K_\infty/9$ if n_o were equal to n_∞ , the saturation density of nuclear matter. In fact one has:

$$9 \frac{dP}{dn} \Big|_{n_o} = K_\infty + \frac{n_o - n_\infty}{n_\infty} K_\infty + 9 \left(\frac{n_o - n_\infty}{n_\infty} \right)^2 n_\infty^2 \frac{d^3 \mathcal{E}}{dn^3} \Big|_{n_\infty}. \quad (6.2)$$

Remembering that n_o can be obtained from eqs. (2.18) and (2.19), one can rewrite K_A as:

$$\begin{aligned} K_A = K_\infty &+ \delta^2 \left[K_{\text{sym}} + 3L - \frac{27L}{K_\infty} n_\infty^2 \frac{d^3 \mathcal{E}}{dn^3} \right] + A^{-1/3} \left[K_{\text{surf}} + 4a_{\text{surf}} \left(1 + \frac{27}{2} \frac{n_\infty^2}{K_\infty} \frac{d^3 \mathcal{E}}{dn^3} \right) \right] \\ &+ Z^2 A^{-4/3} \frac{3}{5} \frac{e^2}{r_o} \left[1 - 27 \frac{n_\infty^2}{K_\infty} \frac{d^3 \mathcal{E}}{dn^3} \right] \end{aligned} \quad (6.3)$$

where we have set:

$$K_{\text{surf}} = 36\pi r_o^2 n_o^2 \frac{d^2 \sigma}{dn_o^2}. \quad (6.4)$$

Let us note that the coefficients of δ^2 , $A^{-1/3}$ and $Z^2 A^{-4/3}$ do not have the simple interpretation of being the second derivatives of the symmetry, the surface and the Coulomb energy respectively. This is because none of these quantities is stationary for $n = n_o$.

All the quantities appearing in the expression (6.3) are known except K_{surf} which can be determined by a fit to the RPA results. The fit is slightly improved if one adds a surface-symmetry term. Thus, one writes K_A in the following way:

$$K_A = K_\infty + K_S A^{-1/3} + (K_\tau + K_{S\tau} A^{-1/3}) \delta^2 + K_c Z^2 A^{-4/3}. \quad (6.5)$$

Such a parametrization was presented in ref. [22]. However better values for the parameters are given in ref. [87]. Table 9 displays numerical values of the various contributions to K_A .

Table 9
Detailed contributions to K_A from the various terms in (6.5).
All the quantities are in MeV

| | K_∞ | $K_S A^{-1/3}$ | $K_\tau \delta^2$ | $K_{S\tau} \delta^2 A^{-1/3}$ | $K_c Z^2 A^{-4/3}$ | K_A |
|-------------------|------------|----------------|-------------------|-------------------------------|--------------------|-----------|
| ^{208}Pb | 356 | -85 | -19 | 6 | -33 | 225 (224) |
| ^{40}Ca | 356 | -148 | 0 | 0 | -18 | 190 (186) |

The parameters entering (6.5) are not determined with a great accuracy. Nevertheless, it would be interesting to pursue such an analysis. For example, information on K_{sym} would provide constraints on the dependence of the Landau parameter F_c on the neutron excess. This would give information on the compressibility of neutron matter. This problem has been examined recently [83].

Figure 14a gives an idea of the accuracy of the fit obtained when one puts $K_\tau = K_{S\tau} = K_c = 0$. The coefficient K_S is mostly determined by the data on ^{40}Ca for which $\delta = 0$. The values of K_S obtained for different forces are plotted versus K_∞ in fig. 14b. Two important points can be extracted from this

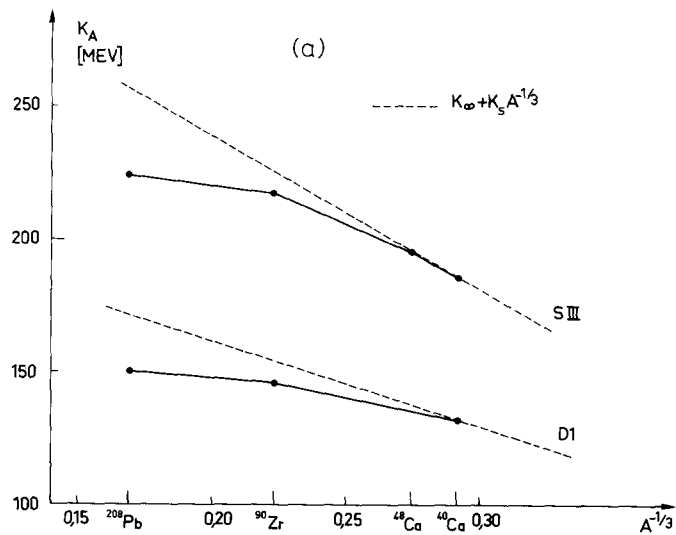


Fig. 14a. The effective compression modulus K_A as a function of $A^{-1/3}$.

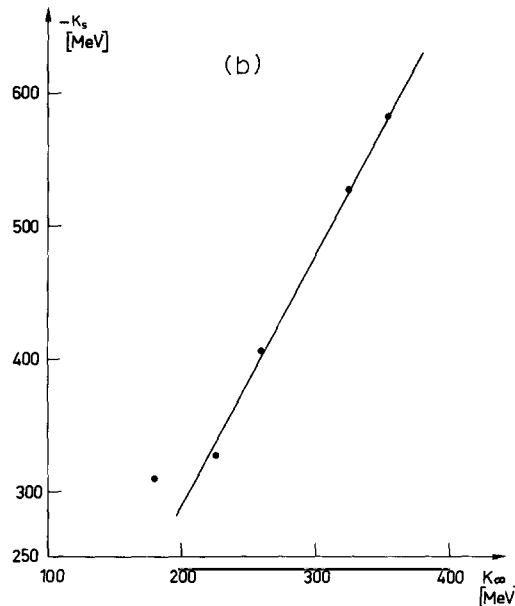


Fig. 14b. Contribution in $A^{-1/3}$ to K_A (coefficient K_S of eq. (6.5)) as a function of K_∞ .

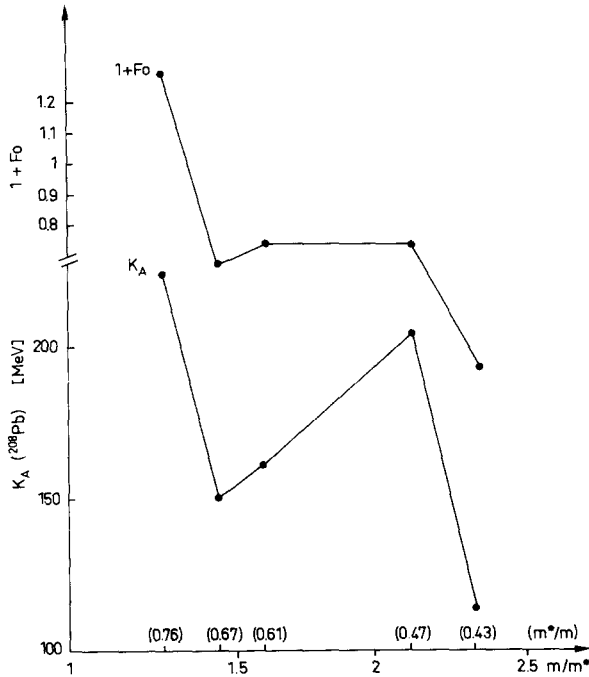


Fig. 15. Variations of the effective compression modulus K_A compared to the variations of the effective mass (in abscissa) and of the Landau parameter F_o (upper curve).

analysis. First of all K_S is large and negative; $K_S \sim -300$ MeV for $K_\infty \sim 200$ MeV. If one considers the various contributions to K_S in formula (6.3), one sees that this implies that K_{surf} is large and negative since the sum of the two other terms in $A^{-1/3}$ is positive. The second point is that K_{surf} varies roughly linearly with K_∞ which guarantees that the surface effects do not destroy the regular behaviour of K_A as a function of K_∞ . These two remarkable properties are easily understood from the model of the nuclear surface developed in section 5.2, or the more complete calculations of ref. [87]. The analysis of the variation of K_A with A just presented relies on the validity of the scaling approximation discussed in section 6.3.

Finally it is instructive to consider the variation of K_A with m^* . From formula (5.11b) ($C = AK_A$), one expects K_A to vary like $\langle(1+F_o)/m^*\rangle$. This behaviour is clearly shown in fig. 15. When F_o remains constant, K_A varies like $1/m^*$. Otherwise, the variations in F_o mostly determine the variations in K_A . On the whole, K_A is really a function of the combination $(1+F_o)/m^*$, i.e. on the compression modulus of nuclear matter, as already shown in fig. 12.

6.3. The transition density

The transition density is given in terms of the RPA amplitudes X_{ph} and Y_{ph} by the following formula:

$$\delta n(r) = \sum_{\text{ph}} (X_{\text{ph}} + Y_{\text{ph}}) \varphi_p(r) \varphi_h(r) \quad (6.6)$$

where $\varphi_p(r)$ and $\varphi_h(r)$ are particle and hole states wave functions, respectively.

The RPA transition densities of the giant monopole resonance of ^{208}Pb , calculated with the Skyrme force S III, are displayed in fig. 16. Neutron and proton transition densities are on the average in phase, and roughly in the ratio N/Z which confirms the isoscalar character of the vibration. The differences which can be observed in the interior, close to the center, are effects of the shell structure. The isoscalar transition density (sum of the neutron and proton transition densities) has a node at about 6.2 fm, i.e. where the total density starts to decrease. The minimum of the transition density lies slightly outside the radius of the nucleus.

These features of the transition density can be reproduced by two simple models of the monopole vibration [40]. In the first one it is assumed that the transition density follows from a simple radial scaling of the ground state density $n_o(r)$:

$$\delta n(r) = -3n_o(r) - r \frac{dn_o(r)}{dr}. \quad (6.7)$$

In this model both the central density and the surface thickness vary. The second model assumes that during the compression of the nucleus, the surface thickness remains constant, only the central density and the radius of the nucleus being allowed to change. In that model, and assuming a Fermi distribution for the ground state density

$$n_o(r) = \frac{n_o}{1 + \exp\{(r - R_o/a_o)\}} \quad (6.8)$$

the transition density is

$$\delta n(r) = -Xn_o(r) - R_o \frac{dn_o(r)}{dr} \quad (6.9)$$

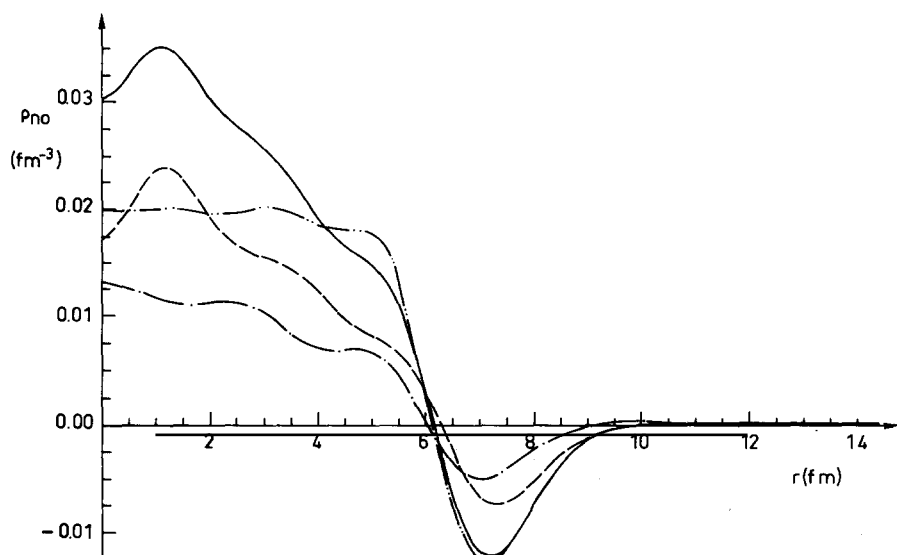


Fig. 16. Transition density of the giant monopole resonance in ^{208}Pb calculated with the interaction S III: ---, neutrons; -·-, protons; —, isoscalar (neutrons + protons); ···, transition density obtained from eq. (6.7).

where:

$$X = 2R_o \frac{\int_0^\infty n_o(r) r dr}{\int_0^\infty n_o(r) r^2 dr} \simeq \frac{3 + (\pi a_o/R_o)^2}{1 + (\pi a_o/R_o)^2}. \quad (6.10)$$

The position r_o of the node obtained with these two models are very close to each other, and also very close to the value obtained for the RPA transition density (see fig. 16). Since the two models yield very similar transition densities it is difficult to say, from their direct comparison with the RPA transition density, whether or not the surface thickness varies during the vibration. A variation of the surface thickness can however be identified on the RPA transition density if one considers the velocity field associated with the collective motion. Such a field is easily obtained by integrating the continuity equation. One gets:

$$u(R) = -\frac{1}{R^2 n_o(R)} \int_0^R r^2 \delta n(r) dr. \quad (6.11)$$

In the case of a pure homologous transformation, $\delta n(r)$ being given by (6.7), $u(R)$ is proportional to R . If $\delta n(r)$ is given by (6.9), $u(R)$ becomes constant in the surface region. Figure 17 shows that the field $u(R)$ obtained from the transition density of fig. 16 is on the average proportional to R , favoring the interpretation of the breathing mode in terms of a simple radial scaling of the ground state density†. This is enforced by the fact that the calculation of K_A (eq. (3.61)) in this model leads to values which become closer and closer to the RPA ones (eq. (3.45)) as A increases (see table 10). That such a model can be so

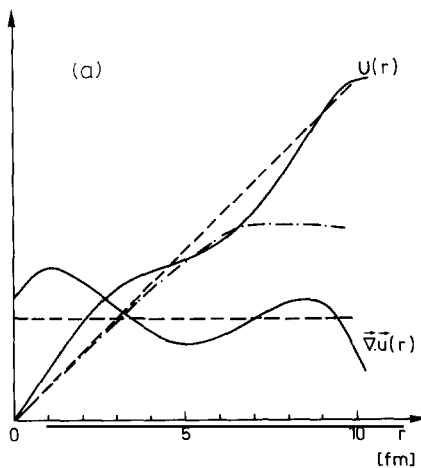


Fig. 17a. Displacement field $u(r)$ (eq. (6.12)) and its divergence $\nabla \cdot u$ calculated with transition densities δn of eq. (6.7) (---) and δn obtained from a RPA calculation in ^{208}Pb with S III (see fig. 16) (—). For comparison, the displacement field calculated with δn of eq. (6.9) is also given (-·-·). All the densities are normalized so as to give the same $B(E_o)$.

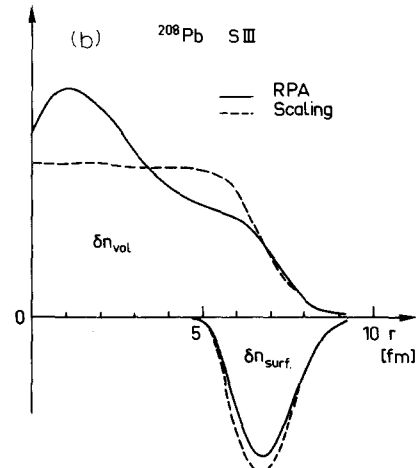


Fig. 17b. Surface and volume contributions to the transition density (see eqs. (6.11b, 6.11c)).

† It has recently been shown that the velocity field in the surface is an increasing exponential [93].

Table 10
Effective compression moduli obtained by performing a scale transformation on the ground state density (see formula (3.61)). In parenthesis we give the value obtained by constrained Hartree-Fock (eq. (3.45))

| | S III | S IV | Sk _a |
|-------------------|-------------|-----------|-----------------|
| ¹⁶ O | 200 (147) | 181 (138) | 147 (117) |
| ⁴⁰ Ca | 227 (186) | 203 (171) | 165 (144) |
| ⁹⁰ Zr | 241.5 (217) | 218 (197) | 175 (160) |
| ²⁰⁸ Pb | 242 (224) | 217 (204) | 174 (161) |
| N.M. | 356 | 325 | 263 |

good in heavy nuclei is of course connected with the fact that the mode depletes almost entirely the sum-rule associated with the operator r^2 .

Knowing the displacement field $\mathbf{u}(R)$, one can separate the transition density into two components:

$$\delta n = \delta n_{\text{vol}} + \delta n_{\text{surf}} \quad (6.12a)$$

with:

$$\delta n_{\text{vol}} = n_o \nabla \cdot \mathbf{u} \quad (6.12b)$$

and:

$$\delta n_{\text{surf}} = \mathbf{u} \cdot \nabla n_o. \quad (6.12c)$$

δn_{surf} is associated with the displacement of the surface, while δn_{vol} is due to the local compression of the matter, proportional in each point to $\nabla \cdot \mathbf{u}$. The quantity $\nabla \cdot \mathbf{u}$ is plotted in fig. 17a. It can be seen that $\nabla \cdot \mathbf{u}$ is on the average equal to 3, the value obtained for $\mathbf{u} = \mathbf{r}$. A plot of δn_{vol} and δn_{surf} is given in fig. 17b. It is important to notice that δn_{vol} is far from being negligible in the surface region.

6.4. The transition potential

When calculated with a zero-range interaction like the Skyrme interaction, the transition potential is local and can be written as follows:

$$\delta V(r) = f_o(r) \delta n(r) \quad (6.13)$$

where $f_o(r)$ is a function which depends only on the ground state density and the kinetic energy density. To simplify the discussion, we shall use a Thomas-Fermi approximation for the later quantity so that f_o depends only on the local density $n_o(r)$. Up to a normalisation factor, $f_o(r)$ is then the local Landau parameter introduced in section 5.1. More precisely one has:

$$f_o(r) = \frac{2\varepsilon_F(r)}{3n_o(r)} F_o(r). \quad (6.14)$$

The transition potential $\delta V(r)$ can be separated in two parts, in the same way as the transition density:

$$\delta V(r) = \delta V_{\text{vol}}(r) + \delta V_{\text{surf}}(r) \quad (6.15a)$$

with:

$$\delta V_{\text{vol}} = f_o(r) \delta n_{\text{vol}} = f_o(r) \nabla \cdot u n_o \quad (6.15b)$$

$$\delta V_{\text{surf}} = f_o(r) \delta n_{\text{surf}} = f_o(r) u \cdot \nabla n_o = u \cdot \nabla V_o(r) \quad (6.15c)$$

where $V_o(r)$ is the ground state potential. The term δV_{surf} is the part of the potential which is associated with the displacement of the surface. In the case of the giant quadrupole resonance for which $\nabla \cdot u = 0$, this is the only component of the transition potential. Since $\nabla \cdot u \neq 0$ for the monopole vibration, one has in each point of the system a compression which generates a change in the local potential; this is δV_{vol} . A plot of δV_{vol} and δV_{surf} is given in fig. 18a. It is important to notice that δV is very much different from δV_{surf} in the surface region, because δV_{vol} is not negligible at all in the surface and interferes destructively with δV_{surf} . The effect is of the order of 35%. Thus the "effective surface potential" to be used in the calculation of the monopole resonance is only 65% of the one used in the calculation of the giant quadrupole resonance.

The behaviour of δV_{vol} in the surface region can be understood from very general arguments. First of all it has been noticed in section 2.3 that F_o must be smaller than -1 for densities lower than 2/3 of the saturation density (see fig. 2). Therefore one expects $f_o(r)$ to be negative in the surface. Moreover, the shape of $f_o(r)$ in the surface is quite universal as can be seen from the following argument. In the local

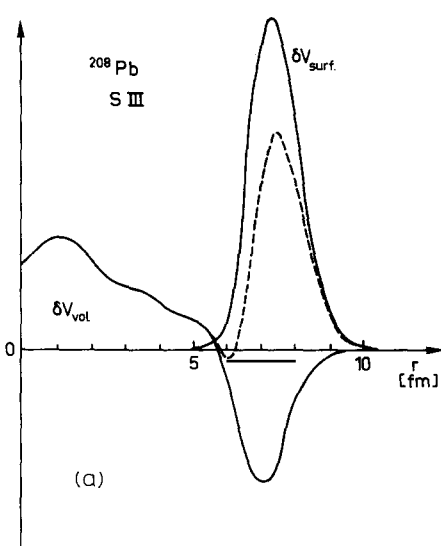


Fig. 18a. Surface and volume contribution to the transition potential (see eqs. (6.15b), (6.15c)). The sum of the two terms is indicated by dotted lines.

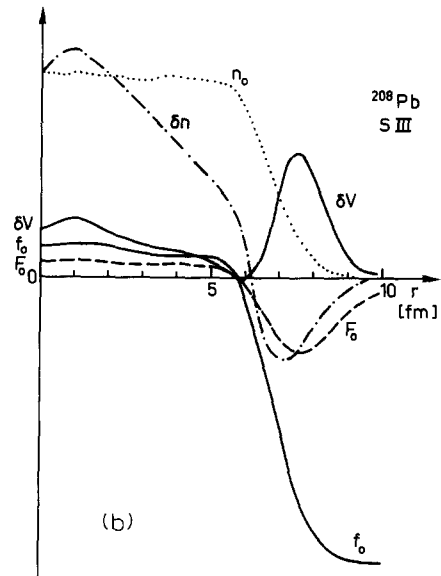


Fig. 18b. Ground state density $n_o(r)$. Transition density $\delta n(r)$. Transition potential $\delta V(r)$. Landau parameters $F_o(r)$ and $f_o(r)$ (see eq. (6.4)).

density approximation, $f_o(r) = f_o(n_o(r))$. Therefore:

$$f_o(r) = \frac{dV_o}{dn} \Big|_{n_o(r)} = \frac{(dV_o/dr)}{(dn_o/dr)}. \quad (6.16)$$

Assuming that both $n_o(r)$ and $V_o(r)$ have a Fermi shape with radii R_1 and R_2 respectively:

$$n_o(r) = \frac{n_o}{1 + \exp\{(r - R_1)/a\}}, \quad V_o(r) = \frac{-V_o}{1 + \exp\{(r - R_2)/a\}}. \quad (6.17)$$

One gets:

$$f_o(r) = -\frac{V_o}{n_o} \operatorname{ch}^2\left(\frac{R_2 - R_1}{2a}\right) \left[1 + \operatorname{th}\left(\frac{R_2 - R_1}{2a}\right) \operatorname{th}\left(\frac{r - R_2}{2a}\right) \right]^2. \quad (6.18)$$

The change of f_o in the surface is given by:

$$\Delta f_o = 2 \frac{V_o}{n_o} \operatorname{sh}\left(\frac{R_2 - R_1}{a}\right). \quad (6.19)$$

In ^{208}Pb , typical parameters are: $R_2 \sim 7.3$ fm, $R_1 \sim 6.8$ fm, $a \sim 0.5$ fm. Taking $V_o \sim 50$ MeV and $n_o \sim 0.17$ fm $^{-3}$ one gets $\Delta f_o \sim 700$ MeV fm 3 which is quite appreciable. The quantity $f_o(r)$ is plotted in fig. 18b together with various other quantities. One sees that it has the shape predicted by the formula (6.18). The change in the surface has the same order of magnitude as the one which we have just calculated. (See also the discussion of this effect in ref. [92].)

6.5. Review of other calculations

Besides the ones we have extensively discussed here, many calculations of the monopole excitations of nuclei have been performed up to now, using different formalisms. The first calculations were carried out in simple macroscopic models, such as the liquid drop model [39], or refined versions of it [42]. Many authors have used variational methods, such as the constrained Thomas–Fermi method [43, 44] or the Hartree–Fock method [45]. Calculations have also been performed using the time-dependent Hartree–Fock [46] approach, the generator coordinate method [47, 48, 49, 50], the hyperspherical formalism [51], Migdal’s theory [52, 53] and the Random Phase Approximation [54, 55, 56].

If one forgets about the macroscopic models, the limitations of which we have already discussed, or those papers discussing only light nuclei [57], the other calculations can be grouped into two categories: those which are self consistent and those which are not. We have already pointed out that it is hard to extrapolate from non self-consistent calculations of nuclei to nuclear matter.

The self-consistent calculations are carried out within more or less the same theoretical framework as the RPA calculations presented here. Namely they use phenomenological effective interactions and independent particle wave functions as a starting point. Some of these calculations could, in principle, go beyond RPA, such as the generator coordinate or the time dependent Hartree–Fock methods. In practice, however the calculations are performed assuming a definite collective mode, which is a limitation. In heavy nuclei, where such a collective mode is well defined and corresponds precisely to

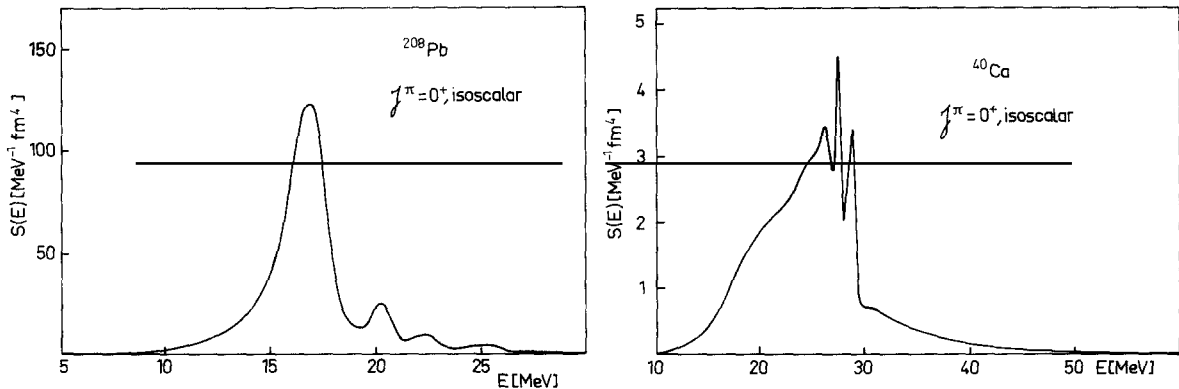


Fig. 19. Monopole strength function in ^{208}Pb and ^{40}Ca , calculated with the interaction S III, with a correct treatment of the continuum. I acknowledge N.V. Giai for communication of this figure.

the ansatz usually used one recovers the RPA results, which indicates that anharmonic corrections are indeed small. Those corrections are not found small in light nuclei such as ^{16}O [58], but there, the RPA results indicate also that the “breathing mode” is much less well defined.

The RPA calculations we have presented, have been performed by discretizing the single particle continuum [29]. A proper treatment of the continuum has been done with the Skyrme interaction [59, 60, 61]. The results of such a calculation is given in fig. 19. For heavy nuclei down to ^{40}Ca , it can be seen that the predictions concerning the average location of the strength agrees remarkably well with our calculations. In ^{16}O the discretized basis yields a broad distribution but located too high. The weakness of the discretization of the continuum in the case of ^{16}O has also been pointed out in ref. [58]. Other calculations using sum rules can also be compared directly with our calculations of the restoring force parameter K_A . These calculations can be expected to be very accurate. Again one finds excellent agreement in heavy nuclei with our results. (Compare table 10 with table 5 of ref. [34].)

Let us finally mention recent hydrodynamical calculations, which are actually approximations to the RPA, similar to the one presented in section 5.1 [85, 86]. When comparison is possible, one finds again agreement with RPA.

7. The effective mass

The discussion of the giant monopole resonance would not be complete without a more careful study of the influence of the single particle spectrum on the properties of the collective mode. This involves a discussion of the effective mass of a nucleon in nuclear matter to which we now proceed.

7.1. The concept of effective mass

Let us recall the definition, already given, in section 2.1, of the effective mass of a nucleon with momentum p and energy ϵ_p :

$$\frac{1}{m^*} = \frac{1}{p} \frac{d\epsilon_p}{dp}. \quad (7.1)$$

The energy ε_p can be split into two parts:

$$\varepsilon_p = \frac{p^2}{2m} + \Sigma(p, \varepsilon_p) \quad (7.2)$$

where $p^2/2m$ is the kinetic energy, and $\Sigma(p, \varepsilon_p)$ is the self-energy resulting from the interaction of the nucleon with the nuclear medium. Actually, in the present-case Σ stands for the real part of the mass operator. The self-energy depends on two variables, a momentum and an energy; here the energy is that defined by eq. (7.2) which is therefore a self-consistent equation for ε_p . Taking the derivative of this equation with respect to p , one easily gets:

$$\frac{m}{m^*} = \frac{1 + (m/p) \partial \Sigma / \partial p}{1 - \partial \Sigma / \partial \varepsilon_p}. \quad (7.3)$$

The numerator and the denominator of expression (7.3) have two distinct physical origins. The numerator arises from the non-locality of the average nuclear potential, the denominator comes from its frequency dependence. The process in fig. 20a corresponds to the non-locality generated by exchange forces. The processes in figs. 20b,c, in which a nucleon couples to a particle-hole pair of the medium or to a collective excitation, generates frequency dependence. These last processes are especially important close to the Fermi surface where they produce a significant increase in the effective mass, as shown by the calculations of ref. [69]. They are not included in the self-consistent calculations described here, where only the process of fig. 20a is explicitly taken into account. Some calculations of nuclear matter indicate that for $k = k_F$ process 20c contributes 2/3, and process 20b for 1/3, the total effective mass being close to the bare mass. Thus, on the Fermi surface, the non-locality and the frequency dependence of the average nuclear field roughly cancel each other. We show in the next section that there is some experimental evidence which indicates that this indeed occurs in finite nuclei.

7.2. Effective mass and static properties of nuclei

The analysis of binding energies and separation energies reveals that the single particle potential must be momentum or energy dependent, and more precisely that nucleons in nuclear matter must have, on the average, an effective mass smaller than unity. This is easily seen using a simple argument originally due to Weisskopf [88], and generalized in a straightforward manner to include the effects of density dependent interactions. The argument goes as follows. Let ε_p be the energy of a particle with

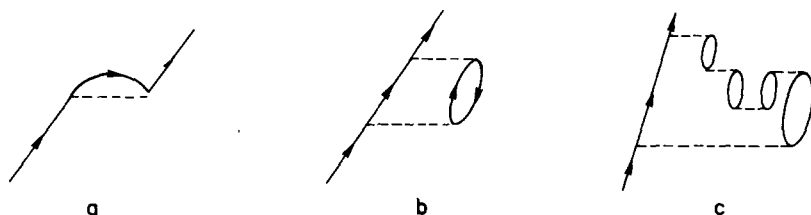


Fig. 20. Microscopic processes which contribute to the momentum dependence (a) and to the energy dependence (b,c) of the mass operator (eq. (7.2)).

momentum p . We can write:

$$\varepsilon_p = p^2/2m + U(p) + R \quad (7.4)$$

where $U(p) + R$ is the potential energy. R is the so-called rearrangement energy coming from the density dependence of the underlying effective interaction. Assuming that this potential energy is generated by two-body forces, and that the state of the system can be well described by independent particle wave-functions, the binding energy $-B/A$ can be written:

$$-\frac{B}{A} = \langle p^2/2m \rangle + \frac{1}{2}\langle U(p) \rangle. \quad (7.5)$$

Now B/A is equal to the separation energy S , i.e. the energy required to remove a nucleon at the top of the Fermi sea:

$$-S = P_f^2/2m + U(P_f) + R. \quad (7.6)$$

From (7.5) and (7.6) one gets:

$$S = -\frac{1}{5} \frac{P_f^2}{2m} + U(P_f) - \langle U(p) \rangle + R \quad (7.7)$$

which indicates that if $R = 0$, U must depend upon p otherwise S is negative and the system is unbound. Let us assume that $U(p)$ can be expanded around $U(p=0)$:

$$U(p) = U(0) + a p^2/2m \quad (7.8)$$

where a is related to the effective mass by:

$$m/m^* = 1 + a. \quad (7.9)$$

This form of momentum dependence is very crude but good enough to get orders of magnitudes. The relations (7.7) and (7.8) imply

$$\frac{m}{m^*} = \frac{3}{2} + \frac{5m}{P_f^2} \left(\frac{B}{A} - R \right) \quad (7.10)$$

i.e. $m^* \sim 0.4m$ for $R = 0$.

With modern effective interactions, the saturation is achieved with a combination of density dependent and velocity dependent (or finite range) forces. It is observed, in agreement with the preceding argument, that in order to achieve saturation with an effective mass close to the bare mass, one needs a strong density dependent component in the interaction. The relation (7.10) shows that in order to get $m^* \sim m$, one must have $R \sim 24$ MeV, a rather large value.

A more direct evidence on the momentum dependence, or equivalently the energy dependence of the average nuclear potential is provided by the analysis of scattering experiment. It is found that the depth of the optical potential for scattering of a nucleon on a nucleus depends on the energy of the

incoming nucleon. Such an energy dependence is compatible with an effective mass $m^*/m \approx 0.7$ for an energy between 10 MeV and 70 MeV [69].

The deep-lying single-particle states are found at energies compatible with a potential depth of about 70 MeV, i.e. 20 MeV more than the depth of the potential required to fit the levels at the Fermi-surface. This is another indication that the effective mass, on the average, is smaller than unity.

It is quite remarkable however that the single-particle levels near the Fermi-surface can be fitted with a static local potential well [66]. This shows that $m^*/m \approx 1$ near the Fermi surface.

Thus the effective mass increases near the Fermi surface. The origin of this phenomenon has been discussed in ref. [67]. As we already mentioned in the preceding section, it can be attributed to the process of figs. 20b,c. That the same effect could explain the single particle spectra of finite nuclei is strongly suggested by the calculations of refs. [68, 62].

7.3. Effective mass and giant quadrupole resonance

In the self-consistent calculations which we are discussing, the giant quadrupole resonances appear as very collective modes, all the strength being concentrated in a single state in double closed shell nuclei such as ^{16}O and ^{40}Ca , and in two states in heavier nuclei such as ^{90}Zr and ^{208}Pb (see fig. 21).

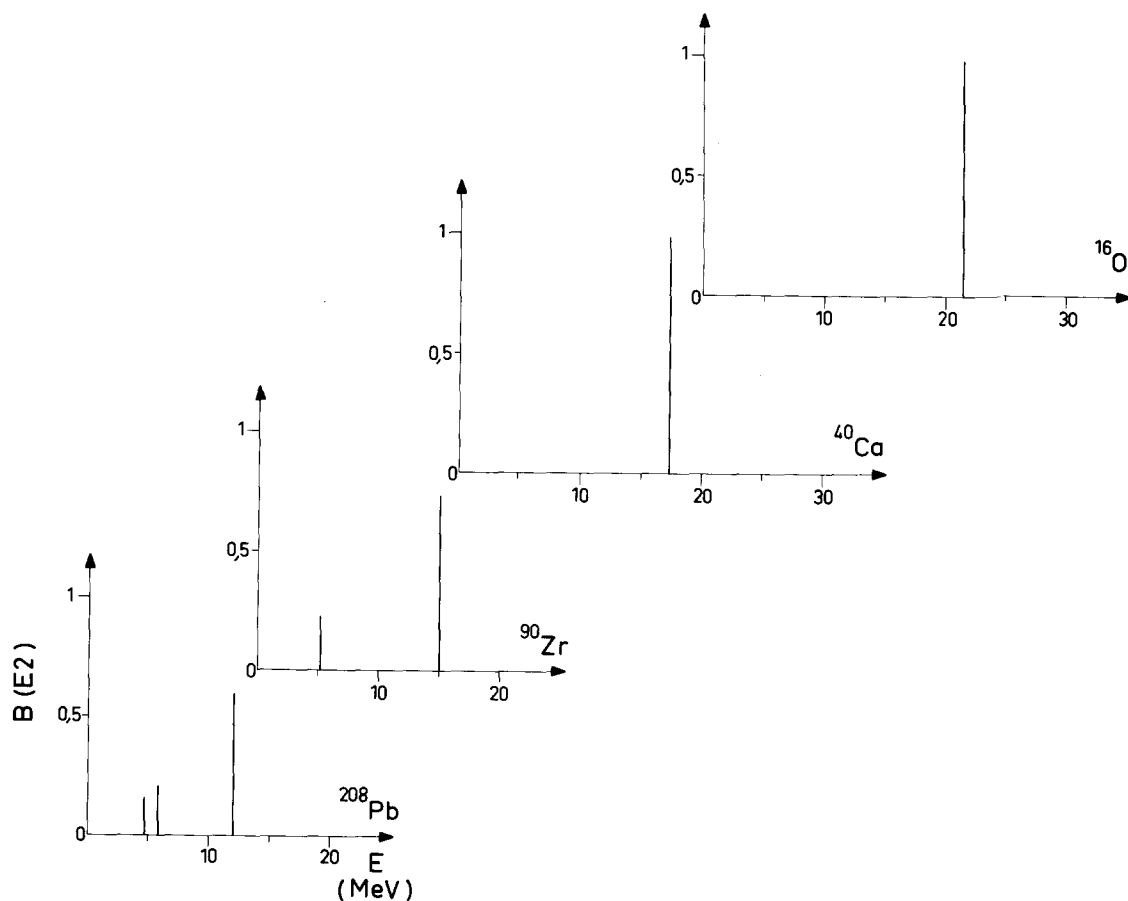


Fig. 21. Giant isoscalar quadrupole resonance in closed shell nuclei, calculated with the interaction S III.

To understand the frequencies of the giant quadrupole resonance, it is convenient to use the approximation discussed in section 5.1 for the monopole resonance. Assuming that the mode is described by a velocity field proportional to $\mathbf{u} = \nabla r^2 P_2(\cos \theta)$ one gets the following results for the mass parameter and the restoring force:

$$B_2 = 2m\langle r^2 \rangle_o. \quad (7.11a)$$

$$C_2 = \frac{24}{5}\langle \epsilon_F(1 + F_2/5) \rangle_o. \quad (7.11b)$$

The mass parameter B_2 is proportional to the expectation value of r^2 in the ground state. If one takes into account that all the interactions we use are fitted in order to reproduce the nuclear radii, one expects very little differences in the mass parameters obtained with various interactions. In this sense, we may say that the mass parameter does not depend upon the interactions, in particular it is insensitive to changes in the effective mass. This last property can be understood as a result of a cancellation. The mass parameter contains indeed two contributions, one from the unperturbed quasiparticle energies:

$$B^{(1)} = 2m \left\langle \frac{m}{m^*} r^2 \right\rangle \quad (7.12a)$$

the other one coming from the particle-hole interaction:

$$B^{(2)} = 2m \left\langle \frac{m}{m^*} r^2 F_1 \right\rangle. \quad (7.12b)$$

Using eq. (2.10) which relates the effective mass to F_1 , one sees clearly the elimination of m^* in the expression of the mass parameter. This cancellation can be understood by invoking the concept of local Galilean invariance, as was done by Bohr and Mottelson [36]. The argument goes as follows. Let us assume that the nucleons are moving in a velocity dependent potential $U(k)$; they acquire an effective mass given by the expression:

$$m^*/m = (1 + \partial U / \partial T_k)^{-1}$$

where $T_k = \hbar^2 k^2 / 2m$. When the particles are moving with an average velocity v , local Galilean invariance implies that the velocities which determine the interaction energy of the particles have to be measured relatively to v . (This argument applies provided the forces which generate the effective mass are of short range.) In other words, the potential energy of a particle with momentum k will be $U(k - mv/\hbar)$. Expanding this potential energy in first order in v one recognizes a new coupling term proportional to $\mathbf{k} \cdot \mathbf{v}$, which restores Galilean invariance, and which is responsible for the term $B^{(2)}$ given by eq. (7.12b).

The interactions have an important effect on the restoring force C_2 , through the effective mass contained in ϵ_F and the Landau parameter F_2 . Now F_2 is typically of the order of -0.3 and its contribution, which is cut down by a factor 5, can be ignored. Therefore the restoring force C_2 depends mainly on ϵ_F , i.e. on the effective mass. The origin of this restoring force is the quadrupole distortion of the local Fermi surface [16, 85]. Since the velocity field is divergence-free there is no local compression, which explains why F_o does not appear in the expression for C_2 . Thus the restoring force for the giant

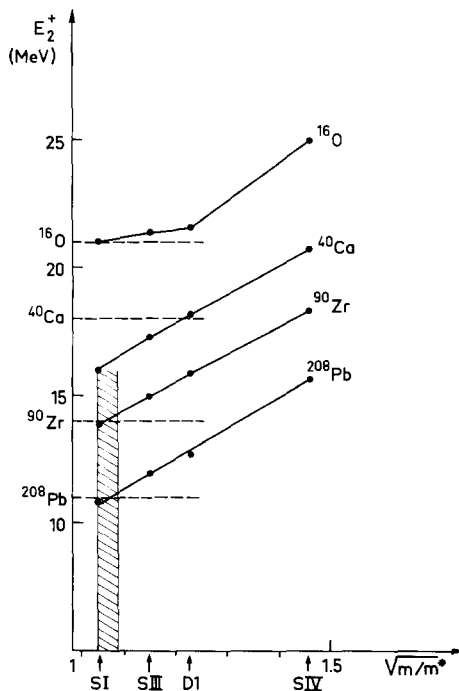


Fig. 22. Energy of the giant quadrupole resonance (E_2^+) as a function of $\sqrt{m/m^*}$. The horizontal dotted lines indicate the experimental values.

quadrupole resonance is proportional to the average, over the nuclear density, of the inverse of the effective mass calculated on the Fermi surface, at the local density.

If m^* is a smooth function of the density, which is a reasonable assumption (see fig. 2), one can expect this average to be mostly determined by the value of m^* in nuclear matter. Therefore one expects the frequency of the giant quadrupole resonance $\omega_2 = \sqrt{C_2/B_2}$ to vary with m^* like $\sqrt{m/m^*}$. This behaviour is confirmed by our numerical calculations as shown in fig. 22. For heavy nuclei, experimental data favor an effective mass close to 1 ($m^*/m \sim 0.9$ from fig. 22) while in light nuclei a smaller effective mass seemed to be required. This may be an indication that the coupling with the collective modes, which is responsible for the enhancement of the effective mass at the Fermi surface in heavy nuclei, may be less important in light nuclei.

7.4. Further remarks

An important limitation of the self-consistent calculations presented here is their inability to reproduce correctly the single particle energies. In particular they predict a constant effective mass, i.e., they neglect the variation of the effective mass with energy. An obvious improvement of the theory would be to include properly the coupling of particles to vibrations, as given by diagrams 20b,c. Such calculations have already been undertaken but they are complicated by divergence problems, particularly important if one derives the particle-hole interaction from a Skyrme force [23].

It has been argued recently [70] that those processes 20b,c should be better left out in the calculation of high frequency modes. One should indeed consider at the same time more complicated couplings which cannot be simply represented by fig. 20c. These couplings are responsible for the spreading of the

strength function but they may be expected not to move significantly the mean energy of a high frequency vibration. Therefore, in the calculation of this mean energy, it may be better to neglect them and at the same time the processes 20b,c which contribute to the effective mass. In other words, it is argued that the high frequency vibrations should be calculated with an effective mass which does not include the coupling to vibrations, i.e. $m^*/m \sim 0.7$. This argument does not apply to the calculation of low-lying collective states in which it is probably better to use empirical single particle energies corresponding to $m^*/m \sim 1$. We are thus led to use different values of the effective mass depending upon the energy of the vibration which we calculate. Up to now no precise calculation has been performed to fix the exact magnitude of this “energy dependence” of the effective mass. The self-consistent calculations would allow a rather small variation, as one can deduce from the analysis of the giant quadrupole resonance (section 7.2) and the energy gap around the Fermi surface (section 2.3.2).

8. Present experimental data on the giant monopole resonance

8.1. Preliminary remarks

For a long time, the giant dipole resonance has been the only “giant resonance” observed in nuclei. This resonance corresponds to a collective excitation of the whole nucleus in which the protons move in opposite phase with the neutrons. Such a mode is easily excited by an oscillating electromagnetic field, spacially uniform, i.e. by long wavelength photons (the wavelength of 13 MeV photons is of the order of 100 fm, i.e. much larger than the size of nuclei). Such long wavelength photons cannot excite, with an appreciable cross section, modes which have a more complicated structure, and the total cross section for photo-absorption in the 10–20 MeV range, is dominated by the giant dipole resonance. This is no longer the case for other projectiles, such as electrons or hadrons. Figure 23 shows some recent data concerning the inelastic scattering of α -particles on ^{90}Zr [71]. The giant resonance, here the quadrupole, appears as a bump in the nuclear continuum at an excitation energy of 10–20 MeV. In the best cases when the experimental background has been almost suppressed, the continuum is made of real transitions having complicated structures. Its strength varies slowly with the energy. On the contrary, the giant resonance region is characterized by a rapid variation of the cross section with the excitation energy. To obtain the cross section for the excitation of the giant resonance, one has to subtract the smooth background. Thus, unlike the case of photo-absorption, the cross section for the excitation of the giant resonances by hadrons constitutes in general only a small fraction of the total cross section. The subtraction of the background is one of the major uncertainties (not the only one) in the determination of the strength or the percentage of the sum rule carried by the resonance. One generally considers that this uncertainty is of the order of 20% or more [72, 73]. This is a difficulty since the absolute magnitude of the peak can help in identifying the nature of the resonance, through sum-rule arguments. For example the peak in fig. 23 cannot correspond to a monopole excitation because the monopole sum-rule would be exceeded; on the other hand it is found to deplete 60% of the quadrupole sum rule; the quadrupole assignment is confirmed by the analysis of the angular distribution.

The study of the angular dependence of the cross section is in fact the best way to establish the multipolarity of a vibration. For example the peak in fig. 23 is much reduced at 20.5° compared to what it is at 17.5° and 22.5° , a behaviour compatible with $L = 2$ and $L = 0$ vibrations. The angular distributions for monopole and quadrupole vibrations differ significantly at small angles. This is clearly seen on fig. 24. The cross section at zero degree is larger for monopole. There is a deep minimum for the

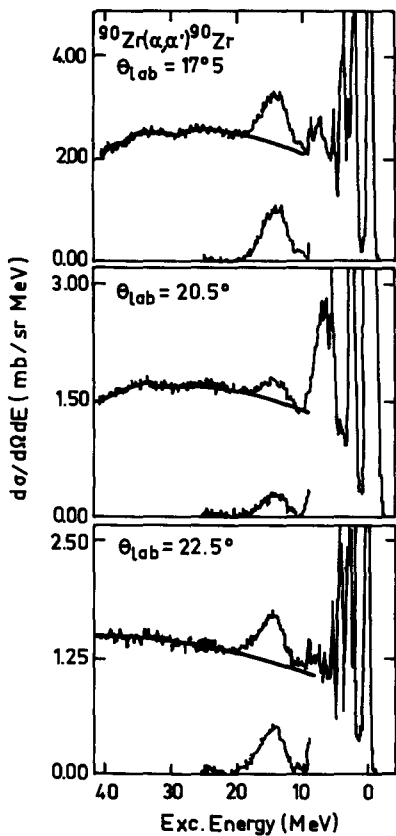


Fig. 23. Inelastic scattering of α -particles on ^{90}Zr : (from ref. [71]). The cross section is given at 3 different angles. The background subtraction is indicated.

monopole around 4° . This allows a clear separation of the two modes which have similar frequencies and therefore are mixed in the cross section (see fig. 25).

This behaviour of the angular distribution at small angles has been used as a “signature” for the monopole excitation in most of the recent experiments.

8.2. Experiments

We enumerate the various experiments which have been performed up to now and which indicate the existence of a collective monopole mode of vibration of nuclei.

(a) Inelastic scattering of α -particles

In ref. [77] one finds the first possible direct observation of a monopole resonance in the (α, α') spectra of ^{206}Pb , ^{208}Pb and ^{209}Bi with 120 MeV α -particles. The “new resonance” was found to deplete the whole monopole sum rule. Unfortunately its angular distribution was also compatible with an $L = 2$ excitation. More recent experiments [74] were performed at very small angles (3°), where as we have seen, the difference between the $L = 0$ and $L = 2$ angular distribution is quite significant. These experiments show that the angular distribution of the new resonance is characteristic of a monopole excitation. Despite a large background – the giant resonance cross section is less than 20% of the total

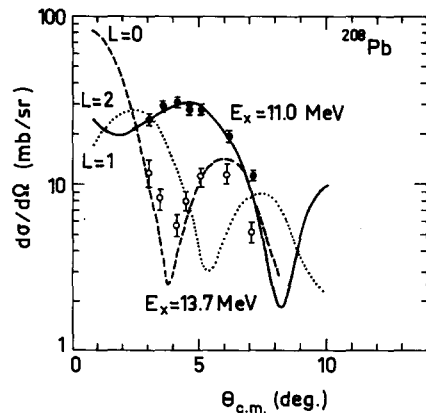


Fig. 24. Inelastic scattering of α -particles on ^{208}Pb (from ref. [74]). Angular distribution at small angles.

cross section – this experiment has brought the first clear evidence for the existence of a giant monopole resonance.

(b) Inelastic scattering of ^3He -particle

These are again scattering experiments at small angle, using 108 MeV ^3He projectiles and ^{208}Pb and ^{90}Zr targets. These experiments show less background than the ones of ref. [74]. The giant monopole resonance is clearly identified (see fig. 25).

(c) Inelastic scattering of deuterons

This is the first report on the observation of a giant monopole resonance at an energy of about $80 \times A^{-1/3}$ MeV [78]. This report was based upon a comparison of deuterons and alpha scattering on ^{40}Ca , ^{90}Zr and ^{208}Pb . It was found that there were extra strength for the deuterons, at an energy close to that of the giant dipole resonance. The deuterons excite very weakly the isovector dipole vibration; furthermore the extra strength seemed to have an angular distribution in agreement with a $L = 0$ excitation. However this experiment was not conclusive. It has been recently repeated at small angles, with a small background: the giant resonance cross section is more than a half of the total cross section. The monopole is clearly identified by its angular distribution [79] in ^{90}Zr , ^{120}Sn , ^{208}Pb (see fig. 26).

(d) Inelastic scattering of electrons

This is again one of the first reports on the possible monopole resonance at an energy of about

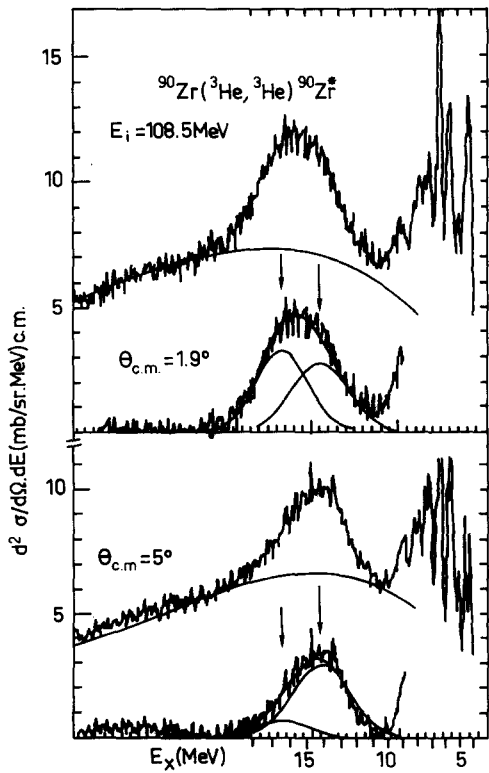


Fig. 25. Inelastic scattering of ^3He on ^{90}Zr (from ref. [75]). Two different angles are shown. The analysis of the giant resonance in two components is shown. The shift of the peak to a higher energy at 1.9° is due to the enhancement of the monopole cross section at this angle.

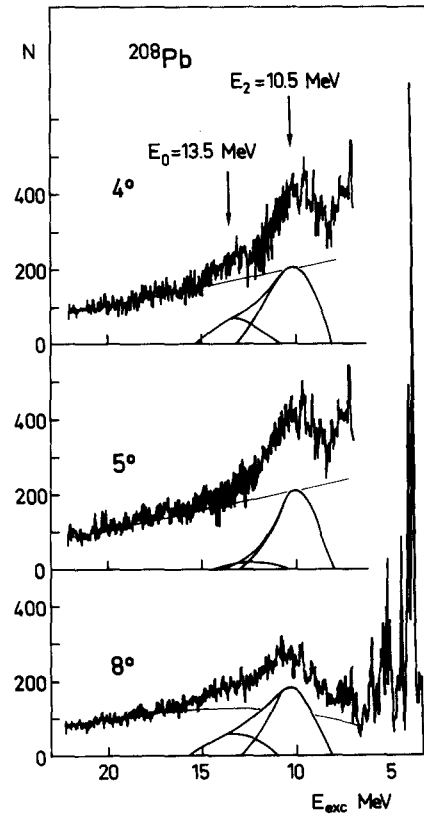


Fig. 26. Inelastic scattering of deuteron on ^{208}Pb . The minimum of the monopole cross section at 5° is clearly seen (from ref. [79]).

$80A^{-1/3}$ MeV in the nuclei ^{40}Ca , ^{90}Zr and ^{208}Pb [81]. However the experiment was hard to analyze and very model dependent results were obtained. In particular the contribution of the giant dipole resonance had to be subtracted from the electron data. Assuming the remaining strength to be monopole, then, for ^{208}Pb , one finds that 100% or 10% of the monopole sum-rule is depleted depending on whether the Goldhaber-Teller or the Jensen-Steinwedel model is used for the dipole resonance.

(e) Inelastic scattering of protons

After the small angle scattering experiments were performed, some data obtained in proton scattering experiments have been reanalyzed [76]. The new analysis takes into account the possibility of exciting the monopole resonance together with the dipole and quadrupole ones. This new analysis is compatible with a systematic existence of a giant monopole resonance in nuclei. Its excitation energy is about $80A^{-1/3}$ MeV. The percentage of the energy weighted sum rule depleted by the resonance is reported to be nearly 100% in nuclei with $A \geq 90$, while it is only 30% in ^{58}Ni and at most 15% in ^{40}Ca .

The results of all these experiments are summarized in the table 11. The experiments on light nuclei such as ^{40}Ca are not yet really conclusive [76, 82] although some monopole strength could have been seen in ^{40}Ca at 20.6 MeV in inelastic pion scattering [80].

8.3. Estimate of the compression modulus

The empirical data are compatible with the results of theoretical calculations such as those described in section 6. The observed resonance exhausts most of the energy weighted sum rule for nuclei with $A > 90$ in agreement with the calculation. In the case of light nuclei the resonance seems to disappear, but the RPA calculations anyhow are not good enough for those nuclei, e.g. they do not predict at all the broadening of the giant quadrupole resonance (see fig. 21). The energy of the monopole resonance is reported consistently in all experiments to be about $80 \times A^{-1/3}$ MeV.

Table 11
Experimental data on the giant monopole resonance

| Nucleus | Excitation energy (MeV) | Width (MeV) | % EWSR | Reaction | Energy | Reference |
|-------------------|-------------------------|---------------|--------------|-------------------------------|---------|-----------|
| ^{209}Bi | 13.7 ± 0.3 | 2.5 ± 0.4 | 100 ± 25 | (α, α') | 120 MeV | 77 |
| ^{208}Pb | 13.9 ± 0.3 | 2.5 ± 0.6 | 110 ± 25 | (α, α') | 120 MeV | 77 |
| | 13.7 ± 0.4 | 3.0 ± 0.5 | 105 ± 20 | (α, α') | 96 MeV | 74 |
| | 13.4 ± 0.5 | 3.0 ± 0.5 | 90 ± 20 | (p, p') | 61 MeV | 76 |
| | 13.5 ± 0.3 | 2.8 ± 0.3 | | (d, d') | 108 MeV | 79, 82 |
| | 13.2 ± 0.3 | 2.8 ± 0.3 | 94 | $(^3\text{He}, ^3\text{He}')$ | 108 MeV | 75 |
| ^{206}Pb | 14.0 ± 0.3 | 2.5 ± 0.4 | 100 ± 25 | (α, α') | 120 MeV | 77 |
| ^{197}Au | 13.6 ± 0.5 | 3.0 ± 0.5 | 100 ± 25 | (p, p') | 61 MeV | 76 |
| ^{154}Sm | 15.5 ± 0.5 | 2.5 ± 0.5 | 100 ± 25 | (p, p') | 67 MeV | 76 |
| ^{144}Sm | 15.1 ± 0.5 | 2.9 ± 0.5 | 100 ± 20 | (α, α') | 96 MeV | 74 |
| | 15.5 ± 0.5 | 2.5 ± 0.5 | 100 ± 25 | (p, p') | 67 MeV | 76 |
| ^{120}Sn | 16.8 ± 0.5 | 3.5 ± 0.5 | 100 ± 25 | (p, p') | 61 MeV | 76 |
| | 16.1 ± 0.4 | 3.0 ± 0.3 | | (d, d') | 108 MeV | 79, 82 |
| ^{90}Zr | 17.5 ± 0.5 | 3.0 ± 0.5 | 60 ± 25 | (p, p') | 61 MeV | 76 |
| | 17.2 ± 0.5 | 4.3 ± 0.3 | | (d, d') | 108 MeV | 79, 82 |
| | 16.4 ± 0.3 | 3.6 ± 0.3 | 60 | $(^3\text{He}, ^3\text{He}')$ | 108 MeV | 75 |
| ^{58}Ni | 19.8 ± 0.5 | 3.5 ± 0.5 | 30 ± 10 | (p, p') | 61 MeV | 76 |

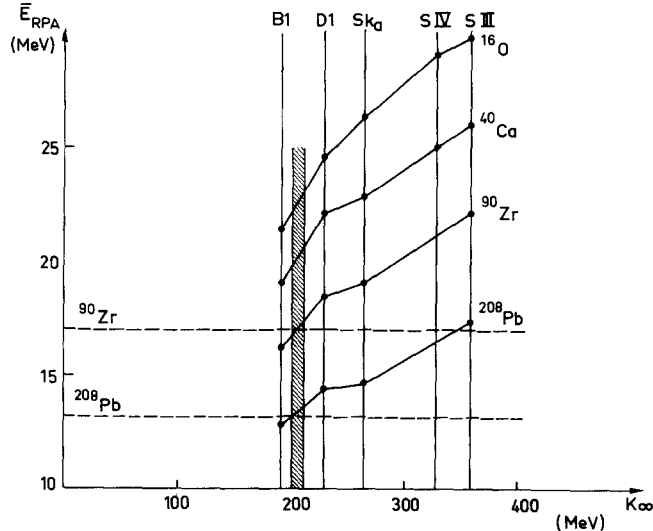


Fig. 27. The energy of the monopole resonance (\bar{E}_{RPA}) as a function of K_∞ . The horizontal dotted lines indicate the experimental data.

In figs. 27 and 28, we have compared our results with these experimental data. One sees that they are compatible with a single value of the compression modulus $K_\infty \sim 210$ MeV. Actually there exists some uncertainty of this value of K_∞ which, to some extent, comes from the experimental determination of the energy, and to the numerical approximations involved in our calculations. Most of the uncertainty however comes from the fact that the variation of the excitation energy with K_∞ is not perfectly regular. Thus we have proposed for K_∞ the value 210 MeV ± 30 MeV [22]. This uncertainty of 30 MeV is only indicative. It means simply that it would be very hard to reproduce within the theory we have used the properties of the giant monopole resonance with a force having a compression modulus outside the range 180–240 MeV. We cannot however exclude such a possibility.

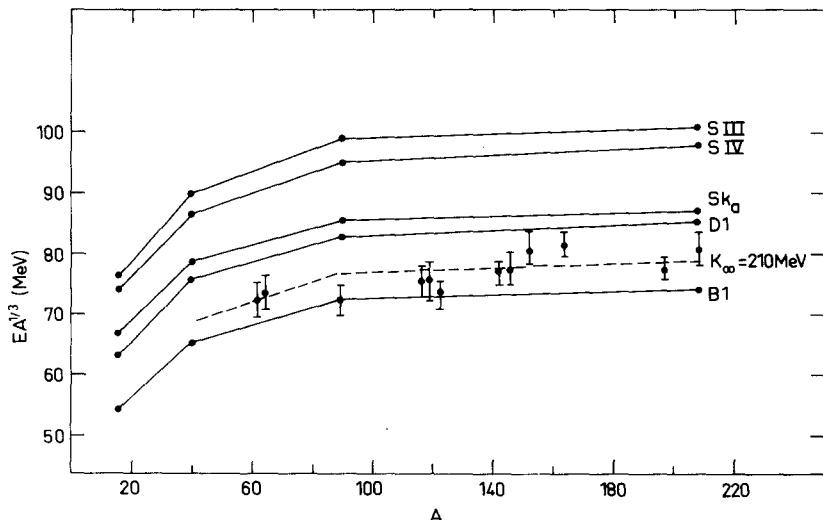


Fig. 28. Energy of the monopole resonance times $A^{1/3}$ as a function of A . The points with error bars are experimental points. (From the review of D.H. Youngblood at the "Giant Multipole Resonance" topical conference Oak-Ridge, USA 15–17 Oct. 1979.) The dotted lines indicate the value of the proposed compression modulus: $K_\infty = 210$ MeV.

9. Conclusions

We summarize the main conclusions of this report and mention some open questions concerning the giant monopole resonance and the determination of the compressibility of nuclear matter.

Most of this paper has been devoted to the theoretical understanding of the compression modes both in finite nuclei and in infinite nuclear matter. As we have emphasized, in order to relate the properties of nuclear matter to those of finite nuclei, the safest way is to use a theory capable of describing both systems on an equal footing, without the introduction of any extra assumption in going from one system to the other. This program is realized in self consistent calculations using phenomenological effective interactions.

Such calculations have been performed in spherical nuclei and they predict the existence of a giant monopole resonance in nuclei heavier than ^{40}Ca . The energy of this resonance is clearly related to the compression modulus of nuclear matter. Recent experimental data have been analyzed in the light of these calculations to extract a value for the compression modulus:

$$K_\infty = 210 \pm 30 \text{ MeV}.$$

The theory we have used to get this estimate describes correctly the properties of giant resonances, other than the monopole, which have been extensively studied already, namely the giant dipole and quadrupole resonances. It incorporates all the important physical features of the various microscopic models which have been used up to now to describe the collective excitations of the nucleus. Furthermore it survives several severe checks of internal consistency (sum rules, conservation laws, etc.). It is this consistency of the theory and the fact that it contains very few phenomenological parameters which gives confidence in its extrapolation from nuclei to nuclear matter.

However, it should be kept in mind that it has certain limitations, the most important one being its inability of describing correctly the energies of the single particle states. In particular the theory does not take into account the coupling between the single particle motion and the collective vibrations of the nucleus. The calculations which have already been done, in an attempt to include this coupling, clearly indicate a reduction of the spreading of the single particle spectrum, i.e., an increase of the effective mass, around the Fermi surface. The corresponding modification of the compression modulus is harder to predict. Furthermore, the effect of this coupling on the frequencies of the vibrations themselves is not easy to determine. Clearly more theoretical work is needed to answer these questions.

There are some reasons however to expect that the relation between the frequency of the breathing mode and the nuclear compression modulus is fairly insensitive to the details of the single particle spectrum. Let us first remark that the structure of the monopole resonance is mainly determined by the bulk shell structure but is insensitive to variations of the single particle energies. For example, self-consistent calculations show then in heavy nuclei, the velocity field of the collective motion is on the average proportional to r^2 , independently of the interaction used and therefore of the effective mass. Thus, in heavy nuclei, the breathing mode is well described by a homologous transformation of the ground state density. This property makes that it is possible to get, via a local density approximation, simple expressions for the mass parameter and the restoring force of the vibrations. The mass parameter is proportional to the size of the system, and is therefore model independent. The restoring force is given by the average over the nucleus of nuclear matter quantities, calculated at the local density. The expression of the restoring force thus obtained explains the relation between the effective compression modulus of the nucleus K_A , the quantity which is measured, and the compression modulus

of nuclear matter K_∞ . K_A depends upon the effective mass, but in precisely the same way as K_∞ does. In particular K_A is identical to K_∞ in an infinite system without surface, or in a finite system with a sharp surface. In a finite nucleus which has a diffuse surface, K_A is much smaller than K_∞ ; this is because the surface energy varies strongly with the density inside the nucleus. This effect can be expressed in terms of a compression modulus of the nuclear surface, which turns out to be proportional to K_∞ . The preceding arguments, which lead to the conclusion that K_A is proportional to K_∞ , do not suppose the validity of the independent particle approximation, although of course it has been checked only in this context. Thus we may expect this conclusion to hold if one improves the present theory.

The “breathing mode” appears to be quite a new type of collective motion of the nucleus and despite the length of this paper, many of its features remain to be explored. The coupling of the monopole and the quadrupole resonances in heavy deformed nuclei [90], the dependence of the frequency of the mode on the neutron excess, the effect of the compression on the transition potential in the surface, the structure of the mode as a function of the number of particles [91], are all interesting subjects for further investigations, both theoretically and experimentally.

Acknowledgments

I would like to express my gratitude to G. Baym, G. Bertsch, A. Bohr, G. Brown, D. Gogny, B. Grammaticos, B. Jennings, B. Mottelson, R. Schaeffer and W. Swiatecki for many useful discussions or suggestions at different stages of this work. Part of this report has been prepared while I was staying at the Niels Bohr Institute at Copenhagen. I am indebted to the Danish Research Council and the Commemorative Association of the Japan World Exposition for financial support during my stay at N.B.I. Finally I would like to thank the secretaries both at N.B.I. and Saclay for their patience in typing the successive versions of the manuscript.

References

- [1] P. Nozières, *Interacting Fermi Systems* (Benjamin, New York, 1964).
- [2] W.D. Myers and W.J. Swiatecki, Ann. Phys. 84 (1974) 211 (and references therein).
- [3] W.D. Myers, in: *Atomic data and nuclear data tables*, ed. K. Way (Academic Press, New York and London, 1975) p. 411.
- [4a] H. von Groote et al., *Atomic data and Nuclear data tables* 17 (1976) 418.
- [4b] F.D. Mackie and G. Baym, Nucl. Phys. A 285 (1977) 332.
- [5] H. Floccard and P. Quentin, Ann. Rev. of Nucl. Sci. 28 (1978) 523 and references cited therein.
- [6] W.D. Myers, Nucl. Phys. A 204 (1973) 465.
- [7] A. Chaumeaux, V. Layly and R. Schaeffer, Ann. Phys. 116 (1978) 247;
S. Shlomo and R. Schaeffer, Phys. Lett. 83 B (1979) 5.
- [8] K. Brueckner and Wada, Phys. Rev. 103 (1956) 1008.
- [9] T.T.S. Kuo and G.E. Brown, Nucl. Phys. 85 (1966) 40;
T.T.S. Kuo, Nucl. Phys. A 103 (1967) 71.
- [10] H.A. Bethe and J. Goldstone, Proc. Roy. Soc. London A 238 (1957) 551.
- [11] H.A. Bethe, Ann. Rev. Nucl. Sci. 21 (1971) 93.
- [12] J.W. Negele, Phys. Rev. C 1 (1970) 1260.
- [13] D.W.L. Sprung and P.K. Banerjee, Nucl. Phys. A 168 (1971) 273.
- [14] L. Zamick, Phys. Lett. 45 B (1973) 313.
- [15] G. Baym, in: *Nuclear physics with heavy ions and mesons*, Les Houches 1977, eds. Balian, Rho and Ripka (North-Holland, Amsterdam).
- [16] J.P. Blaizot, Phys. Lett. 78 B (1978) 367, and in preparation.
- [17] G. Ripka and J.P. Blaizot, *Cours de physique nucléaire théorique*, Note CEA-N-2019.
- [18] D. Gogny, *Nuclear self consistent fields*, eds. G. Ripka and M. Porneuf (North-Holland, Amsterdam, 1975) p. 333.

- [19] H.S. Köhler, Nucl. Phys. A 258 (1976) 301.
- [20] M. Beiner, H. Flocard, N.V. Giai and P. Quentin, Nucl. Phys. A 238 (1975) 29.
- [21] D.M. Brink and E. Boeker, Nucl. Phys. A 91 (1967) 1.
- [22] J.P. Blaizot, D. Gogny and B. Grammaticos, Nucl. Phys. A 265 (1976) 315.
- [23] J.P. Blaizot, Thèse de Doctorat d'Etat. Univ. Paris VII (1977) unpublished.
- [24] D. Gogny, Proc. Intern. Conf. on Nuclear Physics with Electromagnetic Interactions, Mainz (June 1979).
- [25] B.D. Day, Rev. Mod. Phys. 50 (1978) 495.
- [26] S. Babu and G.E. Brown, Ann. Phys. 78 (1973) 1.
- [27] O. Sjöberg, Ann. Phys. 78 (1973) 39.
- [28] P.J. Siemens, Nucl. Phys. A 141 (1970) 141.
- [29] J.P. Blaizot and D. Gogny, Nucl. Phys. A 265 (1976) 315.
- [30] J.P. Blaizot, in: Proc. Intern. School "Enrico Fermi", Elementary modes of excitations in nuclei, Varenna 1976.
- [31] D.J. Thouless, Nucl. Phys. 22 (1961) 78.
- [32] E.P. Wigner, Phys. Rev. 40 (1930) 749.
- [33] L.D. Landau, Sov. Phys. JETP 3 (1956) 920; JETP 5 (1957) 101; JETP 8 (1959) 70.
- [34] O. Bohigas, A.M. Lane and J. Martorell, Phys. Reports 51 (1979) 267.
- [35] A.B. Migdal, Theory of finite Fermi Systems and application to atomic nuclei (Interscience, New York, 1967), Nucl. Phys. A 57 (1964) 29.
- [36] A. Bohr and B. Mottelson, Nuclear Structure I, II (Benjamin, New York, 1975).
- [37] P. Ring and J. Speth, Nucl. Phys. A 235 (1974) 315.
- [38] For a recent review on the collective modes in infinite systems see G. Baym and C. Pethick, in: Physics of Liquid and Solid Helium, eds. K. Benneman and J. Jefferson (Wiley, 1978).
- [39] J.D. Walecka, Phys. Rev. 126 (1962) 653.
- [40] R. Satchler, Particles and Nuclei 5 (1973) 105.
- [41] D. Gogny and R. Padjen, Nucl. Phys. A 293 (1977) 375.
- [42] C. Werntz and H. Überall, Phys. Rev. 149 (1966) 762.
- [43] V.R. Pandharipande, Phys. Lett. 31 B (1970) 685.
- [44] K.A. Brueckner, M.J. Giannoni and R.J. Lombard, Phys. Lett. 31 B (1970) 97.
- [45] S.K.M. Wong, G. Saunier and B. Rouben, Nucl. Phys. A 169 (1971) 294.
- [46] Y.M. Engels et al., Nucl. Phys. A 249 (1975) 215.
- [47] J.J. Griffin, Phys. Rev. 108 (1957) 328.
- [48] E. Caurier, B. Bilwes and Y. Abgrall, Phys. Lett. 44 B (1973) 411.
- [49] A. Faessler, S. Krewald and J.E. Galonska, Phys. Lett. 55 B (1975) 125;
S. Krewald et al., Nucl. Phys. A 269 (1976) 112.
- [50] D. Vautherin and H. Flocard, Phys. Lett. 55 B (1975) 259.
- [51] M. Sotona and J. Zofka, Phys. Lett. 57 B (1975) 27;
K.V. Shiticova, Nucl. Phys. A 331 (1979) 365.
- [52] J. Damgaard et al., Nucl. Phys. A 121 (1968) 625.
- [53] J. Speth, L. Zamick and P. Ring, Nucl. Phys. A 232 (1974) 1.
- [54] G.F. Bertsch and S.F. Tsai, Phys. Reports C 18 (1975) 125.
- [55] K.F. Liu and G.E. Brown, Nucl. Phys. A 265 (1976) 385.
- [56] R.W. Sharp and L. Zamick, Nucl. Phys. A 223 (1974) 333.
- [57] M.K. Kirson, Nucl. Phys. A 257 (1976) 58.
- [58] K. Goeke, Phys. Rev. Lett. 38 (1977) 212.
- [59] S. Krewald et al., Phys. Rev. Lett. 33 (1974) 1386.
- [60] S. Shlomo and G. Bertsch, Nucl. Phys. A 243 (1975) 507.
- [61] K.F. Liu and N.V. Giai, Phys. Lett. 65 B (1976) 23.
- [62] V. Bernard and N.V. Giai, preprint IPNO/TH 79-55 (F-91406 ORSAY Cedex).
- [63] K. Audo and M. Kohno, Prog. Theor. Phys. 60 (1978) 304.
- [64] C.Y. Wong, Phys. Rev. 17 C (1978) 1832.
- [65] R.A. Berg and L. Wilets, Phys. Rev. 101 (1956) 201;
L. Wilets, Rev. Mod. Phys. 30 (1958) 542.
- [66] G.E. Brown, J.H. Goun and P. Gould, Nucl. Phys. 46 (1963) 598.
- [67] G. Bertsch and T.T.S. Kuo, Nucl. Phys. A 112 (1968) 204.
- [68] I. Hamamoto and P. Siemens, Nucl. Phys. A 269 (1976) 199.
- [69] J.P. Jeukenne, A. Lejeune and C. Mahaux, Phys. Reports 25 C (1976) 83.
- [70] G.E. Brown and J. Speth, Neutron Capture Gamma-Ray Spectroscopy, eds. R.E. Chrien and W.R. Kane (Plenum Press, N.Y., 1979).
- [71] D.H. Youngblood et al., Phys. Rev. C 13 (1976) 994.
- [72] F.E. Bertrand, Ann. Rev. Nucl. Sci. 26 (1976) 457.
- [73] R. Satchler, in: Proc. of the Intern. School "Enrico Fermi", Elementary modes of excitations in nuclei, Varenna 1976.

- [74] D.H. Youngblood et al., Phys. Rev. Lett. 39 (1977) 1188.
- [75] M. Buenerd et al., Phys. Lett. 48 B (1979) 305;
D. Lebrun, M. Buenerd, P. Martin, P. de Saintignon, J. Chauvin and G. Perrin, to be published.
- [76] F.E. Bertrand, G.R. Satchler, D.J. Horen, A. Van der Woude, to be published in Phys. Rev. Lett.
- [77] M.N. Harakeh, K. Van der Borg, T. Ishimatsu, H.P. Morsch, A. Van der Woude and F.E. Bertrand, Phys. Rev. Lett. 38 (1977) 676.
- [78] N. Marty et al., Orsay Rpt. No. IPNO-Ph-N-75-11 (1975) unpublished and Proc. Intern. Conf. on highly excited states in nuclei, Julich 1975.
- [79] N. Marty et al., in: Proc. of Conf. Large amplitude collective motion, Lake Balaton June 1979.
- [80] J. Arvieux et al., Phys. Rev. Lett. 42 (1979) 753.
- [81] S. Fukuda and Y. Torizuka, Phys. Lett. 62 B (1976) 146;
M. Sasao and Y. Torizuka, Phys. Rev. C 15 (1977) 217.
- [82] N. Marty et al., contribution to the Conference on giant multipole resonances, Oak Ridge Oct. 1979.
- [83] P. Haensel, Phys. Lett. 81 B (1979) 276.
- [84] Yamejaka, Phys. Rev. Lett. 40 (1978) 1628.
- [85] G. Holzwarth and G. Eckart, Z. Phys. A 284 (1978) 291; Nucl. Phys. A 325 (1979) 1 and to be published in Phys. Lett.:
H. Sagawa and G. Holzwarth, Prog. Theor. Phys. 59 (1978) 12.
- [86] H. Krivine, J. Treiner and O. Bohigas, Nucl. Phys. A 336 (1980) 155.
- [87] J.P. Blaizot and B. Grammaticos, to be published in Nuclear Physics.
- [88] Weisskopf, Nucl. Phys. 3 (1957) 423.
- [89] T. Suzuki, Nucl. Phys. A 217 (1973) 182;
J.P. Blaizot and H. Schulz, in: Proc. workshop "Time dependent Hartree Fock Method", eds. Bonche, Giraud and Quentin, Gif-sur-Yvette 1979.
- [90] Y. Abgrall, B. Morand, E. Caurier and B. Grammaticos, to be published.
- [91] B.K. Jennings and A.D. Jackson, to be published in Nucl. Phys.
- [92] F. Serr, G. Bertsch and J.P. Blaizot, to appear in Phys. Rev. C.
- [93] F. Serr and G. Bertsch, MSU theor. nucl. phys. preprint 1980/204-1.